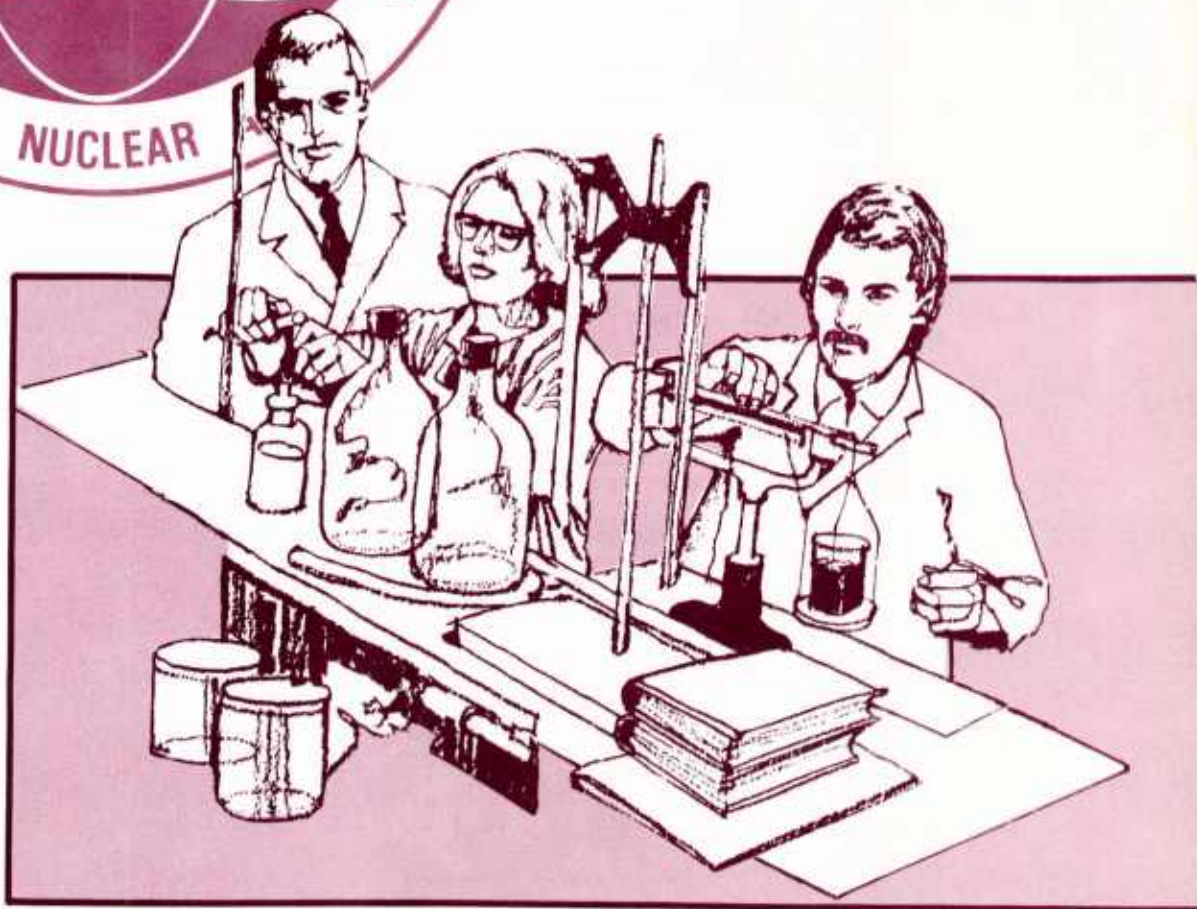


# Abstracts



JULY  
AUG **1986**  
SEP



**Defense Nuclear Agency**

**Armed Forces Radiobiology Research Institute**

**Bethesda, Md 20814-5145**

UNCLASSIFIED

SECURITY CLASSIFICATION OF THIS PAGE

REPORT DOCUMENTATION PAGE				
1a. REPORT SECURITY CLASSIFICATION UNCLASSIFIED		1b. RESTRICTIVE MARKINGS		
2a. SECURITY CLASSIFICATION AUTHORITY		3. DISTRIBUTION/AVAILABILITY OF REPORT  Approved for public release; distribution unlimited.		
2b. DECLASSIFICATION/DOWNGRADING SCHEDULE				
4. PERFORMING ORGANIZATION REPORT NUMBER(S) SR86-23 through SR86-33, TR86-2, and CR86-1		5. MONITORING ORGANIZATION REPORT NUMBER(S)		
6a. NAME OF PERFORMING ORGANIZATION Armed Forces Radiobiology Research Institute	6b. OFFICE SYMBOL (If applicable) AFRRI	7a. NAME OF MONITORING ORGANIZATION		
6c. ADDRESS (City, State and ZIP Code)  Defense Nuclear Agency Bethesda, Maryland 20814-5145		7b. ADDRESS (City, State and ZIP Code)		
8a. NAME OF FUNDOING/SPONSORING ORGANIZATION Defense Nuclear Agency	8b. OFFICE SYMBOL (If applicable) DNA	9. PROCUREMENT INSTRUMENT IDENTIFICATION NUMBER		
8c. ADDRESS (City, State and ZIP Code)  Washington, DC 20305		10. SOURCE OF FUNDING NOS.		
11. TITLE (Include Security Classification) AFRRI Reports, Jul-Sep 1986		PROGRAM ELEMENT NO.	PROJECT NO.	TASK NO.
12. PERSONAL AUTHOR(S)		WORK UNIT NO.		
13a. TYPE OF REPORT Reprints/Technical	13b. TIME COVERED FROM _____ TO _____	14. DATE OF REPORT (Yr., Mo., Day)		15. PAGE COUNT 120
16. SUPPLEMENTARY NOTATION				
17. COSATI CODES		18. SUBJECT TERMS (Continue on reverse if necessary and identify by block number)		
FIELD	GROUP	SUB. GR.		
		N/A		
19. ABSTRACT (Continue on reverse if necessary and identify by block number)  This volume contains AFRRI Scientific Reports SR86-23 through SR86-33, Technical Report TR86-2, and Contract Report CR86-1 for Jul-Sep 1986.				
20. DISTRIBUTION/AVAILABILITY OF ABSTRACT  UNCLASSIFIED/UNLIMITED <input type="checkbox"/> SAME AS RPT. <input type="checkbox"/> DTIC USERS <input type="checkbox"/>		21. ABSTRACT SECURITY CLASSIFICATION UNCLASSIFIED		
22a. NAME OF RESPONSIBLE INDIVIDUAL Junith A. Van Deusen		22b. TELEPHONE NUMBER (Include Area Code) (202) 295-3536	22c. OFFICE SYMBOL ISDP	

DD FORM 1473, 83 APR

EDITION OF 1 JAN 73 IS OBSOLETE

UNCLASSIFIED  
SECURITY CLASSIFICATION OF THIS PAGE

## CONTENTS

### Scientific Reports

**SR86-23:** Cockerham, L. G., Cervený, T. J., and Hampton, J. D. Postradiation regional cerebral blood flow in primates.

**SR86-24:** Durakovic, A. Heart function studies in dogs after acute gamma irradiation of the precordium.

**SR86-25:** Durakovic, A. The effect of anesthetic, sedative or narcotic drugs on intrahepatic and extrahepatic biliary kinetics.

**SR86-26:** Freschi, J. E., and Moran, A. Effect of gamma radiation on sodium channels in different conformations in neuroblastoma cells.

**SR86-27:** Hunt, W. A., and Mullin, M. J. Effects of ethanol exposure on brain sodium channels.

**SR86-28:** Mullin, M. J., Hunt, W. A., and Harris, R. A. Ionizing radiation alters the properties of sodium channels in rat brain synaptosomes.

**SR86-29:** Neta, R., Schwartz, G. N., MacVittie, T. J., and Douches, S. D. Thymic hormones in thymus recovery from radiation injury.

**SR86-30:** Parker, G. A., Bogo, V., and Young, R. W. Acute toxicity of petroleum- and shale-derived distillate fuel, marine: Light microscopic, hematologic, and serum chemistry studies.

**SR86-31:** Rabin, B. M., Hunt, W. A., Chedester, A. L., and Lee, J. Role of the area postrema in radiation-induced taste aversion learning and emesis in cats.

**SR86-32:** Snyder, S. L., Walden, T. L., Patchen, M. L., MacVittie, T. J., and Fuchs, P. Radioprotective properties of detoxified lipid A from Salmonella minnesota R595.

**SR86-33:** Stevens, K. E., Mickley, G. A., and McDermott, L. J. Brain areas involved in production of morphine-induced locomotor hyperactivity of the C57B1/6J mouse.

### Technical Report

**TR86-2:** Zeman, G. H., Dooley, M., and Mohaupt, T. M. Preliminary evaluation of U.S. Army RADIAC detector DT-236/PD and RADIAC computer-indicator CP-696/UD.

### Contract Report

**CR86-1:** McDonald, J. C. Calorimetric dose measurements and calorimetric system developed for the Armed Forces Radiobiology Research Institute.



Reprint & Copyright © by  
Aerospace Medical Association, Washington, DC

# 

L. G. COCKERHAM, Ph.D., T. J. CERVENY, Ph.D., and J. D. HAMPTON

*Physiology Department, Armed Forces Radiobiology Research  
Institute, Bethesda, Maryland 20814-5145*

COCKERHAM LG, CERVENY TJ, HAMPTON JD. *Postradiation regional cerebral blood flow in primates*. *Aviat. Space Environ. Med.* 1986; 57:578-82.

Early transient incapacitation (ETI) is the complete cessation of performance during the first 30 min after radiation exposure and performance decrement (PD) is a reduction in performance at the same time. Supralethal doses of radiation have been shown to produce a marked decrease in regional cerebral blood flow in primates concurrent with hypotension and a dramatic release of mast cell histamine. In an attempt to elucidate mechanisms underlying the radiation-induced ETI/PD phenomenon and the postradiation decrease in cerebral blood flow, primates were exposed to 100 Gy (1 Gy = 100 rads), whole-body, gamma radiation. Pontine and cortical blood flows were measured by hydrogen clearance, before and after radiation exposure. Systemic blood pressures were determined simultaneously. Systemic arterial histamine levels were determined preradiation and postradiation. Data obtained indicated that radiated animals showed a decrease in blood flow of 63% in the motor cortex and 51% in the pons by 10 min postradiation. Regional cerebral blood flow of radiated animals showed a slight recovery 20 min postradiation, followed by a fall to the 10 min nadir by 60 min postradiation. Immediately, postradiation systemic blood pressure fell 67% and remained at that level for the remainder of the experiment. Histamine levels in the radiated animals increased a hundredfold 2 min postradiation. This study indicates that regional cerebral blood flow decreases postradiation with the development of hypotension and may be associated temporally with the postradiation release of histamine.

**E**ARLY TRANSIENT incapacitation (ETI) is the complete cessation of performance, occurring transiently and within the first 30 min following

exposure to supralethal doses of ionizing radiation (17), and performance decrement (PD) is a reduction in performance at the same time. A possible explanation for ETI may occur when supralethal exposure to ionizing radiation, such as gamma photons, results in postradiation hypotension (6) with the arterial blood pressure often decreasing to less than 50% of normal (11). One investigation (3) was able to closely correlate PD with postradiation hypotension, usually with the decrement following, within a few minutes, the initial fall in blood pressure.

Postradiation hypotension may produce a decreased cerebral blood flow (CBF) even though the central nervous system (CNS) can often maintain CBF under conditions of severe hypotension through the mechanism of autoregulation. One study (5) demonstrated a dramatic fall of CBF immediately following a single, 25 Gy (1 Gy = 100 rads) <sup>60</sup>Co exposure. Blood pressure fell 59% by 5 min postradiation, with the CBF falling to only 30% of its preradiation value at the same time. Following a postradiation mean systemic blood pressure decrease of 50% (5,11), the ETI/PD phenomenon may result then from a decreased cerebral blood flow.

Studies have reported elevations of circulating blood histamines in humans undergoing radiation therapy (19), decreases in tissue histamine levels in rats (13), and increases in canine plasma histamine levels (7,8) following radiation. Histamine is released under the stimulus of ionizing radiation (1,12) and is implicated in radiation-induced hypotension. One study (11) even reported the prevention or modification of radiation-induced performance changes and hypotension by the preradiation administration of an antihistamine. This study was designed to determine if the postradiation release of histamine, postradiation hypotension,

Address reprint requests to: Dr. Lorris G. Cockerham, who is Chief, General Physiology Division, Physiology Department, Armed Forces Radiobiology Research Institute, Bethesda, MD 20814-5145.

This manuscript was received for review in May 1985. The revised manuscript was accepted for publication in August 1985.

and reduced cerebral blood flow can be correlated chronologically.

Two contrasting regions of the brain were selected for this study. The reticular formation of the pons was selected because of its possible influence on levels of alertness (2,22) and, therefore, its possible involvement in postradiation ETI. The second region of interest, the precentral gyrus, or motor cortex, is an area more highly susceptible to hypoxia than the sensory cortex or postcentral gyrus (20) and a decrease in blood flow to that area may be responsible for a postradiation decrement in motor performance.

## MATERIALS AND METHODS

In this study, 12 male rhesus monkeys (*Macaca mulatta*), from 25 to 44 months of age ( $31.6 \pm 1.5$  S.E.M.), weighing between 2.8 and 4.8 kg ( $3.7 \pm 0.16$  S.E.M.) were used. The animals were divided randomly into two groups of six animals each. The animals were grouped as follows: Group I, six sham-radiated monkeys; Group II, six radiated monkeys.

Research was conducted according to the principles enunciated in the "Guide for the Care and Use of Laboratory Animals" prepared by the Institute of Laboratory Animal Resources, National Research Council. The monkeys were initially anesthetized in their cages with an i.m. injection of 60 mg of ketamine hydrochloride (to facilitate removal from cages) with 0.04 mg atropine sulfate (to facilitate intubation) and were then moved to surgery where the remainder of the experiment was conducted. (Ketamine and atropine were given on a one-time basis.)

Approximately 3 h before radiation or sham-radiation, the animals were intubated with a cuffed endotracheal tube and ventilated using a forced volume respirator to maintain a stable normal blood pH and oxygen tension. After insertion of the endotracheal tube, each animal was placed on a circulating water blanket to maintain body temperature between 36 and 38°C. A rectal probe was inserted to monitor body temperature. A femoral arterial catheter was used to withdraw blood for blood gas determinations and to measure systemic arterial blood pressure using a Statham P23 Db pressure transducer. A systemic venous catheter was used to administer physiological saline and maintenance doses of anesthetic ( $\alpha$ -Chloralose, as needed, for a total dose of 100 mg·kg<sup>-1</sup>).

The animal's head was positioned on the headholder of a stereotaxic instrument (David Kopf Instruments, Tujunga, CA) and the scalp shaved and incised, allowing access to the skull. Using the stereotaxic micromanipulator, the skull was marked for insertion of four electrodes and small burr holes were drilled through the skull at these marks. Again, using the micromanipulator, one electrode was placed in the left and one in the right pons (21). In the same manner, one electrode was placed in the left and one in the right precentral gyrus of the parietal cortex, 4 mm each side of the longitudinal fissure. The latter two electrodes were placed so that the tips were 2 mm below the surface to ensure that measurements would be taken from the cortical grey matter. The electrodes

were Teflon-coated, platinum-iridium wire of 0.178 mm diameter, encased in, but insulated from, stainless steel tubing (standard 22-gauge spinal needle) for rigidity, with exposed tips of approximately 2 mm. The exposed dura was covered with moistened pledgets and the electrodes were sealed and secured to the skull with dental acrylic. A stainless steel reference electrode was placed in nearby tissue.

Regional cerebral blood flow was measured by the hydrogen clearance technique for 30 min before radiation or sham-radiation and for 60 min after. This technique is essentially an amperometric method of blood flow measurement and is described in previous publications (6-8).

After 30 min of recording, the animals were disconnected from the respirator and recording apparatus to facilitate radiation in a separate room. The animals were reconnected to the respirator and recording apparatus at 4 min postradiation or sham-radiation and measurements were continued for a minimum of 60 min. At 30 and 10 min preradiation or sham-radiation, and at 6, 10, 15, 30, 45, and 60 min postradiation or sham-radiation, blood samples were taken via the arterial catheter to monitor stability of blood pH and oxygen tension, and respiration was adjusted to maintain preradiation levels. Simultaneously, body temperature was monitored and maintained with the water blanket. Mean systemic arterial blood pressure was determined via the arterial catheter for the duration of the experiment. After termination of the measurements the electrodes were examined visually for verification of placement.

At 10 and 30 min preradiation and 2 and 4 min postradiation blood samples for plasma histamine determinations were drawn from the arterial catheter with plastic syringes and transferred to prelabelled, chilled collection tubes contained EDTA. Determinations of plasma histamine levels was then accomplished as described in previous publications (7,8). All blood samples were replaced with an equal volume of saline.

Radiation was accomplished with a bilateral, whole-body, exposure to gamma ray photons from a cobalt-60 source located at the Armed Forces Radiobiology Research Institute. Exposure was limited to a mean of 1.38 min at 74 Gy·min<sup>-1</sup> steady state, free-in-air. Dose rate measurements at depth were made with an ionization chamber placed in a tissue equivalent model. The measured midline tissue dose rate was 69 Gy·min<sup>-1</sup>, producing a calculated total dose of 100 Gy, considering rise and fall of the radiation source.

Blood pressure and blood flow data were grouped into 10 min intervals, measured in relation to midtime of radiation, and plotted at the middle of the interval. The Wilcoxon Rank Sum Test was used to analyze statistically the blood pressure, blood flow and histamine data. A 95% level of confidence was employed to determine significance. Since all the animals were treated identically before radiation or sham-radiation, and since the preradiation data for the control and test animals showed no significant difference, the preradiation data for the radiated and sham-radiated animals were combined.

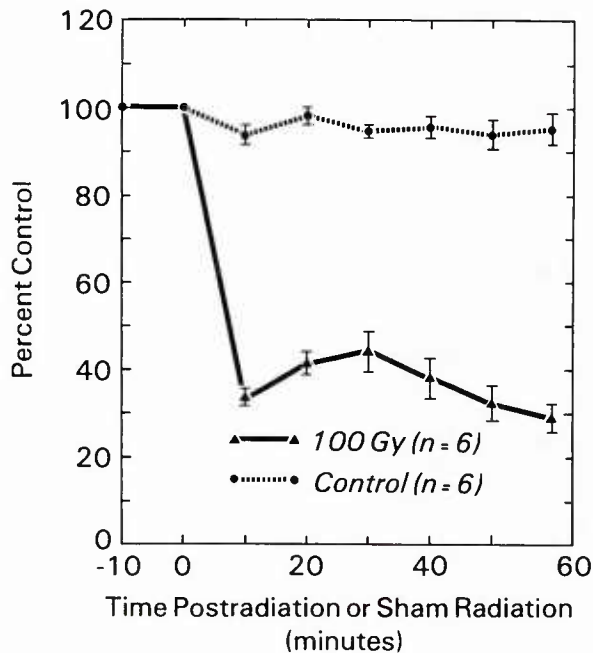


Fig. 1. Percent of control mean blood pressure. Values expressed as percentage change in postradiation mean arterial blood pressure ( $\pm$  S.E.M.) compared to preradiation mean of  $116.1 \pm 2.4$  mm Hg. All 100 Gy postradiation points were significantly different ( $p \leq 0.05$ ) from control.

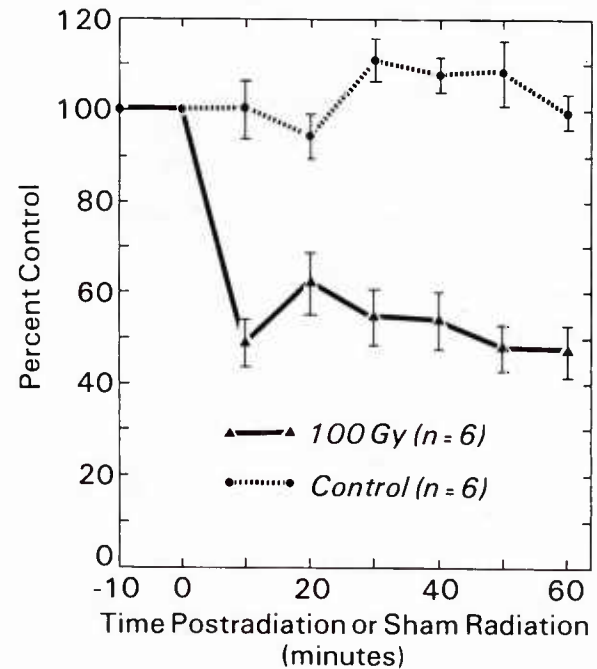


Fig. 2. Percent of control blood flow in the pons. Values are expressed as percentage change in postradiation pontine regional cerebral blood flow ( $\pm$  S.E.M.) compared to preradiation mean of  $73.4 \pm 4.0$  ml·100g<sup>-1</sup>·min<sup>-1</sup>. All 100 Gy postradiation points were significantly different ( $p \leq 0.05$ ) from control.

## RESULTS

Mean systemic arterial blood pressure ( $\bar{P}_a$ ), as seen in Fig. 1, displayed a 66% decrease from a preradiation mean ( $116.1 \pm 2.4$  mm Hg) in the radiated animals within 10 min postradiation. A slight recovery was seen at 30 min postradiation, followed by a decline to a 60-min postradiation level that was 71% below the preradiation values. After sham-radiation there was no significant change in  $\bar{P}_a$  for the six control monkeys. The  $\bar{P}_a$  values for the radiated group are statistically different ( $p \leq 0.05$ ) from the sham-radiated, control group.

Fig. 2 displays a preradiation mean blood flow of  $73.4 \pm 3.1$  ml · 100 g<sup>-1</sup> · min<sup>-1</sup> of tissue in the reticular formation of the pons. The postradiation blood flow values for the sham-radiated, control monkeys showed an overall average increase during the 60 min after sham-radiation. However, postradiation values for radiated animals showed a rapid and significant decline to 51% below preradiation levels 10 min postradiation. Following a slight recovery at 20 min postradiation, the blood flow gradually decreased to 48% of the preradiation level by 60 min postradiation. There was a significant difference ( $p \leq 0.05$ ) between the two groups at all postradiation times of measurement.

Preradiation cortical blood flow, as shown in Fig. 3, was  $48.9 \pm 4.0$  ml · 100 g<sup>-1</sup> · min<sup>-1</sup> of tissue. Postradiation flow for the sham-radiated group of monkeys showed only a 13% decrease for the 60 min observation period. However, postradiation blood flow values for radiated monkeys showed a precipitous

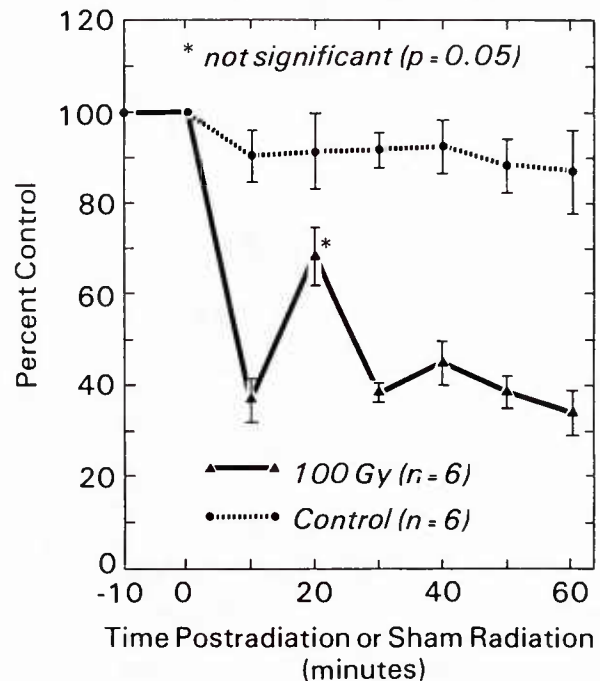


Fig. 3. Percent of control blood flow in the pre-central gyrus. Values are expressed as percentage change in postradiation blood flow in the pre-central gyrus ( $\pm$  S.E.M.) compared to preradiation mean of  $48.9 \pm 4.0$  ml·100g<sup>-1</sup>·min<sup>-1</sup>. All Gy postradiation points, except 20 min (\*), were significantly different ( $p \leq 0.05$ ) from control.



decline to 63% below preradiation levels by 10 min postradiation. This was followed by a sharp, partial recovery at 20 min postradiation and a decline to 66% below baseline levels by 60 min postradiation. These levels are significantly different ( $p \leq 0.05$ ) from those of the control group at all postradiation observations with the exception of the 20 min postradiation recovery point.

When preradiation systemic arterial plasma histamine levels from the two groups were compared, no significant difference was seen at the 95% level of confidence (Table I). However, when postradiation histamine levels from the two groups were compared, there was a significant difference ( $p \leq 0.05$ ) at both the 2 min and 4 min determinations. Plasma histamine levels in radiated animals at these points were determined to be almost a hundred times greater than that found in control animals.

TABLE I. PLASMA HISTAMINE LEVELS ( $\text{ng} \cdot \text{ml}^{-1}$ ).

TIME (min)	CONTROL ( $\pm$ S.E.M.)	100 Gy RADIATED ( $\pm$ S.E.M.)
0	6.09 $\pm$ 0.23	6.55 $\pm$ 0.36
2	6.19 $\pm$ 0.18	599.40 $\pm$ 89.4*
4	6.56 $\pm$ 0.08	480.30 $\pm$ 78.9*

\*Postradiation values significantly different ( $p \leq 0.05$ ) from control.

## DISCUSSION

Postradiation hypotension has been well documented in the rhesus monkey, and a critical postradiation mean arterial blood pressure ( $\bar{P}_a$ ) of 50%–60% of the preradiation  $\bar{P}_a$  must be maintained for adequate autoregulation of cerebral circulation (5,11,14). The initial precipitous decline in  $\bar{P}_a$  to 66% below preradiation levels may, then, be associated with the similar immediate decrease in regional cerebral blood flow (rCBF) seen in both the pons and cerebral cortex of the radiated animals. A similar decrease in cerebral blood flow accompanied by symptoms and signs of cerebral ischemia has been reported in man in response to drugs (15). On the basis of diminished cerebral blood flow reported in these animals, one might expect a severe functional impairment of the CNS following radiation. In fact, postradiation early transient incapacitation (ETI) has been reported in monkeys starting as early as 2 min postradiation, lasting for 10–30 min and often accompanied by severe systemic hypotension during which  $\bar{P}_a$  decreased to less than 50% of normal (4,10). This is supported by Suzuki *et al.* (24) who reported that spontaneous activity in cortical neurons ceased within 60 s after the onset of ischemia. The decline in  $\bar{P}_a$  and rCBF and the temporary recovery of rCBF reported here corresponds closely in time with the observed occurrence of ETI (4,9,11) and suggests a temporal relationship between the depressed  $\bar{P}_a$ , rCBF, and the appearance of ETI. Although seemingly similar, this report differs from an earlier report by Chapman and Young (5) in that it gives regional cerebral blood flow rather than total cerebral blood flow as obtained with

a flow transducer placed unilaterally on the internal carotid or common carotid artery.

Another complication in cerebral ischemia is the opening of the blood-brain barrier as reported by Suzuki *et al.* (23) and which may be associated with the development of cerebral vasogenic edema (18). Gross *et al.* (16) has reported an increase in the permeability of the blood-brain barrier following infusion of histamine into the internal carotid artery. Therefore, histamine may be implicated, not only in postradiation hypotension, but in the decrease in rCBF and its associated neurological dysfunction and in an increase in the permeability of the blood-brain barrier following radiation. Further, since these mechanisms may be involved in the production of cerebral edema, the postradiation release of histamine may be involved with the production of cerebral edema and its associated neurological dysfunction.

Even though a temporal relationship does seem to exist between cortical blood flow and ETI, the presence of other factors must not be excluded. Some other chemical factor could be released by radiation, cause the release of histamine from mast cells, and produce ETI by acting as a neurotransmitter in the central nervous system. However, before a temporal relationship, and definitely a causal relationship, can be established, postradiation measurements of blood chemistry, cerebral blood flow and behavioral effects must be accomplished on the same animal subject.

## ACKNOWLEDGMENTS

The authors thank Dr. M. A. Donlon for helpful advice and guidance, E. A. Helgeson for technical assistance and Mrs. M. H. Owens for manuscript preparation.

This work was supported by the Armed Forces Radiobiology Research Institute, Defense Nuclear Agency, under Research Work Unit MJ 00053. The views presented in this paper are those of the authors; no endorsement by the Defense Nuclear Agency has been given or should be inferred.

## REFERENCES

1. Alter WA III, Hawkins RN, Catravas GN, Doyle TF, Takenaga JK. Possible role of histamine in radiation induced hypotension in the rhesus monkey. *Radiat. Res.* 1983; 94:654.
2. Brodal A. The reticular formation. In: *Neurological anatomy*. New York: Oxford University Press, 1969: 304–49.
3. Bruner A, Bogo V, Henderson EA. Dose-rate effects of  $^{60}\text{Co}$  irradiation on performance and physiology in monkeys. Albuquerque, NM: Lovelace Foundation for Medical Education and Research, 1975; Topical Report DNA 3660T.
4. Bruner A. Immediate dose-rate effects of  $^{60}\text{Co}$  on performance and blood pressure in monkeys. *Radiat. Res.* 1977; 70:378–90.
5. Chapman PH, Young RJ. Effect of cobalt-60 gamma irradiation on blood pressure and cerebral blood flow in the *Macaca mulatta*. *Radiat. Res.* 1968; 35:78–85.
6. Cockerham LG, Doyle TF, Trumbo RB, Nold JB. Acute postradiation canine intestinal blood flow. *Int. J. Radiat. Biol.* 1984; 45:65–72.
7. Cockerham LG, Doyle TF, Donlon MA, Helgeson EA. Canine postradiation histamine levels and subsequent response to Compound 48/80. *Aviat. Space Environ. Med.* 1984; 55:1041–5.
8. Cockerham LG, Doyle TF, Donlon MA, Gossett-Hagerman CJ. Antihistamines block radiation-induced increased intestinal blood flow in canines. *Fundam. Appl. Toxicol.* 1985; 5:597–604.

9. Curran CR, Young RW, Davis WF. The performance of primates following exposure to pulsed whole-body gamma-neutron radiation. Bethesda, MD: Armed Forces Radiobiology Research Institute Scientific Report, 1973; AFRRI SR73-1.
10. Doyle TF, Turns JE, Strike TA. Effect of an antihistamine on early transient incapacitation of monkeys subjected to 4000 rads of mixed gamma-neutron radiation. *Aerospace Med.* 1971; 42:400-3.
11. Doyle TF, Curran CR, Turns JE. The prevention of radiation-induced, early transient incapacitation of monkeys by an antihistamine. *Proc. Soc. Exp. Biol. Med.* 1974; 145:1018-24.
12. Doyle TF, Strike TA. Radiation-released histamine in the rhesus monkey as modified by mast-cell depletion and antihistamine. *Experientia* 1977; 33:1047-8.
13. Eisen VD, Wilson CWM. The effect of B-irradiation on skin histamine and vascular responses in rat. *J. Physiol.* 1957; 136:122-30.
14. Farrar JK, Gamache FW Jr, Ferguson GG, Barker J, Varkey GP, Drake CG. Effects of profound hypotension on cerebral blood flow during surgery for intracranial aneurysms. *J. Neurosurg.* 1981; 55:857-64.
15. Finnerty FA Jr, Guillaudeau RL, Fazekas JF. Cardiac and cerebral hemodynamics in drug induced postural collapse. *Circ. Res.* 1957; 5:34-9.
16. Gross PM, Teasdale GM, Angerson WJ, Harper AM. H<sub>2</sub>-receptors mediate increases in permeability of the blood-brain barrier during arterial histamine infusion. *Brain Res.* 1981; 210:396-400.
17. Kimeldorf DJ, Hunt EL. Neurophysiological effects of ionizing radiation. In: Kimeldorf DJ, Hunt EL, eds. *Ionizing radiation: neural function and behavior.* New York: Academic Press, 1965: 59-108.
18. Klatzo I, Suzuki R, Orzi F, Schuier F, Nitsch C. Pathomechanisms of ischemic brain edema. In: Go KG, Baathmann A, eds. *Recent progress in the study and therapy of brain edema.* New York: Plenum Press, 1984:1-17.
19. Lasser EC, Stenstrom KW. Elevation of circulating blood histamine in patients undergoing deep roentgen therapy. *Am. J. Roentgenol.* 1954; 72:985-8.
20. Pluta R, Gajkowska B. Ultrastructural changes in the sensorimotor cortex of the rabbit after complete 30-min brain ischemia. *J. Neurosci. Res.* 1984; 11:35-47.
21. Snider RS, Lee JC. A stereotaxic atlas of the monkey brain (*Macaca mulatta*). Chicago: The University of Chicago Press, 1961.
22. Somjen GG. The cycle of sleeping and waking. In: *Neurophysiology—the essentials.* Baltimore, MD: Williams and Wilkins, 1983:483-501.
23. Suzuki R, Yamaguchi T, Kirino T, Orzi F, Klatzo I. The effects of 5-minute ischemia in mongolian gerbils: I. Blood-brain barrier, cerebral blood flow, and local cerebral glucose utilization changes. *Acta Neuropathol.* 1983; 60:207-16.
24. Suzuki R, Yamaguchi T, Li C-L, Klatzo I. The effects of 5-minute ischemia in mongolian gerbils. II. Changes of spontaneous neuronal activity in cerebral cortex and CA1 sector of hippocampus. *Acta Neuropathol.* 1983; 60:217-22.



# Heart Function Studies in Dogs After Acute Gamma Irradiation of the Precordium

LTC Asaf Durakovic, MC USA

In order to study the development of post-irradiation cardiac dysfunction, we irradiated the precordia of 18 adult beagle dogs with 30, 60, or 100 Gy of Co-60 photons, and measured cardiac histology, electrocardiograms, Tc-99m pyrophosphate cardiac tissue distribution, and serial left ventricular ejection fraction (LVEF). Although the electrocardiograms and tissue distribution of Tc-99m were unaffected by these dose levels, the LVEF was reduced by day 58 for all the irradiated dogs. The delay in the onset of cardiac function impairment parallels the delay in the onset of fibrosis in irradiated hearts.

MILITARY MEDICINE, 151, 5:275, 1986

## Introduction

Because of the large number of patients who have received cardiac irradiation for the treatment of thoracic neoplasms, as well as isolated exposures to the heart from nuclear accidents,<sup>1</sup> there has been considerable interest in the effects of radiation on the heart itself. Although earlier studies had suggested a relative resistance of the heart to radiation damage,<sup>2</sup> there is now substantial evidence for dose-dependent radiation induced cardiac damage in both man and experimental animals. Early studies by Stone et al.,<sup>3</sup> and Phillips, et al.<sup>4</sup> in dogs receiving X-ray doses of 50–200 Gy demonstrated congestive heart failure, pericarditis, ventricular conduction defects, focal necrosis, and fibrosis. Later studies by Fajardo and Stewart<sup>5</sup> using the rabbit model showed an acute pancarditis followed by a latency period and eventual progressive fibrosis.

In a review of cardiac complications suffered by patients treated with irradiation for chest neoplasma, Cohn, et al.<sup>6</sup> noted pericarditis, mitral insufficiency, left ventricular conduction defects, and myocardial infarction. Recent studies of left ventricular ejection fraction (LVEF) by Gottidiener et al.<sup>7</sup> and Gomez et al.,<sup>8</sup> have shown decreased resting and exercise LVEF in patients formerly treated with chest irradiation for Hodgkins disease. In order to determine if the decrease in ejection fraction following cardiac irradiation occurs in the acute or chronic phase of post irradiation, we studied the effects of localized cardiac irradiation on dogs.

## Methods

All experiments were performed on male bea-

gle dogs maintained on standard laboratory food and water ad libitum. Eighteen dogs were divided into three groups which received respectively 30, 60, and 100 Gy of gamma irradiation applied bilaterally to the precordium from a Theratron-80 Co-60 teletherapy unit. The beam was confined to a radiographically determined outline of the precordium, and dosimetry measurements were made on one of the experimental animals. Isodose curves (Fig. 1) were constructed using the Treatment Planning Computer at the Naval Medical Center, Bethesda, MD. By this method, the dose uniformity over the heart was  $\pm 5\%$ , and the major portion of the lungs were beyond the edges of the direct beams.

Multiple gated blood pool scintigraphic heart function studies were obtained prior to irradiation, and at 7, 21, 30, 50, 58, and 70 days post irradiation. Tc-99m pyrophosphate scans were obtained prior to irradiation, and on days 2, and 12 after irradiation on the dogs receiving 30 and 60 Gy Co-60 photons. Selected dogs receiving Tc-99m pyrophosphate were euthanitized at either 2 or 12 days post irradiation, and tissue samples from the heart, lungs, aorta, and pulmonary artery were analyzed for tissue uptake by counting in an LKB ultrogamma well counter. Tc-99m activity was expressed as percent dose per gram of tissue. The tissue samples were also examined histologically by light microscopy, and single lead precordial electrocardiograms were obtained on all dogs. The Student t-test was used for statistical comparisons.

## Results

Samples taken from the atrium, right and left ventricle, and papillary muscle of dogs irradiated with 30, 60, and 100 Gy all showed focal area of perivascularitis. No evidence of focal necrosis was detected in any of the irradiated dogs. The electrocardiograms remained normal following irradiation at all of the above doses.

Radiation Sciences Department, Nuclear Science Division, Armed Forces Radiobiology Research Institute, Defense Nuclear Agency, Bethesda, Maryland 20814-5145.

## BILATERAL IRRADIATION FIELD OF THE HEART

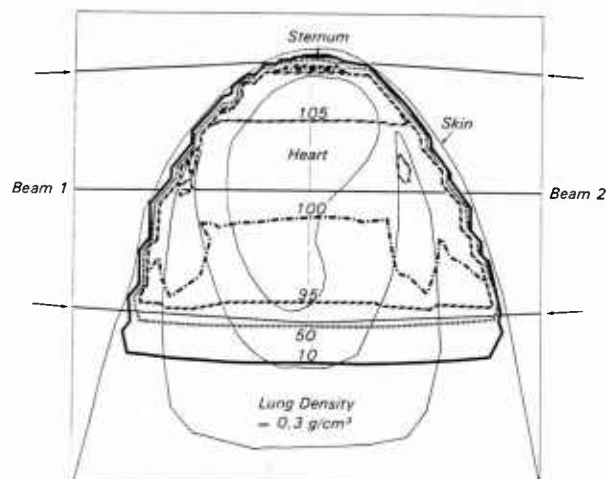


Fig. 1. Isodose Curves of Irradiated Canine Precordium. The intensities are represented as percent of the maximum dose received by the heart.

TABLE I

TISSUE DISTRIBUTION OF Tc-99m (% DOSE/GM TISSUE  $\times 10^3$ , MEAN  $\pm$  SEM)

Region	Radiation Dose		
	0 Gy (N = 5)	30 Gy (N = 4)	60 Gy (N = 12)
Left Atrium	0.4 $\pm$ 0.1	0.6 $\pm$ 0.2	0.9 $\pm$ 0.2
Right Atrium	0.7 $\pm$ 0.1	0.7 $\pm$ 0.2	0.7 $\pm$ 0.0
Left Ventricle	0.5 $\pm$ 0.1	0.3 $\pm$ 0.0	0.7 $\pm$ 0.0
Right Ventricle	0.5 $\pm$ 0.1	0.3 $\pm$ 0.0	0.6 $\pm$ 0.0
Apex	0.5 $\pm$ 0.1	0.4 $\pm$ 0.0	0.7 $\pm$ 0.0
Septum	0.5 $\pm$ 0.1	0.4 $\pm$ 0.0	0.7 $\pm$ 0.0
Papillary Muscle	0.6 $\pm$ 0.2	0.5 $\pm$ 0.1	0.7 $\pm$ 0.0
Aorta	0.9 $\pm$ 0.1	1.1 $\pm$ 0.3	1.3 $\pm$ 0.0
Pulmonary Artery	0.8 $\pm$ 0.1	1.9 $\pm$ 0.3	1.3 $\pm$ 0.2
Left Lung	1.1 $\pm$ 0.2	1.4 $\pm$ 0.0	1.2 $\pm$ 0.1
Right Lung	0.9 $\pm$ 0.2	1.0 $\pm$ 0.1	1.4 $\pm$ 0.0

The Tc-99m pyrophosphate (PYP) scans of the dogs post-irradiation failed to show any evidence of increased uptake of Tc-99m PYP in the cardiac regions. Gamma counts of samples taken from the ventricles, atria, and papillary muscle were not statistically different from the tissue distribution obtained in control dogs (C.F. Table I).

The LVEF's of the dogs receiving 30, 60, and 100 Gy Co-60 photons are shown in Figure 2. The ejection fraction of the dogs receiving 30 Gy decreased gradually until day 57, at which time it was  $38.2 \pm 4.9\%$  compared to the baseline value of  $52.5 \pm 3.4\%$  ( $p < .05$ ). Dogs receiving 60 Gy Co-60 photons showed similar tendency of LVEF decrease on days 7 and 21 post-irradiation reaching the value of  $37.3 \pm 6.2\%$  on day 58. This decrement was not statistically significant. Dogs irradiated with 100 Gy Co-60 did not differ

## Left Ventricular Ejection Fraction in Dogs After Gamma Irradiation to Precordium

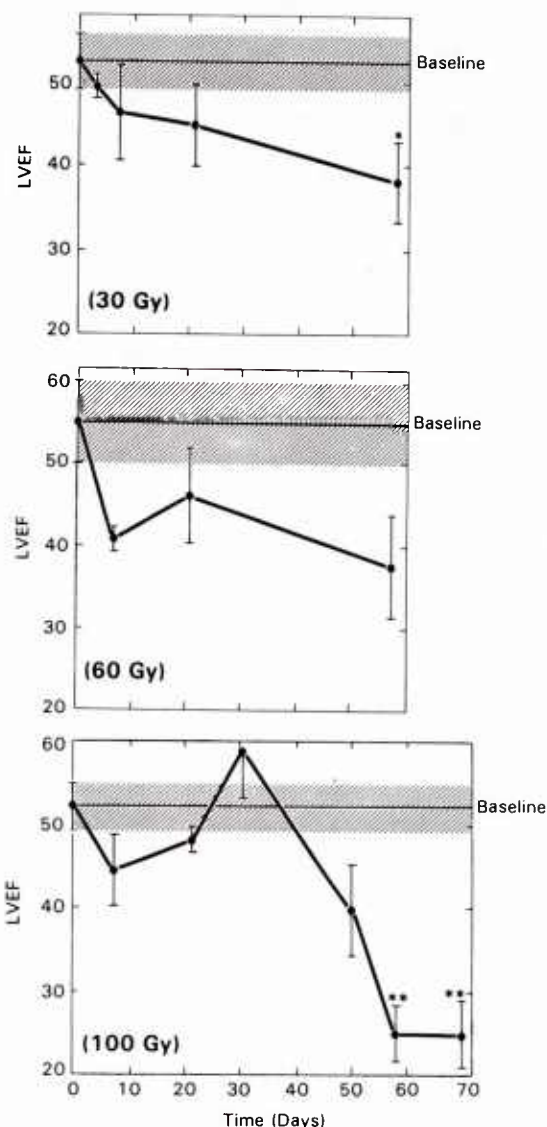


Fig. 2. Left Ventricular Ejection Fraction in Dogs after Gamma Irradiation to the Precordium. (A) 30 Gy. (B) 60 Gy. (C) 100 Gy. LVEF is expressed as percent  $\pm$  S.E.M. \* =  $p < .05$ , \*\* =  $p < .005$ .

from the baseline until day 50 when the LVEF decreased to  $39.8 \pm 5.4\%$  ( $p < .05$ ). Further reductions in LVEF were observed on day 58 ( $25.0 \pm 3.3\%$ ,  $p < .005$ ) and day 70 ( $25.0 \pm 4.2\%$ ,  $p < .005$ ).

## Discussion

Numerous investigators have attempted to correlate the dosage of radiation to the heart with specific pathological lesions. Although Moss et al.<sup>9</sup> reported an absence of detectable lesions in dogs receiving 50–100 Gy photons, Phillips et

al.<sup>4</sup> noted pericarditis and areas of focal necrosis in canine hearts exposed to 50–70 Gy. Fajardo and Stewart<sup>5,10</sup> found a transient diffuse infiltration of neutrophils and histiocytes between six and 48 hours following precordial irradiation of rabbits receiving 20–90 Gy of X-rays. They also noted a subsequent latency period lasting 48 to 70 days during which no pathological lesions were present, followed by the development of progressive myocardial fibrosis. In the range of 135–380 Gy, several authors have reported moderate to severe myocardial necrosis,<sup>5,9,11</sup> and muscle degeneration.<sup>12</sup>

In our work we have examined the time course of the development of cardiac dysfunction in canine hearts following irradiation with Co-60 gamma rays. At each of the three dose levels, which are in the same range of doses used by Fajardo and Stewart,<sup>5</sup> we have observed an absence of a statistically significant decrease in LVEF until the later time periods of 58 to 70 days, when a marked impairment of heart function was observed. It appears that there is a very close correspondence between the duration of this latency period preceding diminution in LVEF and the latency period preceding the onset of fibrosis in irradiated rabbit hearts. Since the cardiac dysfunction is frequently caused by structural defects within the heart, the eventual decrease in LVEF in our canine model could have been due to delayed diffuse fibrosis, especially at the higher dose levels. The fact that significant decrements in LVEF were detected by 58 days suggests that the onset of subtle cardiac dysfunction in patients irradiated for mediastinal neoplasms occurs much earlier than previously reported.<sup>7,8</sup>

### Acknowledgements

I wish to thank J. Stewart, E. Corral, M. Flynn, N.

Flemming, and J. Warrenfeltz for their valuable technical assistance.

### References

1. Karus JS, Stanbury JP: Fatal radiation syndrome from an accidental nuclear excursion. *N Engl J Med* 272:755–761, 1965
2. Warren S: Effect of radiation on normal tissue. VI. Effects of radiation on the cardiovascular system. *Arch Pathol* 34:1070–1079, 1942
3. Stone HL, Bishop VS, Guyton AC: Progressive changes in cardiovascular function after unilateral heart irradiation. *Am J Physiol* 206:289–293, 1964
4. Phillips SJ, Reid JA, Rugh R: Electrocardiographic and pathologic changes after cardiac x-irradiation in dogs. *Am Heart J* 68:524–533, 1964
5. Fajardo LF, Stewart JR: Experimental radiation-induced heart disease: I. Light microscopic studies. *Am J Pathol* 59:299–315, 1970
6. Cohn KE, Stewart JR, Fajardo LF, et al: Heart disease following radiation. *Med* 46:281–298, 1967
7. Gottdiener JS, Katin MJ, Borer JS, et al: Late cardiac effects of therapeutic mediastinal irradiation. *N Eng J Med* 308(10):569–572, 1983
8. Gomez GA, Park JJ, Panahon AM, et al: Heart size and function after radiation therapy to the mediastinum in patient with Hodgkin's disease. *Can Treatment Reports* 67:1099–1103, 1983
9. Moss AJ, Smith DW, Michaelson S, et al: Radiation induced acute myocardial infarction in the dog. University of Rochester Atomic Energy Project UR-625, Rochester, NY 1963, pp 23
10. Stewart JR, Fajardo LF: Radiation-induced heart disease: Clinical and experimental aspects. *Radiol Clin North Amer* 9:511–531, 1971
11. Davis KS: Intrathoracic changes following x-ray treatment: A clinical and experimental study. *Radiology* 44:335, 1945
12. Michaelson SM, Schreiner B, Jr., Hansen CL, Jr., et al: Cardiopulmonary changes in the dog following exposure to x-rays. University of Rochester Atomic Energy Project UR-596, Rochester, NY, 1961, pp 16



# The Effect of Anesthetic, Sedative or Narcotic Drugs on Intrahepatic and Extrahepatic Biliary Kinetics

LTC Asaf Durakovic, MC USA

The purpose of this study was to evaluate hepatobiliary kinetics of Tc-99m-DISIDA in dogs after administration of anesthetic, sedative or narcotic agents. Four groups of six male Beagle dogs were studied as a non-treated control group and after parenteral administration of ketamine (30 mg/kg i.m.), pentobarbital (25 mg/kg i.v.) or morphine (1 mg/Kg i.v.). Each animal was injected with 4 mCi Tc-99m-DISIDA and hepatobiliary scintigraphic studies were obtained using a gamma camera with parallel hole multipurpose collimator and an A<sup>3</sup> MDS computer. We determined: 1) peak activity of Tc-99m-DISIDA in the liver, 2) visualization and peak activity of gallbladder, and 3) intestinal visualization of Tc-99m-DISIDA. Pentobarbital significantly ( $p < 0.01$ ) delayed intestinal visualization of Tc-99m-DISIDA ( $140 \pm 12$  min) compared to untreated controls ( $43 \pm 14$  min); morphine further delayed intestinal visualization ( $237 \pm 28$  min;  $p < 0.01$ ). Neither pentobarbital nor morphine altered intrahepatic kinetics of DISIDA. In contrast, ketamine significantly accelerated both intestinal visualization ( $18 \pm 6$  min;  $p < 0.01$ ) and intrahepatic biliary kinetics compared to control. Thus, two commonly used anesthetics and sedatives (ketamine and pentobarbital) have dramatic and opposite effects on extrahepatic biliary kinetics. Furthermore, ketamine, but not pentobarbital, significantly accelerates intrahepatic biliary kinetics. Finally, as expected, morphine delayed extrahepatic biliary kinetics. Thus, studies of biliary kinetics should be interpreted with caution when measurements are made after administration of anesthetic, sedative or narcotic agents.

MILITARY MEDICINE, 151, 7:368, 1986.

## Introduction

Hepatobiliary dynamic studies with the technetium-99m iminodiacetic acid analogues has superseded and replaced other radioisotope techniques of scintigraphic evaluation of biliary tract.<sup>1</sup> Early studies of hepatobiliary examination with Tc-99m IDA derivatives have proven to be a safe, simple and noninvasive diagnostic procedure<sup>2</sup> with a characteristic excellent hepatic extraction and rapid intrahepatic transit time.<sup>3,4</sup> They are superior to other diagnostic modalities, in visualization of the biliary tree in the presence of even severe cholestasis.<sup>5</sup> This represents a distinct advantage to intravenous cholangiography (IVC) because of frequent adverse reactions<sup>2</sup> with i/v contrast media and failure to visualize biliary tree in the presence of mild or moderate hyperbilirubinemia.<sup>6</sup> Oral cholecystography (OCG) frequently fails to visualize biliary tree and gallbladder in the presence of inflammatory changes, with additional disadvantage of a relatively long time required for a diagnostic study<sup>7</sup> and strong uricosuric properties of oral cholecystographic agents.<sup>8</sup> Transhepatic cholangiography (THC) has been associated with reported cases of pneumothorax<sup>9</sup> requiring a chest-tube drainage.<sup>10</sup> Fine-needle technique of trans-

hepatic cholangiography (FNTC) was reported to cause sepsis in the patients with biliary obstruction with 3.3% of serious complications and 0.14% mortality rate.<sup>11</sup> Similar complication rates were reported in the use of endoscopic retrograde cholangiopancreatography.<sup>12</sup> Ultrasonography (US) by the high-resolution real-time technique or gray-scale method is a non-invasive and inexpensive diagnostic procedure for a rapid evaluation of the biliary tree and gallbladder. This technique is a method of choice for calculous gallbladder disease,<sup>13</sup> and should be used as first imaging procedure in evaluating dilatation of the biliary tract, and in differentiating between surgical and medical jaundice.<sup>14</sup> Computed tomography (CT) is similar in accuracy to ultrasonographic techniques in diagnosis of surgical jaundice, and provides a better visualization of the distal common bile duct.<sup>15</sup> CT technique, provides a superior resolution in diagnosis of space occupying lesions, or hepatic abscesses.<sup>16</sup> Nuclear scintigraphy with Tc-99m-IDA derivatives remains the method of choice in the diagnosis of acute cholecystitis, evaluation of post-cholecystectomy patients, surgical resections, cholestasis, biliary leakage, chronic cholecystitis and dynamic studies of the hepatobiliary tract.<sup>17</sup>

Preoperative management of the patients with an acute biliary colic includes administration of preanesthetic medication such as morphine, barbituric acid derivatives or nonbarbiturate sedative drugs. Administration of morphine in the

Chief, Nuclear Medicine Division, Armed Forces Radiobiology Research Institute, Defense Nuclear Agency, National Naval Medical Center, Bethesda, Maryland 02814-5145.

usual dose of 8–10 mg (l/m) has been widely used to reduce preoperative anxiety and pain of acute abdominal colic in which cases it has been one of the drugs of choice. Its side-effects, including stimulant effect on the smooth muscle may cause spasm of the lower end of the common bile duct (sphincter of Oddi) which may lead to exacerbation of biliary colic due to increased intraductal pressure from normal 20 to 200–300 mm of water. This effect may confuse diagnostic assessment of hepatobiliary kinetics by rentgenographic, manometric or scintigraphic evaluation.<sup>19</sup> Barbiturates in hypnotic doses (Pentobarbital, Secobarbital) have been used in relief of acute abdominal pain mainly due to their central depressant action, decreased intestinal motility and reduced gastric secretion.

It has been reported that administration of phenobarbital (5 mg/kg/day) for five days prior to scintigraphic examination accelerates biliary excretion of IDA derivatives.<sup>19</sup> This property of phenobarbital was utilized in the diagnostic assessment of extrahepatic biliary atresia from neonatal hepatitis, thus overcoming a problem of a slow excretion of tracer in severe cases of neonatal hepatitis. Delayed excretion of Tc-99m IDA derivatives in neonatal jaundice did not permit late imaging studies due to a physical half life of Tc-99m (6.02 hrs.), which was used in advocating I-131 labeled Rose Bengal (I-131  $T_{1/2}$  = 8.2 days), as a method of choice in distinguishing between hepatitis and neonatal biliary atresia.<sup>20</sup> While some authors have postulated the action of phenobarbital on hepatic microsomal enzymes,<sup>21</sup> others have suggested that this accelerated choleresis may be due to the synthesis of the components of canalicular membranes, possible Na<sup>+</sup>-K<sup>+</sup> Adenosine-Triphosphatase. The mechanism of phenobarbital-induced acceleration of bile secretion and canalicular bile flow, still remains an area of controversy.<sup>22</sup>

Non-barbiturate analgesic agents used in hepatobiliary clinical management include several compounds, causing psychologic indifference from the environmental stimuli without a hypnotic effect, thus producing dissociative anesthesia and analgesia. Ketamine (cyclohexylamine) chemically related to hallucinogenic drugs, but without disadvantages of their side effects has been synthesized and used in experimental and clinical medicine.

### Materials and Methods

All experiments were performed on male adult Beagle dogs (10 kg) maintained on standard laboratory Dog Feed and water ad libitum. All animals had an overnight fast for 14 hours prior to scintigraphic studies. Four groups of six dogs were used in the study, as a nontreated control

group and after parenteral administration of Ketamine hydrochloride (Ketaset, Bristol Laboratories, Division of Bristol-Myers Co., Syracuse, New York), Pentobarbital (Nembutal, Abbott Laboratories, Chicago, Illinois) or Morphine Hydrochloride (Wyeth Laboratories, Philadelphia, Pennsylvania). Ketamine was administered by intramuscular injection (30 mg/kg), pentobarbital (25 mg/kg) and morphine (1 mg/kg) by intravenous administration. Each animal was injected intravenously with 4 mCi Tc-99m DISIDA and hepatobiliary dynamic studies were obtained by the use of a gamma camera with a parallel-hole multipurpose collimator and an MDS-A<sup>3</sup> computer. The parameters studied were (1) peak activity of the liver, (2) half-time of the radiopharmaceutical in the liver, (3) visualization of the gallbladder, (4) peak activity of the gallbladder and (5) intestinal visualization of Tc-99m DISIDA. Radionuclide imaging studies were obtained in the anterior view, every 5 minutes after the administration of Tc-99m DISIDA until the intestinal visualization was obtained. All scintigraphic studies were performed immediately after the administration of the radiopharmaceutical.

Results were expressed as a mean-time of the tracer visualization, with a standard error of the mean. Statistical significance was determined by paired t-test.

### Results

Peak activity of Tc-99m DISIDA in the liver was not affected by the administration of either Nembutal or Morphine (Fig. 3). Ketamine administration (Fig. 3) resulted in significantly shorter time of the liver peak activity than control value ( $p < 0.01$ ). Similarly, half-time of the radiopharmaceutical in the hepatic phase was not affected by either Nembutal or Morphine, (Fig. 4) whereas it was significantly decreased ( $p < 0.01$ ) in ketamine treated animals (Fig. 4). Gallbladder vi-

### GALL BLADDER VISUALIZATION (mean $\pm$ S.E.)

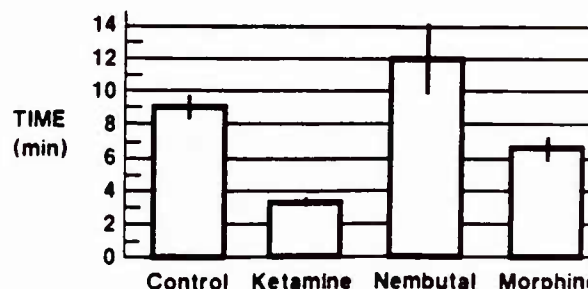


Fig. 1. Gallbladder visualization of Tc-99m DISIDA after the administration of ketamine, numbutal or morphine.

### GALL BLADDER PEAK ACTIVITY (mean $\pm$ S.E.)

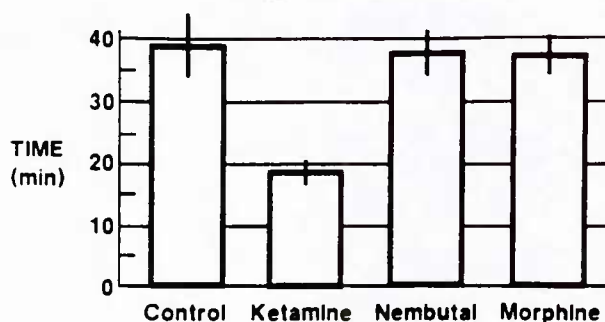


Fig. 2. Gallbladder peak activity of Tc-99m DISIDA.

### LIVER PEAK ACTIVITY (mean $\pm$ S.E.)

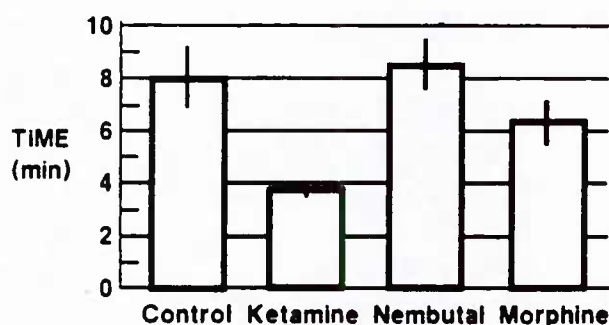


Fig. 3. Liver peak-activity of Tc-99m DISIDA.

### T1/2 OF Tc-99m DISIDA IN THE LIVER (mean $\pm$ S.E.)

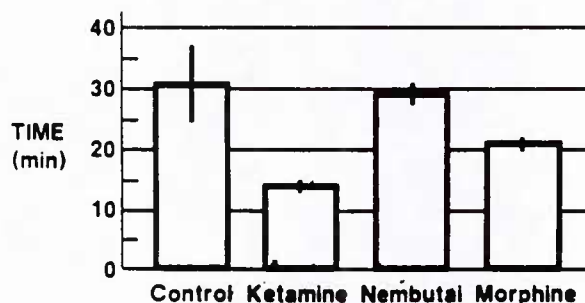


Fig. 4. Tc-99m DISIDA half-time in the liver.

sualization was observed earlier in ketamine treated animals (Table 1, Fig. 1) than in the control, Nembutal or Morphine group ( $p < 0.01$ ). Gallbladder peak activity (Fig. 2) was not different between Nembutal or Morphine treated animals as related to control, whereas gallbladder peak activity was achieved in a significantly shorter time after ketamine injection than in either control, Nembutal or Morphine-treated animals ( $p < 0.01$ ). These results demonstrate that

neither Nembutal nor Morphine altered intrahepatic biliary kinetics, whereas all intrahepatic parameters of Tc-99m DISIDA transit time were significantly accelerated by ketamine administration (Table 1).

Intestinal visualization was observed significantly earlier in ketamine treated animals (Fig. 6) than in control ( $p < 0.01$ ). In contrast, Nembutal treated animals had significantly delayed intestinal visualization longer than three times of the control values (Table 1, Fig. 5). This delay in the intestinal visualization was more dramatic in morphine-treated animals (Fig. 7) where intestinal visualization was observed at over 5 times longer interval as compared to control value ( $p < 0.001$ ).

These results indicate that a single dose of pentobarbital significantly delays intestinal visualization of Tc-99m DISIDA compared to untreated controls ( $p < 0.01$ ). Morphine further delayed intestinal visualization of Tc-99m DISIDA ( $p < 0.001$ ). Neither Nembutal nor Morphine had any effect on intrahepatic biliary kinetics. A dramatic contrast was observed by ketamine administration which accelerated both intrahepatic and extrahepatic biliary kinetics.

## Discussion

Delayed biliary to bowel-transit time of Tc-99m DISIDA after administration of narcotic drugs (morphine, meperidine) has been well documented.<sup>23,24</sup> Therapeutic doses of morphine produce a characteristic increase in the biliary pressure which may exacerbate the pain in patients with a biliary colic, with radiographic and manometric evidence of a spasm at the lower end of the common bile duct (sphincter of Oddi). Our experimental data confirm morphine-induced alterations in extrahepatic phase of the biliary transit time, with a delayed appearance of Tc-99m DISIDA in the duodenum ( $237.5 \pm 28.2$  min.) compared with the control values ( $43.8 \pm 14.0$ ). This, five times longer arrival time of Tc-99m DISIDA in the small intestine without altered liver peak activity and a half-time or gallbladder visualization and peak activity is consistent with the data of the opiate-induced constriction of the extrahepatic biliary ducts.<sup>25</sup>

Effects of barbiturates on the gastrointestinal tract are characterized by a decreased tonus of gastrointestinal musculature and contraction amplitudes. The effect of barbiturates on the hepatobiliary kinetics is still an area of controversy. Phenobarbital has been shown to facilitate choleresis and in patients with cholestasis. Phenobarbital-induced choleresis has not been observed with other barbiturates. The effect of phenobarbital on the canalicular bile flow has



TABLE I

**HEPATOBIILIARY KINETICS OF Tc-99m DISIDA  
IN DOGS AFTER ADMINISTRATION OF  
SEDATIVE, ANESTHETIC OR NARCOTIC AGENTS  
(mean  $\pm$  S.E.)**

n = 6	Control	Ketamine	Nembutal	Morphine
<b>Liver</b>				
Peak Activity	8.0 $\pm$ 1.1	3.7 $\pm$ 0.3	8.5 $\pm$ 0.8	6.3 $\pm$ 0.8
Half-time	31.0 $\pm$ 6.1	13.4 $\pm$ 1.1	29.4 $\pm$ 2.3	20.7 $\pm$ 1.8
<b>Gall Bladder</b>				
Visualization	9.0 $\pm$ 0.9	3.3 $\pm$ 0.2	12.0 $\pm$ 2.1	6.5 $\pm$ 0.6
<b>Gall Bladder</b>				
Peak Activity	38.5 $\pm$ 5.3	18.5 $\pm$ 2.2	36.1 $\pm$ 4.0	37.3 $\pm$ 3.5
<b>Intestinal</b>				
Visualization	43.8 $\pm$ 14.0	18.3 $\pm$ 6.2	140.2 $\pm$ 12.3	237.5 $\pm$ 28.2

**INTESTINAL VISUALIZATION  
(mean  $\pm$  S.E.)**

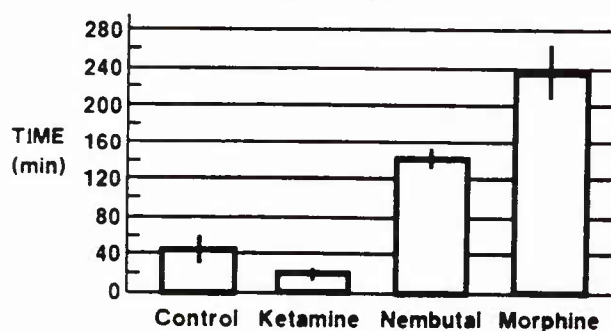
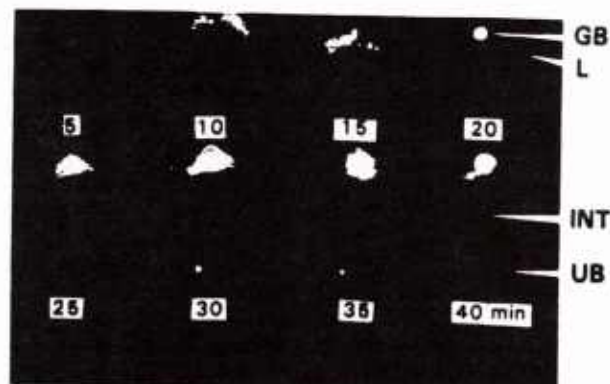


Fig. 5. Intestinal visualization of Tc-99m DISIDA after the administration of ketamine, nembutal or morphine.

been postulated as a consequence of increased bilirubin conjugation and excretion by its action on hepatic microsomal enzymes,<sup>26</sup> but this hypothesis has been challenged by the observations that pentobarbital increases bile flow without inducing hepatic microsomal enzymes, and several enzymes-inducers did not cause an increase in the bile flow.<sup>27</sup>

Recent studies<sup>27,28</sup> support the view that phenobarbital-induced hypercholerisis is principally due to its effect on canalicular membranes likely Na<sup>+</sup>/K<sup>+</sup> ATP-ase, rather than its effect on the activity of the hepatic microsomal enzymes. The controversy over barbiturate action on the hepatobiliary dynamics is still being evaluated.

In our experiments we have not observed any effect of a single therapeutic dose of pentobarbital on intrahepatic biliary kinetics, while extrahepatic biliary flow has been adversely affected by pentobarbital administration with a three-fold delay in the intestinal visualization of Tc-99m DISIDA ( $p < 0.01$ ). These findings are in a sharp contrast with the results of other authors<sup>22</sup> who observed an increase in bile flow 12 hours after a single intraperitoneal injection of phenobarbi-



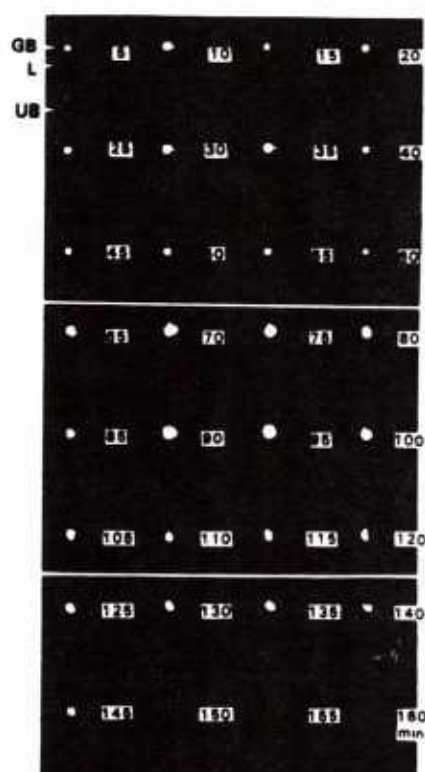
GB = Gallbladder

L = Liver

UB = Urinary Bladder

INT = Intestine

Fig. 6. Anterior sequential images (5 min intervals) of Tc-99m DISIDA in the hepatobiliary system of the control dogs.



GB = Gall Bladder

L = Liver

UB = Urinary Bladder

Fig. 7. Anterior sequential images of delayed gallbladder emptying after morphine administration.

tal, reaching maximum at 18 hours and returning to control values 72 hours after administration.

In our experimental design the transit time of Tc-99m DISIDA was studied in an early phase

after drug administration and this might account for disparate findings on barbiturate hepatobiliary action. Other authors have not observed alterations in biliary excretion of indocyanine green, but did observe enhanced biliary excretion of eosine in phenobarbital-pretreated rats.<sup>29</sup> These data were viewed as an accelerated transport of nonmetabolized compounds from the hepatocytic phase to biliary canaliculi by the effect of phenobarbital. In these experiments the biliary flow was enhanced in phenobarbital pretreated rats as compared to the controls.

In our experiments we were not able to observe any significant effect of a single intravenous therapeutic dose of pentobarbital on intrahepatic biliary transit time of Tc-99m DISIDA. Gallbladder visualization and peak activity of Tc-99m DISIDA were also unchanged after pentobarbital administration, whereas the intestinal visualization was significantly delayed ( $p < 0.01$ ). Our experimental protocol was different from the conventional protocols used in clinical trials of phenobarbital-induced enhancement of biliary excretion of IDA derivatives, where phenobarbital is administered in a dose of 5 mg/kg/day for 5 days prior to scintigraphic examination.<sup>29</sup> Although a difference in the experimental protocols can explain certain disparity in the results of various authors, our findings are in contradiction with the conventional data on barbiturate-induced hepatobiliary alterations and contribute to already existing controversy.

Effects of ketamine on hepatobiliary kinetics have not been reported in the literature. Clinical and experimental use of arylcycloalkylamines in inducing dissociative anesthesia has not been associated with alterations of intrahepatic or extrahepatic biliary kinetics. Our results demonstrate a dramatic effect of ketamine on the processes of both intra and extrahepatic biliary flow. These observations warrant a cautious interpretation of hepatobiliary studies after administration of anesthetic, sedative or narcotic drugs.

### Acknowledgements

The author is indebted to J. D. Stewart, M. E. Corral, J. K. Warrenfeltz, M. E. Flynn and N. L. Fleming for their valuable technical assistance.

### References

1. Taplin GY, Meredith OM, Kade H: The radioactive (131-tagged) rose bengal uptake: Excretion test for liver function using external gamma ray scintillation counting techniques. *J Lab Med* 45:665, 1955
2. Harvey E, Loberg M, Cooper M: 99m-Tc-HIDA—A new radiopharmaceutical for hepatobiliary imaging. *J Nucl Med* 16:553, 1975
3. Nunn AD, Losberg MD, Conley RA, et al: The development of a new cholescintigraphic agent, TC-SQ 26962 using a structure distribution relationship approach. *J Nucl Med* 22:51, 1981
4. Wistow BW, Subramanian G, Van Hebrum RL, et al: An evaluation of 99m-Tc labeled hepatobiliary agents. *J Nucl Med* 18:455, 1977
5. Fonseca C, Rosenthal L, Greenberg D, et al: Differential diagnosis of jaundice by 99m-Tc IDA hepatobiliary imaging. *Clin Nucl Med* 4:135, 1979
6. Scholz FJ, Larsen CR, Wise MD: Intravenous cholangiography: Recurring Concepts. *Seminars in Roentgenology*, XI No. 3, 197, 1976
7. Berk NR, Loeb PM: Pharmacology and physiology of the biliary radiographic contrast materials. *Seminars in Roentgenology*, XI No. 3, 147, 1976
8. Mudge GH: Uricosuric action of cholecystographic agents: A possible factor in nephrotoxicity. *N Engl J Med* 385:929, 1971
9. Flemma RJ, Capp MP, Shingleton WW: Percutaneous transhepatic cholangiography. *Arch Surg* 90:5, 578, 1974
10. Isley JK, Schauble JF: Interpretation of the percutaneous transhepatic cholangiogram. *Am J Roentgenol* 88:772, 1962
11. Peretras R Jr, Chiprut RO, Greenwald RA, et al: Percutaneous transhepatic cholangiograph with the "skinny needle". A rapid, simple and accurate method in the diagnosis of cholestasis. *Ann Intern Med* 86:562, 1977
12. Bilbao MK, Dotter CT, Lee TG, et al: Complications of endoscopic retrograde cholangiopancreatography (ERCP). A study of 10,000 cases. *Gastroenterology* 70:314, 1976
13. Cooperberg PL, Burhenne HJ: Real-time ultrasound: Diagnostic technique of choice in calculous gallbladder disease. *N Engl J Med* 302:1277, 1980
14. Rosenthal L: Nuclear medicine of the biliary tract. In: *Alimentary Tract Radiology* edited by A. R. Margulis, H. J. Burhenne, Vol. 2, 3rd Edition, The C. V. Mosby Co., St. Louis, Toronto, London, 1554, 1983
15. Pedrosa CS: Computed tomography in obstructive jaundice. II. The cause of obstruction. *Radiology* 139:635, 1981
16. Ralls PW: Gray-scale ultrasonography of hepatic amoebic abscesses. *Radiology* 132:125, 1979
17. Weissmann HS, Freeman LM: The biliary tract. In: *Freeman and Johnson's Clinical Radionuclide Imaging*, edited by L. M. Freeman, 3rd Edition, Vol. 2, 879, Grune & Stratton Inc., 1984
18. Bogoch A, Roth JLA, Bochus HL: The effects of morphine on serum amylase and lipase. *Gastroenterology* 26:697, 1954
19. Majd M, Reba R, Altman PR: Effect of phenobarbital on 99m-Tc-IDA scintigraphy in the evaluation of neonatal jaundice. *Seminars in Nucl Med*, XI, No. 3, 194, 1981
20. Collier DB, Traves, Davis M, et al: Simultaneous 99m-Tc-P-Butyl-IDA and 131-I-Rose Bengal scintigraphy in neonatal jaundice. *Radiology* 134:719, 1980
21. Gunucio JJ, Accatino L, Macho AH, et al: Effect of phenobarbital on the ethinyl estradiol-induced cholestasis in the rat. *Gastroenterology* 65:651, 1973
22. Chivrac D, Dumont M, Erlinger S: Lack of parallelism between microsomal enzyme induction and phenobarbital-induced hypercholesterolemia in the rat. *Digestion* 17:516, 1978
23. Murphy P, Solon J, Roseman DL: Narcotic analgesic drugs: Their effect on biliary dynamics. *Arch Surg* 115:710, 1980

24. Dedrick DF, Tanner WE, Bashkin FL: Common bile duct pressure during enflurane anesthesia. Effects of morphine and subsequent naloxone. *Arch Surg* 115:820, 1980
25. Jaffe JH, Martin WR: Opiate analgesics and antagonists. In: Goodman and Gilman's. *The Pharmacological Basis of Therapeutics*, 7th Edition, MacMillan Publishing Co., New York, 491, 1985
26. Yaffe SJ, Juchan MR: Perinatal pharmacology. *Ann Rev Pharmacol* 14:219, 1974
27. Reichen J, Paumgartner G: Relationship between bile flow and Na<sup>+</sup>, K<sup>+</sup> adenosine triphosphatase in liver plasma membranes enriched in bile canaliculi. *J Clin Invest* 60:429, 1977
28. Simon FR, Sutherland E, Acatino L: Stimulation of hepatic sodium and potassium-activated adenosine triphosphatase activity by phenobarbital. Its possible role in regulation of bile flow. *J Clin Invest* 59:849, 1977
29. Fischer E, Varga F, Gregus Z, et al: Bile flow and biliary excretion rate of some organic anions in phenobarbital-pretreated rats. *Digestion* 17:211, 1978

Continued from page 367

### Books Received

**THE AGING BRAIN**, Hanna K. Ulatowska, Ph.D., College Hill Press, \$20.

**OTOLOGIC RADIOLOGY**, Ramon Ruenes, M.D./Antonio De la Cruz, M.D., Macmillan Publishing Company, \$49.95.

**THE FACIAL NERVE**, Mark May, M.D., Thieme-Stratton Inc., \$118.

**GOLDFRANK'S TOXICOLOGIC EMERGENCIES, THIRD EDITION**, Lewis R. Goldfrank, M.D./Neal E. Flomenbaum, M.D./Neal A. Lewin, M.D./Richard S. Weisman, Pharm.D./Mary Ann Howland, Pharm.D./Alan G. Kulberg, M.D., Appleton-Century-Crofts, \$85.

**A CLINICAL MANUAL OF PEDIATRIC INFECTIOUS DISEASE**, Russell W. Steele, M.D., Appleton-Century-Crofts, \$19.95.

**DRUGS FOR THE ELDERLY**, Professor F. I. Caird, WHO Regional Office for Europe, \$25.

**FECHNER'S INTRAOCULAR LENSES**, John J. Alpar, M.D./Paul U. Fechner, M.D., Thieme-Stratton Inc., \$75.

**ATLAS OF PEDIATRIC ORTHOPEDIC RADIOLOGY**, Alan E. Oestreich/Alvin H. Crawford, Thieme-Stratton Inc., \$80.

**DRUG THERAPY IN CARDIOVASCULAR DISEASES**, Adam Schneeweiss, M.D., Lea & Febiger, \$84.50.

**STUDY GUIDE AND SELF-EXAMINATION REVIEW FOR UNDERSTANDING HUMAN BEHAVIOR IN HEALTH AND ILLNESS, THIRD EDITION**, Marita J. Keeling, M.D./Richard C. Simons, M.D., Williams & Wilkins, \$15.95.

**ESTATE PLANNING STRATEGIES FOR PHYSICIANS**, Lawrence Farber, Medical Economics Books, \$19.95.

**HOSPICE, COMPLETE CARE FOR THE TERMINALLY ILL, SECOND EDITION**, Jack M. Zimmerman, M.D., Urban & Schwarzenberg, \$29.50.

**DIAGNOSTIC IMAGING OF THE ACUTELY INJURED PATIENT**, Thomas H. Berquist, M.D., Urban & Schwarzenberg, \$47.50.

**CONTRARY INVESTING**, Richard E. Band, McGraw-Hill Book Company.

**MENTAL DISABILITY IN AMERICA SINCE WORLD WAR II**, Don Martindale/Edith Martindale, Philosophical Library, \$15.

**MEDICAL CONSEQUENCES OF NATURAL DISASTERS**, Lazar Belnin, Springer-Verlag New York, Inc., \$39.

**POCKET REFERENCE FOR MEDICAL INTENSIVE CARE**, Barbara Anne Phillips, M.D., F.C.C.P., An Aspen Publication, \$23.50.

**POCKET ATLAS OF HEMATOLOGY**, Harald Thieml, Thieme-Stratton, Inc., \$15.

**POCKET ATLAS OF RHEUMATOLOGY**, Dieter Wessinghage, Thieme-Stratton Inc., \$15.

**INFECTION IN THE FEMALE, SECOND EDITION**, William J. Ledger, M.D., Lea & Febiger, \$38.50.

**THE PERSISTING OSELER**, Jeremiah A. Burondess, M.D./John P. McGovern, M.D./Charles G. Roland, M.D., University Park Press, \$45.

**EXERCISE PHYSIOLOGY, SECOND EDITION**, William D. McArdle/Frank L. Katch/Victor L. Katch, Lea & Febiger, \$32.50.

**BIOMECHANICAL MEASUREMENT IN ORTHOPAEDIC PRACTICE, OXFORD MEDICAL ENGINEERING SERIES: 5**, Michael Whittle/Derek Harris, Oxford University Press, \$49.95.

**CURRENT MEDICAL DIAGNOSIS & TREATMENT 1986**, Marcus A. Krupp, M.D./Milton J. Chatton, M.D./Lawrence M. Tierney, Jr., M.D., Lange Medical Publications, \$29.50.

**A MANUAL OF PRACTICAL PSYCHIATRY**, P. E. Bebbington/P. D. Hill, Blackwell Scientific Publications.

**A PRACTICAL APPROACH TO ENDOCRINE DISORDERS**, Richard G. Larkins, M.D., Ph.D., FRACP, Williams & Wilkins, \$30.

**DRUG THERAPY IN INFANTS AND CHILDREN WITH CARDIOVASCULAR DISEASES**, Adam Schneeweiss, M.D., Lea & Febiger, \$45.

**OSTEOLOGY FOR RADIOGRAPHERS**, Christina Shillingford, Blackwell Scientific Publications.

**THE CIBA COLLECTION OF MEDICAL ILLUSTRATIONS, VOLUME I, NERVOUS SYSTEM, PART II, NEUROLOGIC AND NEUROMUSCULAR DISORDERS**, Frank H. Netter, M.D., Ciba.

**SURGERY OF THE ESOPHAGUS, SECOND EDITION**, R. W. Postlethwait, M.D., Appleton-Century-Crofts, \$110.



## Effect of gamma radiation on sodium channels in different conformations in neuroblastoma cells

Joseph E. Freschi \* and Arie Moran \*\*

*Physiology Department, Armed Forces Radiobiology Research Institute, Bethesda, MD 20814 (U.S.A.)*

(Received November 11th, 1985)

(Revised manuscript received February 24th, 1986)

**Key words:** Na<sup>+</sup> channel; Batrachotoxin; Ionizing radiation; Gamma radiation; (Neuroblastoma cell)

We studied the dose-response relationship between gamma radiation and batrachotoxin-stimulated sodium influx in neuroblastoma cells in tissue culture. We also tested the hypothesis that changes in sodium channel conformation may alter the radiosensitivity of the channel. We found that gamma radiation inhibited toxin-stimulated <sup>22</sup>Na uptake at doses beyond a threshold of 200–300 Gy. No effects were seen following doses below 100 Gy. This inhibition of sodium permeability was seen when the cells were irradiated with sodium channels in the closed or inactivated, nonconducting states. However, when the channels were in the toxin-opened, conducting state, gamma radiation had no effect at doses up to 2000 Gy. Our results support earlier electrophysiological studies that showed that high doses of ionizing radiation are required to produce a measureable decrease in sodium permeability. In addition, our data suggest that by changing the sodium channel conformation, batrachotoxin appears to alter radiosensitive chemical bonds in the gating or ion-conducting portion of the channel.

### Introduction

Both chemical and physical agents can be useful in demonstrating structural and functional properties of biological membrane macromolecules. In differentiated post-mitotic cells, such as neurons, alterations of proteins by ionizing radiation may have greater immediate functional consequences than does disruption of nucleic acids.

Enzymes vary considerably in the extent to which they are inactivated by ionizing radiation [1], and other protein species are likely to show a similar spectrum of radiosensitivity. A large body of biophysical data exists showing that voltage-sensitive sodium channels are inactivated by ultraviolet radiation at doses that do not affect potassium channel function [2–4]. One might expect that ionizing radiation, comprising a higher energy spectrum than does ultraviolet radiation, may interact with integral membrane proteins in a different way than does ultraviolet radiation. Few studies, however, have used cellular biophysical techniques to study the effects of ionizing radiation on neuronal ion channels. Schwarz and Fox [5] reported that monochromatic X-rays, at doses in excess of 100 Gy (1 Gy = 100 rads), selectively reduce sodium currents in isolated frog sciatic nerves under voltage-clamp. At no dose did they

\* To whom correspondence should be addressed at (present address): Emory University School of Medicine, Department of Neurology, 401 Woodruff Memorial Research Bldg., Atlanta, GA 30322, U.S.A.

\*\* Present address: Unit of Physiology, Faculty of Health Sciences, Ben Gurion University of the Negev, Beersheva, Israel.

Abbreviations: Hepes, 4-(2-hydroxyethyl)-1-piperazineethanesulphonic acid; Tris, 2-amino-2-hydroxymethylpropane-1,3-diol.

find an effect that could underlie neuronal excitation earlier reported as a consequence of ionizing radiation (reviewed in Ref. 6). They suggested that earlier studies reporting an increase in excitability in isolated nerve preparations might be explained by injury currents. Wixon and Hunt [7], studying sodium fluxes in isolated rat brain synaptosomes, found that high-energy electrons decreased sodium uptake beginning at doses as low as 0.5 Gy.

The purpose of these studies was two-fold. First, we wished to establish a dose-response relationship between gamma radiation and sodium influx through voltage-dependent channels to see if the radiosensitivity reported by Wixon and Hunt [7] is present in a whole-cell preparation. Second, we investigated whether the conformational state of the channel could influence its radiosensitivity.

## Materials and Methods

### *Tissue culture*

Cells from the neuroblastoma clone N18 were grown in Dulbecco's modified Eagle medium (GIBCO) supplemented with fetal bovine serum (10% v/v). The cells were seeded into 24-well cluster trays and, after 1 or 2 days, were fed medium plus 0.5% fetal bovine serum (GIBCO) and 1 mM dibutyl cAMP (Sigma). Without this latter treatment, cells grew rapidly to confluency and began to slough from the well bottoms. In the presence of dibutyl cAMP, a drug which induces electrophysiological and morphological differentiation [8], the cells divided more slowly and adhered well to the trays. Cells were then used for experiments after growing in the presence of dibutyl cAMP for 3–4 days, at which time they had formed a confluent, adherent monolayer.

### *Irradiation*

N18 cells in the cluster trays were washed three times with Dulbecco's phosphate-buffered saline (GIBCO, pH 7.3) (normal saline) and allowed to incubate in either normal saline or other test solutions (described in Results) for 30 min prior to and during irradiation. Irradiation was done in the cobalt-60 facility of the Armed Forces Radiobiology Research Institute at constant dose rates whenever possible. For wide dose ranges that included doses below 100 Gy, two different dose

rates were required. The facility contains approx. 100 000 Ci of  $^{60}\text{Co}$  in 104 separate elements. Unilateral dose rates of 0.01–25 Gy/min and bilateral dose rates of 0.08–57 Gy/min can be administered with error bounds of  $\pm 5\%$ . Dosimetry was done using tissue-equivalent ion chambers and thermoluminescent dosimeters within the wells of the plastic trays.

### *Sodium flux assay*

We used, with slight modifications, the methods developed by Catterall [9,10]. Cells were incubated for 60 min at 26°C in toxin-incubation medium comprising 135.4 mM KCl, 50 mM Hepes-Tris (pH 7.4), 5.5 mM glucose, 0.8 mM  $\text{MgSO}_4$ , 1 g/l bovine serum albumin, and various concentrations of batrachotoxin (kindly supplied by Dr. John W. Daly, NIAMDD, National Institutes of Health, Bethesda, MD). This medium allows the toxin to reach equilibrium with the receptor site without altering ion gradients. The toxin-containing medium was removed and the cells were rinsed twice in 15 s using a standard medium consisting of 5.4 mM KCl, 130 mM *N*-methyl-D-glucamine, 50 mM Hepes (pH 7.4), 5.5 mM glucose and 0.8 mM  $\text{MgSO}_4$ . The cells were then incubated for 30 s in assay medium containing 5.4 mM KCl, 120 mM *N*-methylglucamine, 10 mM NaCl, 5 mM ouabain, 50 mM Hepes, 5.5 mM glucose, 0.8 mM  $\text{MgSO}_4$  and 1  $\mu\text{Ci/ml}$   $^{22}\text{NaCl}$ . Because of the very slow dissociation rate of batrachotoxin, it was not necessary to include the toxin in the assay medium [11]. Under these conditions the initial rates are measured with the sodium pump inhibited and the membrane potential held constant. The uptake was then terminated by washing the cells three times with a stop solution containing 163 mM *N*-methyl-D-glucamine, 5 mM Hepes, 5.5 mM glucose, 0.8 mM  $\text{MgSO}_4$ , 1.8 mM  $\text{CaCl}_2$  and 3  $\mu\text{M}$  tetrodotoxin (Sigma). This medium allows the extracellular  $^{22}\text{Na}$  to be removed under conditions that stop influx and prevent efflux of  $^{22}\text{Na}$ . The cells were then solubilized in 0.5% Triton X-100 in water, and the radioactivity of the solubilized cell samples was determined in a liquid scintillation counter.

Proteins were determined from three separate wells per tray using the Bio-Rad protein assay.

Our choice of 30 s uptake assay time was justified by initial experiments that confirmed that the rate of  $^{22}\text{Na}$  influx remained linear for more than 2 min. Nonspecific Na uptake was measured as the uptake in cells without batrachotoxin. This was not significantly different from the uptake in 3  $\mu\text{M}$  tetrodotoxin, without batrachotoxin. The rationale for using the above solutions has been reviewed by Catterall [9].

## Results

### Batrachotoxin-stimulated Na influx

The influx of sodium that resulted from activation of the sodium channels by batrachotoxin was reproducible from experiment to experiment and agreed with the results published by Catterall [9,12]. Fig. 1 shows the effect of batrachotoxin on initial rates of  $^{22}\text{Na}$  uptake in unirradiated cells. The data were pooled from three different experiments performed during a 3-month period. Each experiment was normalized to the response obtained in the presence of 1  $\mu\text{M}$  batrachotoxin. Since the rate of  $^{22}\text{Na}$  influx is directly proportional to the fraction of sodium channels activated by batrachotoxin, as shown by Catterall [12], the relationship between the rate of uptake and toxin concentration can be described by a modified Michaelis-Menten equation of the form:

$$v = V_{\max} (1 + K_m/x)^{-1},$$

where  $v$  is the rate of  $^{22}\text{Na}$  uptake at various toxin concentrations ( $x$ ) and is linearly proportional to the fraction of activated sodium channels;  $V_{\max}$  is the maximum rate of  $^{22}\text{Na}$  uptake at infinite toxin concentration; and  $K_m$  is the toxin concentration at half-maximum uptake and reflects the degree of binding or affinity of the toxin to its binding site. The pooled data in Fig. 1 were well fit by this equation; the calculated values of  $V_{\max}$  and  $K_m$  were 127 nmol/mg protein per min and 0.54  $\mu\text{M}$ , respectively. This toxin dose-response relationship is quantitatively similar to that reported by Catterall [9,12].

### Radiation dose-response relationship

There was considerable variability from experiment to experiment in the degree to which sodium

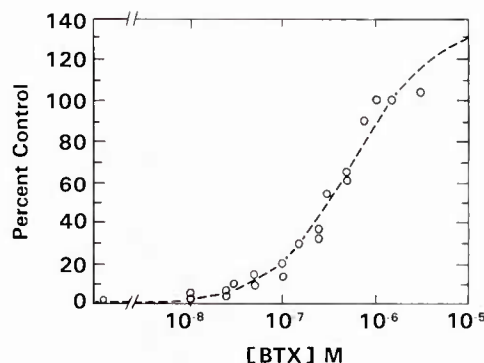


Fig. 1. Dose-response relationship between batrachotoxin concentration and  $^{22}\text{Na}$  uptake. Data were pooled from three separate experiments. The data were normalized as a percent of the response obtained with 1  $\mu\text{M}$  batrachotoxin in each experiment (this point is termed control). Each point is the average of measurements from three separate wells at that batrachotoxin dose. The curves were fitted to a modified Michaelis-Menten equation using a computer-generated least-squares method ( $R^2 = 0.98$ ). The calculated values of the parameters  $V_{\max}$  and  $K_m$  were 127 nmol/mg protein per min and 0.54  $\mu\text{M}$ , respectively (mean value of  $v$  at 1  $\mu\text{M}$  batrachotoxin was 91 nmol/mg protein per min;  $V_{\max}$ , as a percent of the control value, was 137).

influx was inhibited by gamma irradiation. Such experiment-to-experiment variability in the effects of ionizing radiation has been noted by other investigators (e.g., Ref. 13), indicating the importance of using each set of cultures as its own non-irradiated control. Within a given set of cultures used for any one experiment, results from triplicate sets of wells were consistent. No effect of radiation was found at doses below 100 Gy. Consistent reduction in maximum Na influx was seen only after doses above 200 Gy. Fig. 2 shows the results of 10 separate experiments, done on different cultures on different days, from which the data have been pooled. Within each experiment, for a given condition, measurements from three separate wells were averaged. In order to pool these averages, data from a range of radiation doses were combined. This was because all experiments did not share the same radiation dose sequence. Thus, for example, data from radiation doses between 200 and 600 Gy were combined. In these experiments the uptake induced by 1  $\mu\text{M}$  batrachotoxin was compared for various radiation doses from 100 to 3000 Gy. Uptake at doses below 200 Gy was not significantly different from



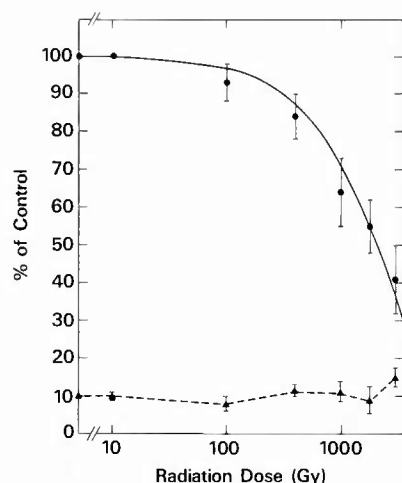


Fig. 2. Dose-response relationship between gamma-radiation and  $^{22}\text{Na}$  uptake. Both the batrachotoxin-stimulated (●) and the non-specific (▲)  $^{22}\text{Na}$  influx at various radiation dose ranges are shown. For batrachotoxin-stimulated flux, data were normalized and pooled from 10 different experiments in the manner described in Fig. 1. In addition, responses obtained over a range of radiation doses were pooled as follows (dose range and number of experimental averages pooled): 0 Gy,  $n = 9$ ; 10–100 Gy,  $n = 4$ ; 200–600 Gy,  $n = 10$ ; 800–1200 Gy,  $n = 7$ ; 1600–2000 Gy,  $n = 5$ ; 2800–3200 Gy,  $n = 5$ . The non-specific uptake, pooled as above (for above dose ranges:  $n = 9, 5, 18, 8, 4, 4$ , respectively), was not normalized and is shown as initial rate of uptake. Each point represents the mean and standard error of the mean of the average uptakes pooled over the indicated dose ranges. The curve for the batrachotoxin-stimulated uptake data is a non-linear least-squares fit to the equation  $y = 100 e^{(-x/k)}$  where  $k$  was computed as 2900 Gy ( $R^2 = 0.99$ ). The radiation dose rates for these and all experiments shown in subsequent figures were similar; between 66 and 67 Gy/min.

control uptake. Thereafter, there was a progressive fall in Na influx as an exponential function of increasing doses of gamma radiation. As shown also in Fig. 2, there was no significant increase in the nonspecific (leak) influx of  $^{22}\text{Na}$  at doses up to 3000 Gy.

It is possible that radiation may alter the affinity of batrachotoxin for the sodium channel. If so, then the apparent inhibition of  $^{22}\text{Na}$  uptake could simply reflect this loss of toxin affinity rather than an effect on the channel. To assess this possibility we examined the dose-response relationship between batrachotoxin and  $^{22}\text{Na}$  uptake at various radiation doses. As shown in the experiment of Fig. 3, the predominant effect of irradiation was a

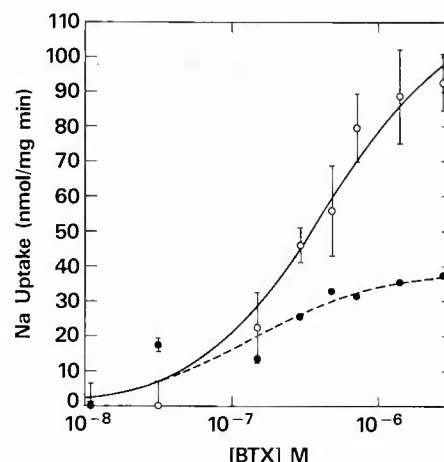


Fig. 3. Dose-response relationship between batrachotoxin concentration and  $^{22}\text{Na}$  influx in irradiated cells (●) and non-irradiated controls (○). Each data point represents the mean and standard error of the mean of measurements from three different wells for each batrachotoxin dose at each radiation dose (0 and 1500 Gy). The curves were fit by the equation described in Fig. 1 ( $R^2 > 0.9$  for each curve). The calculated values of the parameters  $V_{\max}$  and  $K_m$  were respectively: 112 nmol/mg protein per min and  $0.45 \mu\text{M}$  for the control curve; 38 nmol/mg protein per min and  $0.14 \mu\text{M}$  for the data from irradiated cells.

depression of the maximum rate of sodium uptake ( $V_{\max}$ ). The apparent affinity (reflected by  $K_m$ ) of batrachotoxin for its receptor was not reduced; in fact, the curves were consistently shifted to the left.

#### Effect of channel conformation on radiosensitivity

To study the effect of channel conformation on radiosensitivity, N18 cells were irradiated under three conditions. In one group, the cells were irradiated in normal saline. Under this condition, the transmembrane potential is sufficiently negative so that as many as 20% of the sodium channels are in the closed state [14,15]; the rest are inactivated. Cells in the second group were irradiated in high  $\text{K}^+$ -saline (the toxin-incubation medium without batrachotoxin). Under this condition, the cells are depolarized to close to 0 mV transmembrane potential and virtually all the channels are in the inactivated state. The third group was irradiated in the presence of batrachotoxin in the toxin-incubation medium (high  $\text{K}^+$ ). Most of the channels under this condition are activated and remain in the toxin-mod-

ified open state [11,16]. In addition, in some experiments cells were incubated in the presence of 50  $\mu\text{M}$  *N*-bromoacetamide to remove channel inactivation. The drug acts at a different site than does batrachotoxin and inhibits fast inactivation with little effect on activation [17,18]. That *N*-bromoacetamide had an effect from the outside of the membrane was shown in preliminary experiments showing a 40% greater maximum uptake achieved with *N*-bromoacetamide plus batrachotoxin compared with uptake in the presence of batrachotoxin alone. The experiments were done as described in Materials and Methods except that during the 30 min prior to and during irradiation the cells were incubated in either normal saline, high  $\text{K}^+$ -saline, toxin-containing medium with or without *N*-bromoacetamide, or *N*-bromoacetamide in normal saline. Immediately following irradiation, for those cultures not containing batrachotoxin, the uptake assay was carried out as outlined in Methods. For the cultures that contained toxin during irradiation, the toxin-incubation step was omitted, and the uptake assay was

begun immediately following irradiation by washing with the standard medium and proceeding as described in Methods. Thus, for all groups, the toxin-incubation periods were the same.

The effect of radiation on cells with sodium channels in the different conformational states is shown in Fig. 4. The cells in wells containing toxin-free normal saline (data not shown) or toxin-free high  $\text{K}^+$ -saline showed the typical dose-dependent inhibition of  $^{22}\text{Na}$  influx beginning at doses of about 200 Gy. In contrast, the cells in wells containing batrachotoxin during irradiation were remarkably resistant to this effect. No significant inhibition of  $^{22}\text{Na}$  influx was seen up to doses in excess of 2000 Gy. Addition of *N*-bromoacetamide to normal saline during irradiation did not alter the radiosensitivity, and when *N*-bromoacetamide was added to batrachotoxin during irradiation, there was no change in the protection afforded by batrachotoxin alone.

## Discussion

Our results agree with earlier studies that concluded that ionizing radiation causes reduction in neuronal excitability by blocking voltage-sensitive sodium channels. The dose required to reach a threshold effect was of the same order of magnitude as that found using electrophysiological techniques (reviewed in Ref. 6). Thus, Gaffey [19] found that 1600–2000 Gy of 200-kV X-rays were required to attenuate the amplitude of maximal action potentials in isolated frog sciatic nerves. The duration of the compound action potential, however, increased beginning at doses of 100–200 Gy. In the same preparation under voltage clamp, Schwarz and Fox [5] found that a threshold dose of 80 Gy of monochromatic and 100 Gy of continuous-spectrum X-irradiation was required before peak sodium currents were decreased. We could not confirm the results of Wixon and Hunt [7], who found that high-energy electrons decreased the veratridine-stimulated uptake of sodium in rat brain synaptosomes at doses as low as 0.5 Gy. Perhaps this difference in radiosensitivity can be explained by an absence of cellular protective and repair mechanisms in synaptosomes.

What may explain the striking degree of radio-protection afforded by the presence of

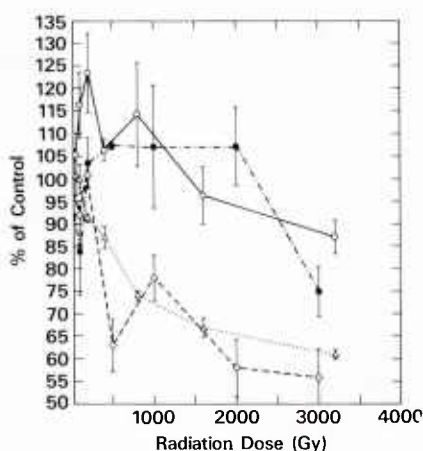


Fig. 4. Dose-response relationship between radiation dose and  $^{22}\text{Na}$  uptake under different incubation conditions. Data were obtained from two separate experiments. Within each experiment cells were irradiated either in the presence of batrachotoxin, 1  $\mu\text{M}$ , in toxin-incubation medium (○, ●), in toxin-incubation medium (high  $\text{K}^+$ ) without batrachotoxin (△, ◇), or in normal saline (not shown). After irradiation, the latter two groups of cells were incubated for 60 min in 1  $\mu\text{M}$  batrachotoxin before uptake assay, as described in Methods. In order to compare the results obtained under these different conditions, data from each group were normalized as a percent of the uptake in the absence of radiation.

batrachotoxin during irradiation? It is unlikely that such a small amount of toxin could have a significant 'quenching' effect. It is possible that irradiation prevents the binding of batrachotoxin to the sodium channel complex. If so, then these experiments would suggest that bound toxin confers protection against subsequent irradiation. We believe, however, that the reduction in sodium uptake is not due to effects on toxin binding. If binding were reduced but not completely blocked, there might be measurable alteration in the affinity of the toxin for its binding site. However, from dose-response curves of batrachotoxin versus  $^{22}\text{Na}$  uptake at different radiation doses, such as those of Fig. 3, we found that the maximum rate of  $^{22}\text{Na}$  uptake ( $V_{\max}$ ) was affected to a much greater extent than was the affinity of batrachotoxin for its binding site (where affinity is inversely related to the parameter ( $K_m$ )). Furthermore, radiation slightly lowered the value of  $K_m$ , thereby suggesting a slight increase rather than a decrease in the affinity of the toxin toward its binding site. If radiation were to prevent the binding of batrachotoxin in an all-or-none manner, there would be a decrease in  $V_{\max}$  indistinguishable from that caused by disruption of the ion-conduction subunits of the sodium channels; but direct measurement of sodium current by voltage-clamp, for which batrachotoxin is not required, showed that radiation specifically inhibits the sodium conductance [5]. We therefore hypothesize that during the conformational change induced by batrachotoxin, certain radiosensitive chemical bonds undergo a transition to a more radioresistant state. In voltage-clamp studies of the effect of ultraviolet radiation on sodium channels of frog nodes of Ranvier, Hof and Fox [20] obtained results similar to our observations. Sodium channels appeared least sensitive to ultraviolet light flashes applied shortly after a depolarizing step from a hyperpolarized prepotential. At that time, most of the sodium channels were in the open, non-inactivated state.

Although specific molecules, such as tyrosine and tryptophan, appear to be involved in ultraviolet photoreaction of the voltage-dependent sodium channel [21], there have been no studies to implicate particular molecular species in the interaction of ionizing radiation with the channel. The inhibition of sodium conductance by ultraviolet

radiation appears sufficiently different from the process by which ionizing radiation interacts with the channel that extrapolation is not possible. For example, Schwarz and Fox [5] found that blocking of sodium conductance by ionizing radiation occurred after a delay of about 10 min and after a threshold dose of 80 Gy. In contrast, the effect of ultraviolet radiation had no threshold and was of immediate onset. This suggests that whereas ultraviolet radiation reacts directly with sensitive molecules of the sodium channel [2–4], ionizing radiation may indirectly react with the channel through multiple photon interactions or the formation of free radicals [5].

Further studies of the radiosensitivity of the sodium channel may lead to an understanding of which chemical structures are involved in the loss of function and may provide additional knowledge of the nature of sodium channel structure-activity relationships.

#### Acknowledgements

We thank Dr. John Daly for providing batrachotoxin, and Dr. Marshall Nirenberg for supplying N18 cells. We are grateful to Drs. Nava Moran and John Pooler for their comments on the manuscript. This research was supported by Armed Forces Radiobiology Research Institute, Defense Nuclear Agency, under Research Work Unit MJ 00013. The views presented in this paper are those of the authors; no endorsement by the Defense Nuclear Agency has been given or should be inferred.

#### References

- 1 Singh, A. and Singh, H. (1982) *Prog. Biophys. Mol. Biol.* 39, 69–107
- 2 Fox, J.M. (1974) *Pfuegers Arch.* 351, 207–229
- 3 Schwarz, W. and Fox, J.M. (1977) *J. Membrane Biol.* 36, 297–310
- 4 Weigle, J.B. and Barchi, R.L. (1980) *J. Neurochem.* 35, 430–435
- 5 Schwarz, W. and Fox, J.M. (1979) *Experientia* 35, 1200–1201
- 6 Kimeldorf, D.J. and Hunt, E.L. (1965) *Ionizing Radiation: Neural Function and Behavior*, pp. 59–108, Academic Press, New York
- 7 Wixon, H.N. and Hunt, W.A. (1983) *Science* 220, 1073–1074



- 8 Chalazonitis, A. and Greene, L.A. (1974) *Brain Res.* 72, 340–345
- 9 Catterall, W.A. (1981) in *Excitable Cells in Tissue Culture* (Nelson, P.G. and Lieberman, M., eds.), pp. 279–317, Plenum Press, New York
- 10 Catterall, W.A. (1982) *Mol. Pharmacol.* 20, 356–362
- 11 Huang, L.Y.M., Moran, N. and Ehrenstein, G. (1982) *Proc. Natl. Acad. Sci. USA* 79, 2082–2085
- 12 Catterall, W.A. (1975) *J. Biol. Chem.* 250, 4053–4059
- 13 Portela, A., Hines, M., Perez, J.C., Brandeis, D., Bourne, G.H., Stewart, P. and Groth, D. (1960) *Exp. Cell Res.* 21, 468–481
- 14 Miyake, M. (1978) *Brain Res.* 143, 349–354
- 15 Moolenaar, W.H. and Spector, I. (1978) *J. Physiol. (Lond.)* 278, 265–286
- 16 Lazdunski, M., Barhani, J., Frelin, C., Hughes, M. and Romey, G. (1983) in *Basic Mechanisms of Neuronal Hyperexcitability* (Jasper, H.H. and van Gelder, N.M., eds.), pp. 171–184, Alan R. Liss, New York
- 17 Oxford, G.S., Wu, C.H. and Narahashi, T. (1978) *J. Gen. Physiol.* 71, 227–247
- 18 Patlak, J. and Horn, R. (1982) *J. Gen. Physiol.* 79, 333–351
- 19 Gaffey, C.T. (1971) *Radiat. Res.* 45, 311–325
- 20 Hof, D. and Fox, J.M. (1983) *J. Membrane Biol.* 71, 31–37
- 21 Oxford, G.S. and Pooler, J.P. (1975) *J. Membrane Biol.* 20, 13–30

## EFFECTS OF ETHANOL EXPOSURE ON BRAIN SODIUM CHANNELS

Walter A. Hunt and Michael J. Mullin  
Behavioral Sciences Department  
Armed Forces Radiobiology Research Institute  
Bethesda, Maryland 20814-5145

### Summary

Ethanol, like other general anesthetics, probably acts through an interaction with excitable membranes. When ethanol is present in membranes, the lipid structure of membranes is disordered. This effect can lead to alterations in functional entities that require a particular lipid environment. Sodium channels, requiring such an environment, have been studied for their sensitivity to ethanol. In synaptosomes, ethanol in vitro reversibly inhibits sodium influx stimulated by batrachotoxin or veratridine in concentrations equivalent to those found in animals during ethanol intoxication. Only the maximum stimulation of the toxins is altered by ethanol. The potencies of aliphatic alcohols are directly related to their lipid solubilities. Acute and chronic ethanol administration reduces the effectiveness of ethanol in vitro. This tolerance dissipates after a single dose of ethanol as it is eliminated from the body. However, after 4 days of ethanol treatment, the tolerance lasts for over 20 days. These data suggest that ethanol might disrupt one of the basic processes of neural function by acting directly on the environment of the sodium channel. The channel appears to be able to adapt to the presence of ethanol through the induction of tolerance.

The site of action of aliphatic alcohols, like other general anesthetics, is believed to be electrically excitable membranes in the brain (11). About the turn of the century, studies with alcohols were undertaken that led to the formulation of the Meyer-Overton principle that states that the potencies of general anesthetics are directly proportional to their lipid solubility. This is a reasonable concept especially for alcohols since they have simple molecular structures that probably preclude them from interacting with specific receptors on membranes and have both lipophilic and hydrophilic properties.

Because of their lipophilic properties, alcohols dissolve into membranes and disorder the lipid structure. Lipid disordering has been demonstrated by both electron paramagnetic resonance spectroscopy and fluorescence spectrometry (5, 9). Alcohols have their greatest disordering effect deep in the membrane where it is most lipophilic. If the temperature of a membrane preparation is reduced or cholesterol is added to the membrane to make it more rigid, the disordering effect of alcohols is less (6). Since the lipid in membranes is largely structural, the significance of alcohol-induced disordering is probably related to the processes that require a lipid environment for optimal activity.

Neuronal membranes contain functional entities that control the

excitability of the cell, including ion channels and various enzymes. Action potentials are generated and propagated through the movement of ions across the membrane. Based on the classic experiments of Hodgkin and Huxley (10), the action potential is initiated by an initial depolarization of the membrane involving the inward movement of sodium ions. These ions move through specific channels that are gated and open and close in response to physiological conditions.

Electrophysiological experiments, mostly in invertebrates, have suggested that ethanol inhibits the transient inward movement of sodium ions and reduces the height of the action potential in neurons that are stimulated (1, 2, 12). However, high concentrations of alcohols are required to induce these effects. However, when electrically stimulated brain slices are incubated with 105 mM ethanol, uptake of sodium into intracellular spaces is reduced (17).

Over the last few years the molecular properties of sodium channels have been extensively characterized in synaptosomes and cultured neurons. With this information it has been possible to examine the direct interactions of alcohols, as well as other drugs, with these channels. The sodium channel is a glycoprotein with multiple polypeptide subunits and traverses the neuronal membrane (4). Through experiments with purified sodium channels reconstituted in artificial membranes, it has been found that the channels have an absolute requirement for the presence of lipid for normal activity (16).

Three functional sites have been identified based on the actions of a number of neurotoxins derived from a variety of animal and plant sources (3). Site I binds water-soluble drugs such as tetrodotoxin and saxitoxin that block the inward movement of sodium into neurons and is located on the membrane surface. Site II binds lipid-soluble drugs such as batrachotoxin and veratridine that activate sodium channels and promote the inward movement of sodium. These sites are located in the lipid core of the membrane. And Site III binds drugs such as scorpion venom and sea anemone toxin that facilitate the actions of the drugs that act on Site II but have no activity alone.

Using a synaptosomal preparation all of the functional properties of the sodium channel can be determined through measurements of radiolabeled sodium influx. The synaptosomes are preincubated in sodium-free medium with or without added alcohols, then stimulated with batrachotoxin or veratridine. Blanks include tetrodotoxin to block the actions of the neurotoxins and measure passive movements of sodium.

Ethanol in vitro reversibly inhibits sodium uptake stimulated by both batrachotoxin and veratridine in a dose-dependent manner (7, 13, 14). No effect of ethanol on passive sodium uptake can be seen. The IC<sub>50</sub> values are 583 mM for batrachotoxin and 345 mM for veratridine. The concentrations required to inhibit uptake (50-600 mM) parallel those associated with behavioral intoxication. In addition, the effect could be observed only when the duration of the incubation is 5 sec or less. When different short-chain aliphatic alcohols are tested, their potencies to inhibit neurotoxin-stimulated uptake are directly related to their lipid solubilities.

Ethanol inhibits only the maximum sodium uptake induced by different concentrations of neurotoxins (14). There is no apparent competition of ethanol for neurotoxin binding sites. The specificity of the action of ethanol on the sodium channel was examined by measuring the effect of ethanol on saxitoxin binding, as an indicator of Site I function and enhanced neurotoxin-stimulated sodium uptake in the presence of scorpion toxin, as an indicator of



Site III function. Concentrations of ethanol as high as 400 mM have no effect on saxitoxin binding or the ability of scorpion toxin to enhance neurotoxin-stimulated sodium uptake (14, 15). This suggests that ethanol acts at Site II in the lipid core of the membrane where ethanol has its greatest disordering effect. Studies using batrachotoxin binding to assess Site II function are currently underway in our laboratory.

The responsiveness of the sodium channel to acute and chronic ethanol administration in vivo has been examined (15). Single doses of ethanol induce, in a dose-dependent manner, a rapidly developing tolerance to ethanol added to synaptosomes in vitro, although no effect is found in neurotoxin-stimulated sodium uptake in the absence of added ethanol. This tolerance is found only while ethanol is present in the blood. After a 4.5 g/kg oral dose of ethanol, the maximum tolerance is observed 6 hours after treatment, but by the time the ethanol is eliminated, in about 24 hours, the tolerance has dissipated.

When animals are rendered behaviorally tolerant and physically dependent on ethanol, sodium channel function is also altered. After four days of ethanol administration, neurotoxin-stimulated sodium uptake in the absence of added ethanol is reduced for at least 5 days after withdrawal. By 10 days, uptake has returned to control values. When ethanol is added to the synaptosomal preparation derived from tolerant and dependent animals, significant tolerance is seen to the usual inhibitory effect of ethanol. Unlike that observed after a single dose of ethanol, the tolerance lasts over 20 days and dissipates by 35 days after withdrawal.

Ethanol can clearly inhibit neurotoxin-stimulated sodium uptake into synaptosomes, an effect that can be modified by animals having prior exposure to ethanol. Because this inhibitory effect of ethanol is observed at concentrations in vitro equivalent to those found in vivo after ethanol administration, it is tempting to conclude that alterations in sodium uptake accompanying neuronal depolarization play a role in the depressant effect of ethanol. This may reflect a reduction in the number of functional sodium channels.

As stated earlier, ethanol disorders the lipid structure of excitable membranes and the lipid environment is important to the normal functioning of the sodium channel. Recent experiments have found that there is a direct correlation between the disordering effect of various membrane perturbing agents and their ability to inhibit neurotoxin-stimulated sodium uptake (8). Consequently, the presence of ethanol in membranes may disturb the microenvironment of the sodium channel in a way that prevents the channel from opening and closing at the proper times. This may impair the ability of the neuron to generate effective action potentials.

The role of sodium channels on the development of tolerance and physical dependence is not clear. Acute and chronic ethanol treatment can alter the responsiveness of the channels to ethanol added in vitro. Whether this action of ethanol treatment contributes to behavioral tolerance or dependence will await further research.

#### References

1. Armstrong, C. M. and L. Binstock. The effects of several alcohols on the properties of the squid giant axon. *J. Gen. Physiol.* 48:265-277, 1964.
2. Bergmann, M. C., M. W. Klee, and D. S. Faber. Different sensitivities to

- ethanol of early transient voltage clamp currents of Aplysia neurons. *Pflug. Arch. Physiol.* 348:139-153, 1974.
3. Catterall, W. A. Neurotoxins and that act on voltage-sensitive sodium channels in excitable membranes. *Annu. Rev. Pharmacol. Toxicol.* 20:15-43, 1980.
  4. Catterall, W. A. The emerging molecular view of the sodium channel. *Trends Neurosci.* 5:303-306, 1982.
  5. Chin, J. H. and D. B. Goldstein. Effects of low concentrations of ethanol of the fluidity of spin-labeled erythrocytes and brain membranes. *Mol. Pharmacol.* 13:435-441, 1977.
  6. Chin, J. H. and D. B. Goldstein. Membrane-disordering action of ethanol: Variation with membrane cholesterol content and depth of the spin label probe. *Mol. Pharmacol.* 19:425-431, 1981.
  7. Harris, R. A. and P. Bruno. Effects of ethanol and other intoxicant-anesthetics on voltage-dependent sodium channels of brain synaptosomes. *J. Pharmacol. Exp. Ther.* 232:401-406, 1985.
  8. Harris, R. A. and P. Bruno. Membrane disordering by anesthetic drugs: Relationship to synaptosomal sodium and calcium fluxes. *J. Neurochem.* 44:1274-1281, 1985.
  9. Harris, R. A. and F. Schroeder. Ethanol and the physical properties of brain membranes: Fluorescence properties. *Mol. Pharmacol.* 20:128-137, 1981.
  10. Hodgkin, A. L. and A. F. Huxley. A quantitative description of membrane current and its application to conduction and excitation in nerve. *J. Physiol. (London)* 117:550-544, 1952.
  11. Hunt, W. A. *Alcohol and Biological Membranes*. New York: Guilford Press, 1985.
  12. Moore, J. W., W. Ulbricht, and M. Takata. Effect of ethanol on the sodium and potassium conductances of the squid giant axon membrane. *J. Gen. Physiol.* 48:279-295, 1964.
  13. Mullin, M. J. and W. A. Hunt. Ethanol inhibits veratridine-stimulated sodium uptake in synaptosomes. *Life Sci.* 34:287-292, 1984.
  14. Mullin, M. J. and W. A. Hunt. Actions of ethanol on voltage-sensitive sodium channels: Effects on neurotoxin-stimulated sodium uptake in synaptosomes. *J. Pharmacol. Exp. Ther.* 232:413-419, 1985.
  15. Mullin, M. J., W. A. Hunt, T. K. Dalton, and E. Majchrowicz. Alterations in neurotoxin-stimulated  $^{22}\text{Na}^+$  influx in synaptosomes after acute and chronic ethanol treatment. *Fed. Proc.* 44:4843, 1985.
  16. Tamkun, M. M., J. A. Talvenheimo, and W. A. Catterall. The sodium channel from rat brain: Reconstitution of neurotoxin-activated ion flux and scorpion toxin binding from purified components. *J. Biol. Chem.* 259:1676-1688, 1984.
  17. Wallgren, H., P. Nikander, P. von Boguslawsky, and J. Linkola. Effects of ethanol, tert. butanol, and clomethiazole, on net movements of sodium and potassium in electrically stimulated cerebral tissue. *Acta Physiol. Scand.* 9:83-93, 1974.

## Ionizing Radiation Alters the Properties of Sodium Channels in Rat Brain Synaptosomes

Michael J. Mullin, Walter A. Hunt, and \*R. Adron Harris

*Behavioral Sciences Department, Armed Forces Radiobiology Research Institute, Bethesda, Maryland; and*

*\*Department of Pharmacology, School of Medicine, University of Colorado, Denver, Colorado, U.S.A.*

**Abstract:** The effect of ionizing radiation on neuronal membrane function was assessed by measurement of neurotoxin-stimulated  $^{22}\text{Na}^+$  uptake by rat brain synaptosomes. High-energy electrons and  $\gamma$  photons were equally effective in reducing the maximal uptake of  $^{22}\text{Na}^+$  with no significant change in the affinity of veratridine for its binding site in the channel. Ionizing radiation reduced the veratridine-stimulated uptake at the earliest times measured (3 and 5 s), when the rate of uptake was greatest. Batrachotoxin-stimulated  $^{22}\text{Na}^+$  uptake was less sensitive to inhibition by radiation. The binding of [ $^3\text{H}$ ]saxitoxin to its receptor in the sodium channel was unaffected by exposure to ionizing radiation. The effect of ionizing radiation on the lipid order of rat brain synaptic plasma membranes was measured by the fluores-

cence polarization of the molecular probes 1,6-diphenyl-1,3,5-hexatriene and 1-[4-(trimethylammonium)phenyl]-6-phenyl-1,3,5-hexatriene. A dose of radiation that reduced the veratridine-stimulated uptake of  $^{22}\text{Na}^+$  had no effect on the fluorescence polarization of either probe. These results demonstrate an inhibitory effect of ionizing radiation on the voltage-sensitive sodium channels in rat brain synaptosomes. This effect of radiation is not dependent on changes in the order of membrane lipids. **Key Words:** Ionizing radiation—Sodium channels—Membrane fluidity—Fluorescent probes—Neuronal membranes. Mullin M. J. et al. Ionizing radiation alters the properties of sodium channels in rat brain synaptosomes. *J. Neurochem.* 47, 489–495 (1986).

Exposure to ionizing radiation has a complex effect on the CNS, an effect that depends on the dose delivered and time elapsed after radiation exposure. In the whole animal, exposure to low to moderate doses (50–400 rad) of radiation produces a conditioned taste aversion in rats (Smith, 1971; Rabin et al., 1982), a reduction in the threshold for electrically induced seizures (Rosenthal and Timiras, 1961; Pollack and Timiras, 1964; Sherwood et al., 1967), and changes in the electroencephalogram of rabbits (Minamisawa and Tsuchiza, 1977). Doses of radiation in the range of 1,000–1,500 rad produce arousal in rats (Kimeldorf and Hunt, 1965) and increased locomotor activity in mice (Mickley et al., 1983a,b). Radiation doses of >10,000 rad depress the CNS, and the irradiated animals demonstrate lethargy, disorientation, ataxia, reduced locomotor activity, and an inability to avoid shock

(Casarett and Comar, 1973; Mickley and Teitelbaum, 1978; Bogo, 1984).

The mechanisms of radiation-induced changes in CNS function are largely unknown. Neurochemical studies have demonstrated a reduction in brain cyclic nucleotide levels (Hunt and Dalton, 1980) and increases in high-affinity choline uptake and  $\text{K}^+$ -stimulated dopamine release (Hunt et al., 1979) after exposure to 5,000–10,000 rad. In addition,  $\beta$ -endorphin like-immunoreactivity is reduced in the brain after 1,500 rad (Mickley et al., 1983a,b).

Electrophysiological studies of the effects of ionizing radiation have yielded conflicting results. Several studies have reported a temporary enhancement of neuronal excitability at doses of <10,000 rad (Bachofer and Gautereaux, 1960; Bachofer, 1962), whereas others have reported no change in the amplitude or rate of rise of the action potential,

Received October 18, 1985; accepted February 14, 1986.

Address correspondence and reprint requests to Dr. M. J. Mullin at Behavioral Sciences Department, Armed Forces Radiobiology Research Institute, Bethesda, MD 20814-5145, U.S.A.

**Abbreviations used:** BTX, batrachotoxin; DPH, 1,6-diphenyl-1,3,5-hexatriene; HEPES, *N*-2-hydroxyethylpiperazine-*N'*-2-ethanesulfonic acid; SPM-2, synaptic plasma membranes; STX, saxitoxin; SV, scorpion venom; TMA-DPH, 1-[4-(trimethylammonium)phenyl]-6-phenyl-1,3,5-hexatriene; TTX, tetrodotoxin.



conduction velocity, or membrane resistance at radiation doses of <10,000 rad (Gerstner and Orth, 1950; Gasteiger and Campbell, 1962). Higher doses of radiation have usually been reported to reduce neuronal excitability.

In many cells, DNA has been shown to be the primary target for ionizing radiation. However, in the mature, postmitotic CNS, radiation-induced changes in the structure and function of neuronal membranes may be the site of action. The interaction of ionizing radiation with water is known to produce a variety of reactive products, including hydroxyl and hydrogen radicals, hydrated electrons, hydrogen peroxide, and superoxide radicals (Okada, 1970). The reactive products of water can then interact with membrane lipids or proteins, resulting in lipid peroxidation or oxidation of sulfhydryl groups (Edwards et al., 1984). Structural modification of membrane components would be expected to cause changes in the functional properties of membranes.

We have examined the effect of ionizing radiation on the properties of voltage-sensitive sodium channels in rat brain synaptosomes. Neuronal sodium channels were studied, because they are believed to be involved in the control of neuronal excitability (Catterall, 1984) and because the functional properties of these channels are sensitive to perturbations of the lipid and protein components in the membrane microenvironment (Baumgold, 1980; Saum et al., 1981; Harris and Bruno, 1985a).

## MATERIALS AND METHODS

### Materials

Scorpion venom (SV; *Leiurus quinquestratus*), tetrodotoxin (TTX), and veratridine were purchased from Sigma Chemical Co. (St. Louis, MO, U.S.A.). Batrachotoxin (BTX) was kindly supplied by Dr. John Daly (Laboratory of Bioorganic Chemistry, National Institute of Arthritis, Metabolism, and Digestive Diseases, National Institutes of Health, Bethesda, MD, U.S.A.). Carrier-free  $^{22}\text{NaCl}$  was obtained from New England Nuclear (Boston, MA, U.S.A.); [ $^3\text{H}$ ]saxitoxin (STX) with a specific activity of 9.3 Ci/mmol and a radiochemical purity of 50% was a generous gift from Dr. Stephen Davio (Pathophysiology Division, U.S. Army Research Institute of Infectious Diseases, Fort Detrick, Frederick, MD, U.S.A.). Fluorescent probes were obtained from Molecular Probes, Inc. (Junction City, OR, U.S.A.). All other chemicals were obtained from commercial sources and were of analytical grade.

### Animals

Male Sprague-Dawley rats weighing 200–300 g (Charles River Breeding Laboratories, Inc., Wilmington, MA, U.S.A.) were housed two per cage with free access to water and standard laboratory chow.

### Measurement of synaptosomal sodium uptake

A crude synaptosomal ( $P_2$ ) fraction was prepared from rat brain after removal of the cerebellum and brainstem

by a modification of the method of Gray and Whittaker (1962). The final pellet was resuspended in ice-cold incubation buffer (8–10 ml/brain) containing 5.4 mM KCl, 0.8 mM  $\text{MgSO}_4$ , 5.5 mM glucose, 130 mM choline chloride, and 50 mM *N*-2-hydroxyethyl-piperazine-*N'*-2-ethanesulfonic acid (HEPES), with the pH adjusted to 7.4 with Tris base. The uptake of  $^{22}\text{Na}^+$  was measured by a slight modification of the method of Tamkun and Catterall (1981). Aliquots (50  $\mu\text{l}$ ) of the synaptosomal suspension were incubated for 2 min at 36°C. BTX or veratridine was then added, and the incubation was continued for an additional 10 min. The samples were then diluted with 300  $\mu\text{l}$  of uptake solution containing 5.4 mM KCl, 0.8 mM  $\text{MgSO}_4$ , 5.5 mM glucose, 128 mM choline chloride, 5 mM ouabain, 2 mM NaCl, 1.3  $\mu\text{Ci}$  of  $^{22}\text{NaCl}/\text{ml}$ , the indicated concentration of BTX or veratridine, and 50 mM HEPES (pH adjusted to 7.4 with Tris). After a 5-s incubation (except where noted), uptake was terminated by addition of 3 ml of ice-cold wash solution containing 163 mM choline chloride, 0.8 mM  $\text{MgSO}_4$ , 1.7 mM  $\text{CaCl}_2$ , 1 mg/ml of bovine serum albumin, and 5 mM HEPES (pH adjusted to 7.4 with Tris). The mixture was rapidly filtered under vacuum through a 0.45 cellulose filter with 0.45- $\mu\text{m}$  pores (041255; Amicon), and the filters were washed twice with 3 ml of wash solution. Radioactivity was determined by liquid scintillation spectrometry. The data are presented as corrected specific uptake (Mullin and Hunt, 1984, 1985) after subtraction of nonspecific uptake (BTX or veratridine plus TTX, 1  $\mu\text{M}$  present in incubation and uptake buffers).

### [ $^3\text{H}$ ]STX binding assay

[ $^3\text{H}$ ]STX binding was measured using a slight modification of the method of Krueger et al. (1979). A synaptosomal ( $P_2$ ) pellet was prepared as described above, but the final pellet was resuspended in an incubation buffer containing 140 mM NaCl and 20 mM HEPES (pH 7.5 at 4°C). An aliquot (200–300  $\mu\text{g}$  of protein) of synaptosomes was mixed with various concentrations of [ $^3\text{H}$ ]STX (0.10–10 nM) in a final volume of 1.5 ml, and the samples were incubated for 60 min at 0–2°C. Following incubation, the samples were diluted with 5 ml of ice-cold incubation buffer and rapidly filtered through glass fiber filters (GF/F; Whatman) under vacuum. The filters were washed twice with 5 ml of ice-cold incubation buffer, and the radioactivity remaining on the filter was determined by liquid scintillation spectrometry. Nonspecific binding was measured in the presence of 10  $\mu\text{M}$  TTX. The  $K_D$  and  $B_{\text{max}}$  values were calculated according to the procedure of Scatchard (1949).

### Fluorescence measurements

A HH-1 T-format polarization spectrofluorimeter (BHL Associates, Burlingame, CA, U.S.A.) with fixed excitation and emission polarization filters was used to measure fluorescence intensity parallel and perpendicular to the polarization phase of the exciting light (Harris and Schroeder, 1982). Polarization of fluorescence and intensity of fluorescence were calculated by an on-line microprocessor. Similar instrumentation is presented in more detail by Johnson et al. (1979). The fluorescent probes 1,6-diphenyl-1,3,5-hexatriene (DPH) and 1-[4-(trimethylammonium)phenyl]-6-phenyl-1,3,5-hexatriene (TMA-DPH) were used. The excitation wavelength was 362 nm, a 03FGG001 filter (Melles Griot, Irvine, CA,

U.S.A.) was used in the excitation beam, and KV389 filters (Schott Optical, Duryea, PA, U.S.A.) were used for emission. Cuvette temperature was maintained by a circulating water bath and monitored continuously by a thermocouple inserted into the cuvette to a level just above the light beam.

Synaptic plasma membrane (SPM-2) preparations were used for all fluorescence measurements. The cerebellum and brainstem were removed from the brain, and SPM-2 preparations were separated by Ficoll and sucrose density centrifugation as described by Harris and Schroeder (1982). Membranes were resuspended in phosphate-buffered saline (8 g/L of NaCl, 0.2 g/L of KCl, 0.2 g/L of  $\text{KH}_2\text{PO}_4$ , 1.15 g/L of  $\text{Na}_2\text{HPO}_4 \cdot 7 \text{H}_2\text{O}$ , and 0.48 g/L of HEPES, pH 7.4) at a concentration of 1–3 mg of protein/ml and were frozen and kept at  $-80^\circ\text{C}$  before analysis. SPM-2 preparations were diluted to 0.05 mg of protein/ml, and fluorescent probes were incorporated at  $35^\circ\text{C}$  for 15 min with frequent vortex mixing. DPH was dissolved in tetrahydrofuran, and TMA-DPH was dissolved in tetrahydrofuran/water (1:1 vol/vol). The probes were added in a volume of 0.3–0.5  $\mu\text{l}$ /ml to give a probe concentration of 40–80 ng/ml. Control levels of fluorescence (baseline) were determined at 20 or  $35^\circ\text{C}$ . In certain cases, an aliquot (1–10  $\mu\text{l}$ ) of ethanol was added to the cuvette, and fluorescence was determined 3–5 min later.

#### Irradiation procedures

The synaptosomes or SPM-2 preparations were placed in glass test tubes in a Plexiglas ice bath and were irradiated with 18.5 MeV electrons from the Armed Forces Radiobiology Research Institute linear accelerator. Pulse duration was 4  $\mu\text{s}$ , and pulses were delivered at a rate of 15/s. Dose rate was  $\sim 12$  rad/pulse. Synaptosomes were exposed to  $\gamma$  radiation using a  $^{60}\text{Co}$  source at a dose rate of 100 rad/min (for the 100-rad dose only) or 7,600 rad/min. Dosimetry was performed using a 0.05- $\text{cm}^3$  tissue equivalent ion chamber whose calibration is traceable to the National Bureau of Standards. The ion chamber was placed in a glass test tube inside the Plexiglas ice bath during dosimetry measurements.

#### Miscellaneous methods

Protein content was determined by the method of Lowry et al. (1951), using bovine serum albumin as the standard. Data are presented as mean  $\pm$  SEM values. In each experiment, triplicate samples were prepared for each concentration of toxin. The number of experiments is given in the legend of each table and figure. Statistical analysis was performed using Student's *t* test. Multiple comparisons with a control were done by analysis of variance and Dunnett's test (Dunnett, 1964).

## RESULTS

#### Ion flux studies

Incubation of synaptosomes with the alkaloid toxin veratridine caused a concentration-dependent increase in synaptosomal  $^{22}\text{Na}^+$  uptake. The effects of exposure to high-energy electrons on  $^{22}\text{Na}^+$  uptake are shown in Fig. 1. Irradiation with doses of 100, 1,000, and 10,000 rad caused a dose-dependent inhibition of veratridine-stimulated  $^{22}\text{Na}^+$  uptake. The uptake of  $^{22}\text{Na}^+$  uptake into irradiated synap-

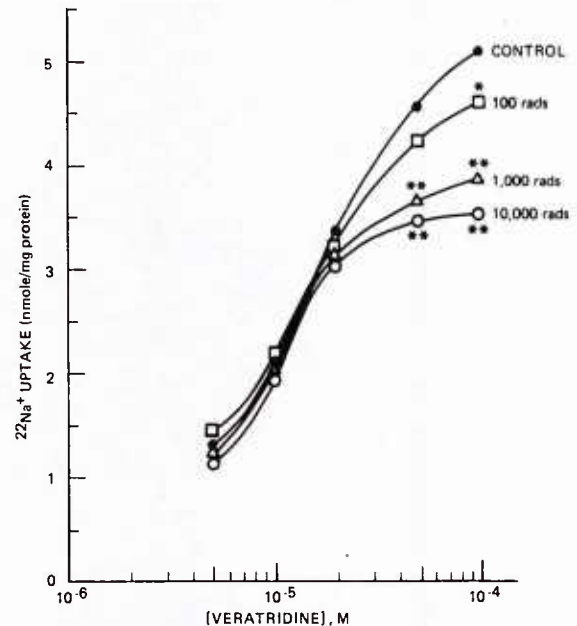


FIG. 1. Effect of high-energy electrons on veratridine-stimulated  $^{22}\text{Na}^+$  uptake by rat brain synaptosomes. In each experiment, triplicate samples were incubated with the indicated concentration of veratridine, and  $^{22}\text{Na}^+$  uptake was measured during a 5-s uptake phase. Data are mean values from four experiments; the SEM was 5–10% of the mean. Significant effects of radiation are indicated as follows: \**p* < 0.05, \*\**p* < 0.01.

tosomes was significantly different from control values only at the higher concentrations of veratridine. A double-reciprocal analysis of these data indicated that the maximal uptake was reduced with no change in the affinity of veratridine for its binding site in the channel (data not shown). In addition, nonspecific sodium uptake in the presence of veratridine and TTX and the uptake in the absence of any added toxins were unaffected by ionizing radiation (data not shown). These findings are in agreement with previous work on ion channels in our laboratory (Wixon and Hunt, 1983).

To determine if other types of ionizing radiation had a similar effect on the sodium channel, we irradiated synaptosomes with  $\gamma$  rays and measured the uptake of  $^{22}\text{Na}^+$  over a range of concentrations of veratridine (Fig. 2). Exposure to  $\gamma$  rays reduced the maximal effect of veratridine with no apparent shift in the concentration-effect curve. The magnitude of the radiation-induced inhibition of veratridine-stimulated  $^{22}\text{Na}^+$  uptake was similar in synaptosomes exposed to high-energy electrons or  $\gamma$  radiation.

When sodium channels were activated by BTX, the effect of radiation was less pronounced at a given dose of radiation (Fig. 3). One thousand rad of high-energy electrons reduced the maximal effect of veratridine by 25%, whereas the maximal effect of BTX was reduced by only 11%. At 3  $\mu\text{M}$

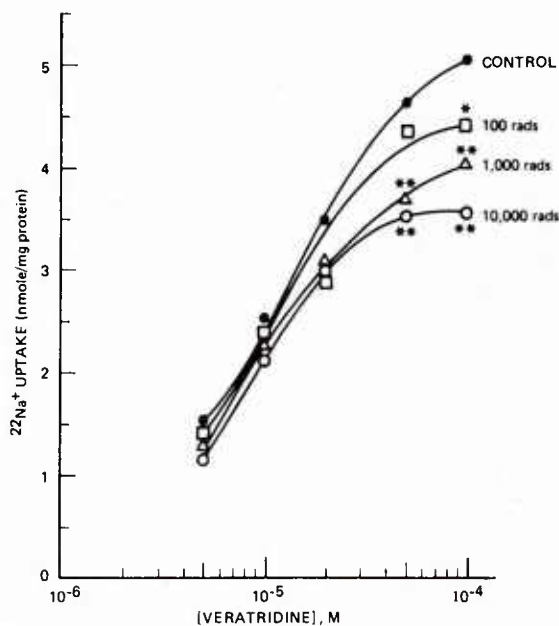


FIG. 2. Effect of  $\gamma$  radiation on veratridine-stimulated  $^{22}\text{Na}^+$  uptake by rat brain synaptosomes. In each experiment, triplicate samples were incubated with the indicated concentration of veratridine, and  $^{22}\text{Na}^+$  uptake was measured during a 5-s period. Data are mean values from three to five experiments; the SEM was 5–10% of the mean. Significant effects of radiation are indicated as follows: \* $p < 0.05$ , \*\* $p < 0.01$ .

BTX, the higher dose of radiation (10,000 rad) caused a significant ( $p < 0.05$ ) reduction in  $^{22}\text{Na}^+$  uptake. This difference in the potency of radiation may be related to the fact that BTX is considered to be a full agonist, whereas veratridine is a partial agonist in stimulating  $^{22}\text{Na}^+$  uptake (Catterall, 1980). In addition, the mechanism by which veratridine and BTX stimulate sodium uptake may be slightly

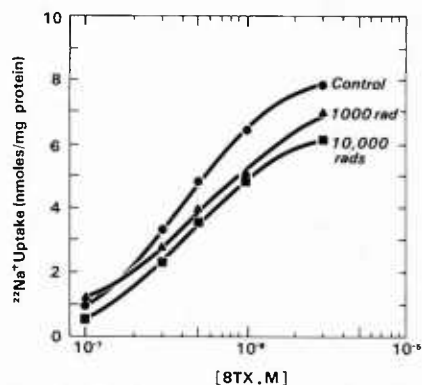


FIG. 3. Effect of high-energy electrons on BTX-stimulated  $^{22}\text{Na}^+$  uptake by rat brain synaptosomes. Triplicate samples were incubated with the indicated concentration of BTX, and  $^{22}\text{Na}^+$  uptake was measured during a 5-s period. Data are mean values from three experiments.

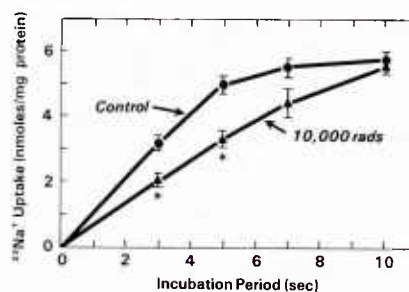


FIG. 4. Time course of veratridine-stimulated  $^{22}\text{Na}^+$  uptake. In each experiment, triplicate samples were incubated with veratridine (200  $\mu\text{M}$ ) for 10 min, and  $^{22}\text{Na}^+$  uptake was measured at the indicated interval. Synaptosomes were irradiated with 10,000 rad of high-energy electrons. Data are mean  $\pm$  SEM (bars) values from three to five experiments. A significant effect of ionizing radiation is indicated as follows: \* $p < 0.05$ .

different because of other properties of the toxins (Miller, 1983; Tanaka et al., 1983).

The time course of veratridine-stimulated  $^{22}\text{Na}^+$  uptake in control and irradiated synaptosomes is shown in Fig. 4. Exposure to 10,000 rad of high-energy electrons significantly reduced veratridine-stimulated  $^{22}\text{Na}^+$  uptake at incubation times of 3 and 5 s but not at later time points. Thus, ionizing radiation reduced the initial rate of neurotoxin-dependent  $^{22}\text{Na}^+$  uptake when the influx was unidirectional and the rates of uptake were greatest.

In synaptosomes and cultured neuroblastoma cells, the small polypeptide toxins present in certain SVs enhance the neurotoxin-dependent influx of sodium through an allosteric mechanism (Catterall, 1980). The data in Table 1 illustrate that the interaction of SV and veratridine remains intact in irradiated synaptosomes.

#### [ $^3\text{H}$ ]STX binding

In addition to the receptor sites for veratridine and SV, sodium channels in synaptosomes also

TABLE 1. Effect of high-energy electrons on SV-induced enhancement of veratridine-stimulated  $^{22}\text{Na}^+$  uptake

Dose (rad)	$^{22}\text{Na}^+$ uptake (nmol/mg of protein/5 s)	
	Veratridine (100 $\mu\text{M}$ )	Veratridine (100 $\mu\text{M}$ ) + SV (100 $\mu\text{g/ml}$ )
0	4.97 $\pm$ 0.10	6.92 $\pm$ 0.22 <sup>a</sup>
1,000	3.91 $\pm$ 0.25 <sup>b</sup>	6.03 $\pm$ 0.36 <sup>a</sup>
10,000	3.51 $\pm$ 0.18 <sup>c</sup>	5.79 $\pm$ 0.27 <sup>a</sup>

After irradiation, synaptosomes were preincubated with SV (100  $\mu\text{g/ml}$ ) for 2 min followed by a 10-min incubation with veratridine, and  $^{22}\text{Na}^+$  uptake was measured after a 5-s uptake phase. Data are mean  $\pm$  SEM values from three experiments.

<sup>a</sup> Denotes a significant effect of SV,  $p < 0.01$ .

<sup>b</sup> Denotes a significant effect of radiation,  $p < 0.05$ .

<sup>c</sup> Denotes a significant effect of radiation,  $p < 0.01$ .



**TABLE 2.** *Effect of ionizing radiation on binding of [<sup>3</sup>H]STX to rat brain synaptosomes*

Group	$B_{\max}$ (pmol/mg of protein)	$K_D$ (nM)
Control	2.80 ± 0.15	1.64 ± 0.10
Irradiated <sup>a</sup>	2.65 ± 0.23	1.76 ± 0.20

Synaptosomes were incubated at 0–2°C for 60 min with [<sup>3</sup>H]STX (0.10–10 nM) in the absence and presence of 10 μM TTX, and binding was measured using a rapid filtration assay. Data are mean ± SEM values from four experiments.

<sup>a</sup> Synaptosomes were irradiated with 10,000 rad of high-energy electrons.

contain a receptor site for TTX and STX. The binding of [<sup>3</sup>H]STX is sensitive to changes in the lipid and protein components of the membrane (Baumgold, 1980). However, exposure to 10,000 rad of high-energy electrons did not alter the equilibrium binding parameters of [<sup>3</sup>H]STX (Table 2). In addition, exposure to 25,000 rad of γ radiation did not affect the concentration of TTX required to inhibit veratridine-stimulated <sup>22</sup>Na<sup>+</sup> uptake by 50% (data not shown).

#### Fluorescence polarization studies

Ionizing radiation in doses of ≥500 rad has been shown to increase the fluidity of erythrocyte membranes (Edwards et al., 1984; Yonei et al., 1984). In addition, there is a strong correlation between inhibition of veratridine-stimulated sodium influx and increased membrane fluidity in mouse brain synaptic membranes (Harris and Bruno, 1985a). The fluorescence polarization of the probes DPH and TMA-DPH in rat brain synaptic plasma membranes after 10,000 rad of ionizing radiation is shown in Table 3. There was no significant difference in the baseline fluorescence polarization of DPH or TMA-DPH in the irradiated membranes compared with the corresponding control. The response of irradiated membranes to the lipid-disordering effect of ethanol was identical to the response in control membranes (Table 4). We conclude that a 10,000-rad dose of ionizing radiation has no effect on the baseline fluidity of synaptic plasma membranes

and, in addition, the response of irradiated membranes to the fluidity-inducing effect of ethanol is also unchanged. Thus, the changes in synaptosomal sodium uptake we observed are not due to changes in the order or arrangement of lipids in the neuronal membranes.

#### DISCUSSION

The CNS has traditionally been considered to be somewhat resistant to the effects of ionizing radiation. However, there is a growing body of evidence that low to moderate doses of radiation cause a wide variety of behavioral effects. In addition, the state of neuronal excitability, as assessed by changes in seizure thresholds, appears to be quite sensitive to radiation (Pollack and Timiras, 1964; Sherwood et al., 1967). Only recently have the possible mechanisms underlying these effects been studied with the methods available to membrane biologists and neurochemists.

The results of the present study confirm and extend our earlier observation that ionizing radiation reduced the veratridine-stimulated uptake of <sup>22</sup>Na<sup>+</sup> by rat brain synaptosomes (Wixon and Hunt, 1983). In addition, we determined that high-energy electrons and γ radiation were equally effective in reducing veratridine-stimulated <sup>22</sup>Na<sup>+</sup> uptake. In this regard, it is interesting to note that high-energy electrons are nearly twice as potent as γ photons in degrading performance in certain behavioral paradigms (Hunt, 1983). Ionizing radiation did not affect the interaction of SV with veratridine or the binding of [<sup>3</sup>H]STX to its receptor site in the sodium channel. Thus, only the receptor site for veratridine was affected by exposure of the membrane to ionizing radiation. Ionizing radiation reduced the maximal effect of veratridine and BTX without affecting the affinity of these toxins for the receptor site in the channel. We are currently studying the effect directly by measuring the effect of radiation on the binding of radiolabeled BTX.

There are several similarities in the effects of ionizing radiation and intoxicant-anesthetic drugs on the function of rat brain sodium channels. These

**TABLE 3.** *Effect of ionizing radiation on baseline fluorescence polarization of DPH and TMA-DPH*

Probe	Temperature	Baseline fluorescence polarization	
		Control	Irradiated
DPH	20°C	0.313 ± 0.002	0.315 ± 0.004
	35°C	0.253 ± 0.002	0.253 ± 0.004
TMA-DPH	20°C	0.335 ± 0.002	0.339 ± 0.003
	35°C	0.303 ± 0.002	0.305 ± 0.003

SPM-2 preparations were irradiated with 10,000 rad of high-energy electrons, and fluorescence polarization was measured as described in Materials and Methods. Data are mean ± SEM values (n = 6).

TABLE 4. Effect of ethanol *in vitro* on fluorescence polarization of DPH

Ethanol concentration (mM)	Change in polarization of DPH	
	Control	Irradiated <sup>a</sup>
75	-0.003 ± 0.001	-0.002 ± 0.001
150	-0.004 ± 0.001	-0.004 ± 0.001
300	-0.007 ± 0.001	-0.008 ± 0.001
600	-0.013 ± 0.001	-0.013 ± 0.002

The indicated concentration of ethanol was added to each cuvette, and the change in the baseline fluorescence polarization of DPH was measured at 35°C. Data are mean ± SEM values (n = 6).

<sup>a</sup> SPM-2 preparations were irradiated with 10,000 rad of high-energy electrons.

drugs and radiation reduce the initial rate of uptake and reduce the maximal effect of the toxins with little or no effect on affinity, and neither the SV-veratridine interaction nor the action of TTX is affected appreciably (Mullin and Hunt, 1984, 1985; Harris and Bruno, 1985b). Also, the effect of BTX is less sensitive than the effect of veratridine to inhibition by these agents (Mullin and Hunt, 1985; Harris and Bruno, 1985b).

Because ionizing radiation has been shown to increase the fluidity of erythrocyte membranes (Yonei and Kato, 1978; Yonei et al., 1984) and because there is a good correlation between increased membrane fluidity and reduced neurotoxin-stimulated sodium influx (Harris and Bruno, 1985a), we investigated the effects of ionizing radiation on the fluidity of synaptic plasma membranes and no difference in the response of these membranes to the lipid-disordering effect of ethanol at radiation doses that reduce the neurotoxin-stimulated uptake of <sup>22</sup>Na<sup>+</sup> by synaptosomes. As DPH is a probe of the lower (methyl terminal) portions of lipid acyl groups and TMA-DPH is a probe of the glycerol backbone and upper (carboxyl) portions of the acyl groups in membranes (Harris et al., 1984), we conclude that a 10,000-rad dose of ionizing radiation does not affect the order or packing of lipids in the neuronal membranes. Although alterations in the order of packing of membrane lipids may be an important determinant of radiation damage in certain biological membranes (Edwards et al., 1984; Yonei et al., 1984), this does not appear to be the case for membranes derived from the CNS. Perturbation of other membrane constituents such as oxidation of sulfhydryl groups and/or changes in protein conformation may be related to the observed effect of ionizing radiation on the functional properties of neuronal sodium channels.

**Acknowledgment:** We thank Mr. Tom Dalton for expert technical assistance and Mrs. Marion Golightly for excellent secretarial assistance in preparing the manuscript.

## REFERENCES

- Bachofner C. S. and Gautreaux M. E. (1960) Bioelectric responses *in situ* of mammalian nerves exposed to x-rays. *Am. J. Physiol.* **198**, 715-717.
- Bachofner C. S. (1962) Radiation effects on bioelectric activity of nerves, in *Response of the Nervous System to Ionizing Radiation* (Haley T. J. and Snider R. S., eds), pp. 573-583. Academic Press, New York.
- Baumgold, J. (1980) <sup>3</sup>H-Saxitoxin binding to nerve membranes: inhibition by phospholipase A<sub>2</sub> and by unsaturated fatty acids. *J. Neurochem.* **34**, 327-334.
- Bogo V. (1984) Effects of bremsstrahlung and electron radiation on rat motor performance. *Radiat. Res.* **100**, 313-320.
- Casarett A. P. and Comar C. L. (1973) Incapacitation and performance decrement in rats following split doses of fission spectrum radiation. *Radiat. Res.* **53**, 455-461.
- Catterall W. A. (1980) Neurotoxins that act on voltage-sensitive sodium channels in excitable membranes. *Annu. Rev. Pharmacol. Toxicol.* **20**, 15-43.
- Catterall W. A. (1984) The molecular basis of neuronal excitability. *Science* **223**, 653-661.
- Dunnett C. W. (1964) New tables of multiple comparisons with a control. *Biometrics* **20**, 482-491.
- Edwards J. C., Chapman D., Cramp W. A., and Yatvin M. B. (1984) The effects of ionizing radiation on biomembrane structure and function. *Prog. Biophys. Mol. Biol.* **43**, 71-93.
- Gasteiger E. L. and Campbell B. (1962) Alteration of mammalian nerve compound action potentials by beta irradiation, in *Response of the Nervous System to Ionizing Radiation* (Haley T. J. and Snider R. S., eds), pp. 597-606. Academic Press, New York.
- Gerstner H. B. and Orth J. S. (1950) Effects of high intensity x-ray irradiation on the velocity of nerve conduction. *Am. J. Physiol.* **130**, 232-286.
- Gray E. G. and Whittaker V. P. (1962) The isolation of nerve endings from brain: an electron-microscopic study of cell fragments derived by homogenization and centrifugation. *J. Anat.* **96**, 79-87.
- Harris R. A. and Bruno P. (1985a) Membrane disordering by anesthetic drugs: relationship to synaptosomal sodium and calcium fluxes. *J. Neurochem.* **44**, 1274-1281.
- Harris R. A. and Bruno P. (1985b) Effects of ethanol and other intoxicant-anesthetics on voltage-dependent sodium channels of brain synaptosomes. *J. Pharmacol. Exp. Ther.* **232**, 401-406.
- Harris R. A. and Schroeder T. (1982) Effects of barbiturates and ethanol on the physical properties of brain membranes. *J. Pharmacol. Exp. Ther.* **223**, 424-431.
- Harris R. A., Baxter D. M., Mitchell M. A., and Hitzemann R. J. (1984) Physical properties and lipid composition of brain membranes from ethanol tolerant-dependent mice. *Mol. Pharmacol.* **25**, 401-409.
- Hunt W. A. (1983) Comparative effects of exposure to high-energy electrons and gamma radiation on active avoidance behaviour. *Int. J. Radiat. Biol.* **44**, 257-260.
- Hunt W. A., and Dalton T. K. (1980) Reduction in cyclic nucleotide levels in the brain after a high dose of ionizing radiation. *Radiat. Res.* **83**, 210-215.
- Hunt W. A., Dalton T. K., and Darden J. H. (1979) Transient alterations in neurotransmitter activity in the caudate nucleus of rat brain after a high dose of ionizing radiation. *Radiat. Res.* **80**, 556-562.
- Johnson D. A., Lee N. M., Cooke R., and Loh H. H. (1979) Ethanol-induced fluidization of brain lipid bilayers: required presence of cholesterol in membranes for the expression of tolerance. *Mol. Pharmacol.* **15**, 739-746.
- Kimeldorf D. J. and Hunt E. L. (1965) Radiation effects on performance capacity, in *Ionizing Radiation: Neural Function and Behavior* (Kimeldorf D. J. and Hunt E. L., eds), pp. 166-213. Academic Press, New York.

- Krueger B. K., Ratzlaff R. W., Strichartz G. R., and Blaustein M. P. (1979) Saxitoxin binding to synaptosomes, membranes and solubilized binding sites from rat brain. *J. Membr. Biol.* 50, 287–310.
- Lowry O. H., Rosebrough N. J., Farr A. L., and Randall R. J. (1951) Protein measurement with the Folin phenol reagent. *J. Biol. Chem.* 193, 265–275.
- Mickley G. A. and Teitelbaum H. (1978) Persistence of lateral hypothalamic-mediated behaviors after a supralethal dose of ionizing radiation. *Aviat. Space Environ. Med.* 49, 868–873.
- Mickley G. A., Stevens K. E., White G. A., and Gibbs G. L. (1983a) Endogenous opiates mediate radiogenic behavioral change. *Science* 220, 1185–1187.
- Mickley G. A., Stevens K. E., Moore G. H., Deere W., White G. A., Gibbs G. L., and Mueller G. P. (1983b) Ionizing radiation alters beta-endorphin-like immunoreactivity in brain but not blood. *Pharmacol. Biochem. Behavior* 19, 979–983.
- Miller C. (1983) Integral membrane channels: studies in model membranes. *Physiol. Rev.* 63, 1209–1242.
- Minamisawa T. and Tsuchiza T. (1977) Long-term changes in the averaged evoked potentials of the rabbit after irradiation with moderate x-ray doses. *Electroencephalogr. Clin. Neurophysiol.* 43, 416–424.
- Mullin M. J. and Hunt W. A. (1984) Ethanol inhibits veratridine-stimulated sodium uptake in synaptosomes. *Life Sci.* 34, 287–292.
- Mullin M. J. and Hunt W. A. (1985) Actions of ethanol on voltage-sensitive sodium channels: effects on neurotoxin-stimulated sodium uptake in synaptosomes. *J. Pharmacol. Exp. Ther.* 232, 413–419.
- Okada S. (1970) Cells, in *Radiation Biochemistry*, Vol. 1. (Altman K. I., Gerber G. B., and Okada S., eds), pp. 3–76. Academic Press, New York.
- Pollack M. and Timiras P. S. (1964) X-ray dose and electroconvulsive responses in adult rats. *Radiat. Res.* 21, 111–119.
- Rabin B. M., Hunt W. A., and Lee J. (1982) Studies on the role of central histamine in the acquisition of a radiation-induced conditioned taste aversion. *Radiat. Res.* 90, 609–620.
- Rosenthal F. and Timiras P. S. (1961) Changes in brain excitability after whole-body x-irradiation in the rat. *Radiat. Res.* 15, 648–657.
- Saum W. R., McGee R. Jr., and Love J. (1981) Alteration of the action potential of tissue cultured neuronal cells by growth in the presence of a polyunsaturated fatty acid. *Cell Mol. Neurobiol.* 1, 319–324.
- Scatchard G. (1949) The attraction of proteins for small molecules and ions, in *Annals of the New York Academy of Sciences*, Vol. 51: *Molecular Interactions* (Fuoss R. M., ed), pp. 660–672. New York Academy of Sciences, New York.
- Sherwood N. M., Welch G. P., and Timiras P. S. (1967) Changes in electroconvulsive thresholds and patterns in rats after x-rays and high-energy proton irradiation. *Radiat. Res.* 30, 374–390.
- Smith J. C. (1971) Radiation: its detection and its effects on taste preferences, in *Progress in Physiological Psychology*, Vol. 4 (Stellar E. and Sprague J. M., eds), pp. 53–117. Academic Press, New York.
- Tamkun M. M. and Catterall W. A. (1981) Ion flux studies of voltage-sensitive sodium channels in synaptic nerve-ending particles. *Mol. Pharmacol.* 19, 78–86.
- Tanaka J. C., Eccleston J. F., and Barchi R. L. (1983) Cation selectivity characteristics of the reconstituted voltage-dependent sodium channel purified from rat skeletal muscle sarcolemma. *J. Biol. Chem.* 258, 7519–7526.
- Wixon H. N. and Hunt W. A. (1983) Ionizing radiation decreases veratridine-stimulated uptake of sodium in rat brain synaptosomes. *Science* 220, 1073–1074.
- Yonei S. and Kato M. (1978) X-ray induced structural changes in erythrocyte membranes studied by use of fluorescent probes. *Radiat. Res.* 75, 31–45.
- Yonei S., Akasaka S., and Kato M. (1984) Studies on the mechanism of radiation-induced structural disorganization of human erythrocyte membranes. *Int. J. Radiat. Biol.* 46, 463–471.



## Thymic Hormones in Thymus Recovery from Radiation Injury

Ruth Neta, Gretchen N. Schwartz, Thomas J. MacVittie, and Susan D. Douches

Experimental Hematology Department, Armed Forces Radiobiology Research Institute, Bethesda, Maryland 20814-5145, USA

### ABSTRACT

The effect of a thymic hormone, thymosin fraction 5 (TF5), in restoring immunocompetence in the thymus of  $\gamma$ -irradiated mice was examined. Three different mouse strains were used in this study, since previous work has established that the response to TF5 varies in different strains. To measure the rate of recovery of immunocompetent cells in the thymus, the responsiveness to comitogenic effect of interleukin-1 (IL-1) was used. This assay was chosen since it has been established that only more mature PNA<sup>+</sup>, Lyt1<sup>+</sup>2<sup>-</sup> medullary cells respond to this monokine. Contrary to several earlier reports that radioresistant cells repopulating the thymus within the first 10 days after irradiation are mature, corticosteroid resistant, immunocompetent cells, the thymic cells from irradiated mice in all strains used had greatly reduced responses to IL-1. Daily intraperitoneal injections of TF5 increased significantly the responses of thymic cells to IL-1 in 10-13 weeks old C57Bl/KsJ, C3H/HeJ, and DBA/1 mice. Older mice, 5 months or more in age, of DBA/1 strain did not respond to treatment with TF5. However, C3H/HeJ mice of the same age were highly responsive. In conclusion, (a) cells repopulating the thymus within 12 days after irradiation contain lower than normal fraction of mature IL-1 responsive cells, (b) thymic hormones increase the rate of recovery of immunocompetent cells in the thymus, and (c) the effect of thymic hormones is strain and age dependent.

Send reprint requests to: Dr. Ruth Neta, Experimental Hematology Department, Armed Forces Radiobiology Research Institute, Bethesda, Maryland 20814-5145.

### INTRODUCTION

The thymus gland is of critical importance in the normal development of T-cells. T-cell precursors acquire functions and phenotypic markers characteristic of mature T-cells in the thymus. Much information has accumulated recently on the phenotype definition of thymic cells subpopulations [1,2] and on modes of acquisition of MHC determined self restriction necessary for their reactivity [3,4]. However, the precise intrathymic events that regulate thymocytes proliferation and differentiation remain unresolved. In particular, the influence of thymic hormones on proliferation and maturation of cells in the thymus remains to be established [5-7]. Much work has shown that administration of these hormones in vivo can restore immunologic reactivities of immunodeficient host [8-12]. Previous work, including our own, also indicated that thymic hormones can correct deficient function but do not augment normal function [13,14]. This immunoregulatory effect awaits an explanation.

Ionizing radiation, even in low doses (150-200 rad), causes a dramatic involution in murine thymus. Regeneration of the thymus, as measured by weight and mitotic index, begins 5-7 days after irradiation [15]. The thymuses of radiation immunocompromised mice presented a convenient model to observe the effect of administration of thymic hormones on the maturation of the cells in the thymus. Two additional aspects were considered in developing the experimental model: (a) Previous work has established that the effectiveness of treatment with TF5 varies widely in different strains of mice. C3H/HeJ mice susceptible to infection with *C. albicans* and low responders in the in vivo release of MIF and IFN- $\gamma$

become resistant and release high titers of the two lymphokines into circulation following daily administration of TF5. In contrast, DBA/1 strain, also susceptible and low-responder, was not affected by hormone administration [14,13]. In addition, C57Bl/KsJ, normally resistant and high responders, became susceptible and low-responders when compromised by induction of a diabetic condition [16]. This compromised strain also responded to treatment with thymosin with enhanced resistance, lymphokine release, and delayed footpad reaction to *C. albicans*. (b) The involution of the thymus that begins at puberty is not understood at present. It is possible that this process depends on reduced production and/or responsiveness to thymic hormones.

Therefore, our experimental model consisted of the three above mentioned mouse strains, varying in their ages from 10 weeks to 6 months and irradiated with 450 rad. As a measure of thymocyte function we have chosen to assay changes in responsiveness to IL-1, since previous work has established that only more mature PNA<sup>+</sup>, Lyt1<sup>+</sup>2<sup>-</sup> cells respond by proliferation in this assay [17-20].

In this presentation we will demonstrate that administration of TF5 into irradiated mice accelerates the rate of recovery of IL-1 responsive cells in the thymus. The effectiveness of treatment with the hormone depends, however, on the strain and the age of the animal.

#### MATERIALS AND METHODS

**Mice.** Inbred strains of female mice (C57Bl/KsJ, DBA/1J, and C3H/HeJ) were obtained from Jackson Laboratories, Bar Harbor, Maine. The mice were housed in the Veterinary Medicine Department facility at the Armed Forces Radiobiology Research Institute in cages of nine mice with filter lids. Standard lab chow and HCL acidified water (pH 2.4) were given *ad libitum*. All cage cleaning procedures and daily injections were carried out in a micro-isolator.

**Irradiation.** Mice were placed in Plexiglas restrainers and given whole-body irradiation at 0.40 Gy/min by bilaterally positioned cobalt-60 elements. The total dose was 4.5 Gy (450 rads).

**Thymosin Fraction 5.** This was obtained through the courtesy of Dr. Allan Goldstein, Department of Biochemistry, The George Washington University School of Medicine, Washington, DC. The control fraction, kidney fraction 5, was also kindly provided by Dr. Goldstein. Both lyophilized fractions were diluted in pyrogen-free saline (Travenol Laboratories) containing 100 U/ml of penicillin and 100 µg/ml of streptomycin to a final concentration of 10 µg/ml. Each mouse

received 0.5 ml daily intraperitoneal injection.

**Thymic Cell Suspensions.** Three to six mice per experimental group were sacrificed via ether anesthesia on the days postirradiation as noted. Thymuses were removed, cleared of any parathymic lymph nodes and placed in Hanks Balanced Salt Solution (HBSS-GIBCO) on ice. Single cell suspensions were prepared by passing the thymuses through a Millipore screen (20 mm diameter) and then a 23 gauge needle and syringe. The cells were washed two times in HBSS (200 g, 10 min, 4°C), and resuspended in complete medium containing RPMI 1640, 10% calf serum (HyClone), 100 U/ml penicillin, 100 µg/ml streptomycin, 10<sup>-5</sup> M 2-beta mercaptoethanol, and 2 mM L-glutamine. Viability for all cell suspensions was found to always be >95%.

**IL-1 Preparations.** Two preparations of IL-1 were used. IL-1 purchased from Genzyme with a specific activity of 100 U/ml was used at a final concentration of 5 U/ml and 1 U/ml (lot numbers 094a, 095a). IL-1 was also prepared in the laboratory according to Gery, et al. [21]. Briefly, resident peritoneal macrophages were lavaged from C57Bl/6 mice. Cell suspensions containing 2 x 10<sup>6</sup> cells/ml were allowed to adhere for 2 hr to the surface of plastic Costar 2506 multiwell dishes and then after removal of nonadherent cells, were incubated for 24 hr at 37°C in 5% CO<sub>2</sub> with 20 µg/ml of lipopolysaccharide (Difco, Detroit, Michigan) and 60 µg/ml of silica (gift from Dr. Alison D. O'Brien, Department of Microbiology, Uniformed Services University of the Health Sciences) prepared as specified [22]. The supernatants were used in dilutions ranging from 1:50 to 1:250. Controls which consisted of cell culture supernatants to which LPS and silica were added at the termination of the culture did not have any stimulatory effect.

**IL-1 Assays.** The assay was performed as previously described [21]. Briefly, triplicate cultures for each IL-1 dilution and background control were set up in 96 well flat bottom microtiter plates (Costar 3596, Cambridge, Massachusetts). Two cell concentrations were used in each assay, usually 0.1 ml/well of 3 x 10<sup>5</sup> cells/ml or 1.5 x 10<sup>5</sup> cells/ml. PHA (Wellcome Burroughs, Greenville, North Carolina) was added to the cell suspensions at a final concentration of 1.0 µg/ml. Following 48 hr incubation at 37°C in 5% CO<sub>2</sub>, cells were pulsed with 1 µCi <sup>3</sup>H-thymidine per well. The cells were harvested 18 hr later (Skatron Cell Harvester, Sterling, Virginia) onto glass filters which were then counted in Scintiverse II on a Mark III Scintillation Counter to determine thymidine

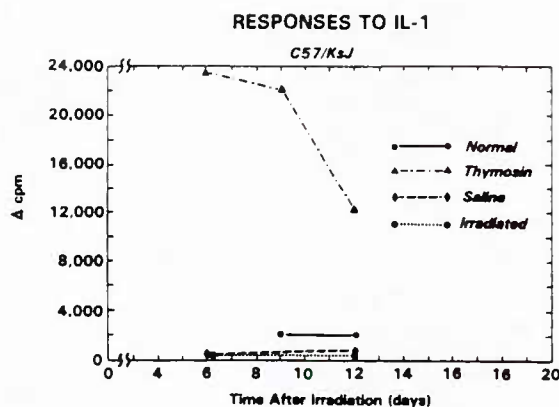


Fig. 1. Effect of TF5 on comitogenic response of thymocytes from C57Bl/6 mice. Thymocytes were recovered at days after irradiation and cultured at a cell concentration of  $1.5 \times 10^6$  cells/well (D + 6) or  $3.0 \times 10^6$  cells/well (D + 9 and D + 12). Results are mean cpm of triplicate cultures with 5 U/ml of IL-1 minus mean cpm of triplicate cultures without IL-1.

uptake. Statistical analyses were performed using Student's T test.

#### RESULTS

**C57Bl/KsJ.** Previous work indicated that treatment of normal C57Bl/KsJ mice with TF5 reduced their immunologic responsiveness, i.e., their resistance to infection with *C. albicans* and the titers of in vivo released lymphokines (IFN- $\gamma$  and MIF). Similar treatment of C57Bl/KsJ mice immunocompromised by induction of diabetic condition and, therefore, susceptible to *C. albicans* and low-responders in in vivo IFN- $\gamma$  and MIF release, resulted in enhanced resistance and greatly increased titers of lymphokines [16]. Presently, groups of mice, 10-12 per group, 3 months old at the time of irradiation with 450 rads, were given daily injections of 5  $\mu$ g TF5 or saline or were not injected. The magnitude of comitogenic effect of IL-1 in the thymocytes of the three above groups and normal controls was compared (Fig. 1). The results are expressed as mean counts per minute of triplicate cultures containing  $1.5 \times 10^6$  or  $3.0 \times 10^6$  cells per well, incubated with and without 5 units/ml of IL-1. The responses of two other concentrations of IL-1 used in each assay indicated the linearity of responsiveness to IL-1 (data not shown). It is apparent that normal C57Bl/KsJ mice can be characterized as low-responders to IL-1. The recovery of cells/thymus on a given day after irradiation is very similar for the individual experimental groups (Fig. 2) and agrees with previously published observations on the initial

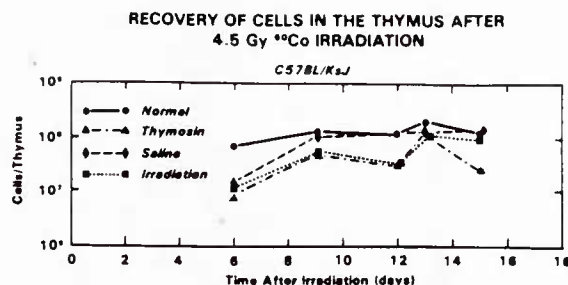


Fig. 2. The numbers of cells recovered per thymus at different days after irradiation (calculated from groups of 3-6 mice).

cell recovery in the thymus of irradiated mice [15]. A striking difference, however, may be observed in the responsiveness of cells to IL-1. The TF5 treated thymocytes responded significantly more than the control and the saline treated for irradiated groups. In two additional series of experiments 10 week old mice were used, since 8-10 weeks old CD-1 mice respond to IL-1 with peak activity [23]. Although much higher number of cells/thymus were recovered from the normal, 10 week old C57Bl/KsJ mice (ranging from  $2.3$  to  $4.0 \times 10^5$  cells), the thymocytes in response to 1:100 dilution of IL-1 incorporated only  $2-4 \times 10^3$  cpm of  $^3\text{H}\text{TdR}$ . Thus, lower levels of response were observed in thymuses with higher cellularity. At day 6, 9, and 13 after irradiation the TF5 treated mouse thymocytes from C57Bl/KsJ mice responded at  $73\%$ ,  $129 \pm 7\%$ , and  $80 \pm 60\%$  of normal control responses, respectively. The saline or kidney fraction 5 treated control groups had only  $19\%$ ,  $41 \pm 37\%$ , and  $10 \pm 9\%$ , and irradiated mice had only  $40\%$ ,  $8 \pm 11\%$ , and  $13 \pm 8\%$  of normal control responses on the same days. Therefore, despite the reduced effect of the treatment with TF5 in 10 week old C57Bl/KsJ mice a marked greater response was still obtained from TF5 treated than from saline/kidney fraction 5 - treated, or irradiated mice. We conclude, therefore, that treatment with TF5 in comparison with saline or kidney fraction 5, enhances the recovery of IL-1 responsive cells in the thymuses of irradiated mice.

**DBA/1.** Mice of this strain were evaluated since in previous experiments TF5 did not affect their resistance to infection with *C. albicans* and their in vivo release of IFN- $\gamma$  and MIF. Animals of two different ages were used to determine whether the responses to TF5 are age dependent. The particular choice of ages, 10 weeks and 5 months, was based on the previous observation [23] that 8-10 week old CDF<sub>1</sub> mice



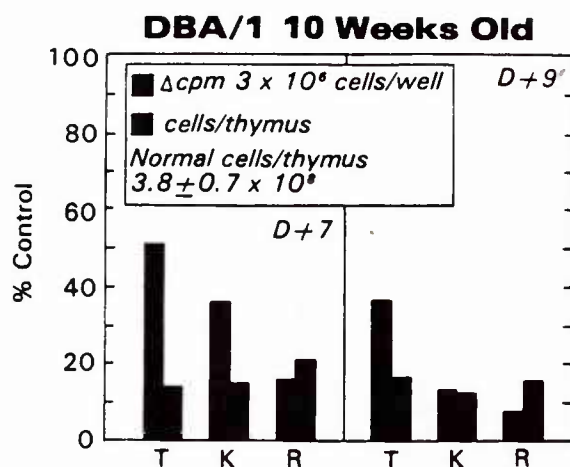


Fig. 3. Effect of TF5 on comitogenic responses of thymocytes from 10 week old DBA/1 mice to IL-1. Thymocytes were recovered at 7 and 9 days after irradiation and cultured at concentration of  $3 \times 10^6$  cells/well with or without IL-1. Results are expressed as percent of control responses. T - thymosin fraction 5, K - kidney fraction 5, R - radiation only.

had maximal responses to IL-1 and 18 week old mice had greatly reduced responses to purified IL-1. The lower responses in older animals may be an indication of reduced levels of immunocompetent T-cells in the thymus, possibly as a result of reduced effectiveness of thymic hormones.

(a) Thymocytes from 10 week old mice at 7 and 9 days after irradiation when treated with TF5 showed consistently higher responses (Fig. 3). The thymocytes responses were lower in animals treated with kidney fraction 5 or irradiated only. Although lower number of cells per thymus were recovered in kidney fraction 5 and TF5 treated animals than in irradiated only mice at 7 days after irradiation, similar numbers of cells were recovered in TF5 treated group and irradiated group at 9 days after irradiation. Depletion of cells, therefore, in the thymuses of TF5 treated mice does not account for the apparent difference in the level of IL-1 reactive cells.

(b) The responses of thymocytes from 5 month old mice evaluated in two series of experiments are summarized in Fig. 4. None of the irradiated experimental groups showed the presence of IL-1 responsive cells at the cell concentrations used in the assay. The cellularity of the thymuses increased with no apparent influence of treatment (Fig. 5). Thus, we can conclude that TF5, although effective in thymic recovery of younger animals, did not affect the recovery of the thymus in older animals. Cell proliferation, however, takes place in these thymuses

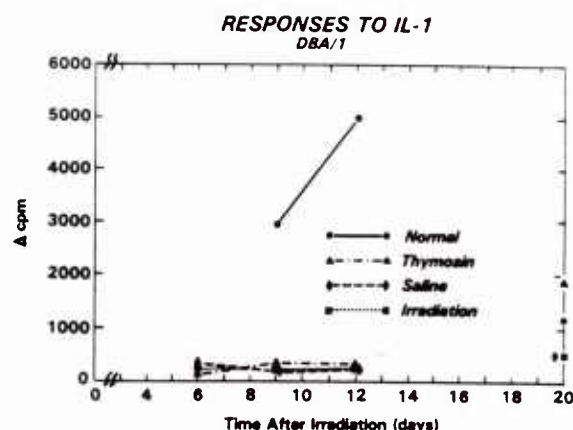


Fig. 4. Effect of TF5 on comitogenic response of thymocytes from 5 month old DBA/1 mice. Thymocytes were recovered at days after irradiation and cultured at  $3 \times 10^6$  cells/well. Results are mean cpm of triplicate cultures with 5 units of IL-1 minus mean cpm of triplicate cultures without IL-1.

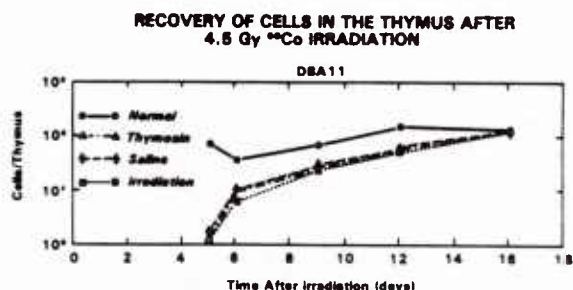


Fig. 5. The numbers of cells recovered per thymus at different days after irradiation, calculated from groups of 3-6 mice.

following radiation injury, and at 12 days the numbers of thymocytes in irradiated mice nears that of normal mice.

**C3H/HeJ.** Mice of this strain, 5-6 months old, were used for comparison with TF5 unresponsive DBA/1 mice of the same age. Two series of the separate experiments are summarized in Table 1. Since on day 6 and 7 after irradiation the recovery of cells in individual groups (6 mice in each group) was low, the cell concentrations were reduced to  $5 \times 10^5$  cells/well on day 6 and to  $7 \times 10^5$  cells/well on day 7. It is evident from Table 1 that on days 6, 7, and 9 after irradiation only thymic cells from TF5 treated mice responded to IL-1 with increased proliferation. In contrast, equal cell concentrations from irradiated only, irradiated and kidney

EFFECT OF THYMOSIN FRACTION 5 ON COMITOGENIC RESPONSE OF  
THYMOCYTES FROM 5 MONTHS OLD C3H/HeJ MICE TO IL 1

TREATMENT	O = 6		O = 7		O = 9	
	IL 1	CONTROL	IL 1	CONTROL	IL 1	CONTROL
Thymosin fraction 5	* 4583 ± 2112 (1.0 × 10 <sup>6</sup> )	753 ± 79	** 1938 ± 174 (3.1 × 10 <sup>6</sup> )	432 ± 188	+ 6324 ± 493 (6.5 × 10 <sup>7</sup> )	1776 ± 619
Kidney fraction 5	* 1367 ± 1000 (1.0 × 10 <sup>6</sup> ) p < 0.02	736 ± 356	** 1225 ± 203 (4.1 × 10 <sup>6</sup> ) p < 0.005	540 ± 328	+ 1410 ± 95 (5.4 × 10 <sup>7</sup> ) p < 0.01	1607 ± 630
Irradiated only	* 1959 ± 2050 (1.0 × 10 <sup>6</sup> ) p < 0.05	1713 ± 1061	** 937 ± 204 (4.1 × 10 <sup>6</sup> ) p < 0.05	540 ± 255	+ 1349 ± 413 (5.1 × 10 <sup>7</sup> ) p < 0.001	1683 ± 198
Normal, non irradiated	* 4096 ± 1391 (7.7 × 10 <sup>7</sup> )	1499 ± 801	- 6162 ± 1189 (1.9 × 10 <sup>6</sup> )	937 ± 101	+ 3252 ± 414 (1.5 × 10 <sup>6</sup> )	1905 ± 249
	* 685 ± 187	475 ± 112	** 264 ± 120	226 ± 77		

\* 5 × 10<sup>5</sup>, \*\* 7 × 10<sup>5</sup>, + 3 × 10<sup>6</sup>

Table 1. Thymocytes were recovered at days after irradiation and cultured at cell concentrations indicated by \* (5 × 10<sup>5</sup>), \*\* (7 × 10<sup>5</sup>), or + (3 × 10<sup>6</sup>) per well. Results are mean cpm ± S.D. of triplicate cell cultures with 2 U/ml of IL-1 or of controls. The numbers in parentheses are number of cells recovered per thymus. P values were calculated by Student's t test for a given group compared to TF5 treatment.

fraction 5 treated, and nonirradiated normal mice were not responsive to IL-1. In conclusion, unlike DBA/1 mice, 5-6 month old C3H/HeJ mice respond to TF5 treatment with enhanced responses of the cells in the thymus to IL-1.

#### DISCUSSION

The experimental results reported here address three questions: (a) are the cells repopulating the thymus in the early postirradiation phase immunologically competent, (b) can thymic hormones exert an effect on these cells (or change their composition), and (c) can genetic factors influence the effect exerted by thymic hormones in irradiated mice.

Thymocytes from all of the strains examined, after irradiation with 450 cGy showed reduction in IL-1 responsiveness throughout the first phase of recovery. Earlier studies by Takada et al. [15], using mitotic index and thymus weight from mice irradiated with 400 cGy concluded that thymus regeneration is a biphasic process. Within 24 hr after irradiation, a precipitous drop in mitosis and in thymic weight developed which was followed by nearly full recovery beginning on days 5-7 until day 12. Following this day a second drop in thymic cellularity was observed which lasted until day 20. Our observation on the recovery of cells in the thymus parallels these findings. The mechanism of this biphasic pattern of thymus repopulation remains speculative.

The immunologic competence of the cells initially repopulating the thymus is controversial. A number of studies concluded that radiation-resistant cells repopulating the thymus are immunocompetent. Blomgren and Anderson [24] compared cells from normal thymuses with corticosteroid resistant cells (CRC) for their radiation resistance. They observed that corticosteroid treatment enriched the radiation resistant cells from 4% in normal mice to 50% CRC populations, and concluded that these two populations may be similar. Studies by Konda et al. [25] examining the buoyant density and T-cell markers of CRC concluded that this population was similar to radio-resistant cells present in the thymus 10 days after 880 cGy irradiation. Using 760 cGy irradiated A/J mice, Kadish and Basch demonstrated that cells recovered 9 days after irradiation had enhanced reactivity to Con-A and PHA [26]. The histology of cortical and medullary regions of the thymus 10 days after irradiation with 750 cGy resembled that of a normal thymus [27]. Therefore it has been proposed that the radioresistant cells in the thymus that repopulate the thymus after irradiation present a population resembling the mature CRC. More recent studies on the phenotypes of cells present in the thymus within 12 days following irradiation demonstrated a relative sparsity of PNA<sup>+</sup>, Lyt1<sup>+</sup>2<sup>-</sup> cells [28], presently recognized as the immunocompetent subpopulation that is responsive to IL-1 [17-20]. Similarly, CTL-precursor cells were found 14 days after lethal irradiation and bone marrow transfer but were not detected at 7 days after irradiation [29]. In another

laboratory the frequency of CTL-precursor cells was about 50-fold lower for up to 12 days after irradiation in the thymuses of bone marrow reconstituted radiation chimeras [30]. The same investigators also analyzed by flow microfluorimetry the Thy-1 phenotype of host derived cells. Despite increasing numbers of Thy-1 bright cells (considered immunologically immature), cells weakly stained with Thy-1 (considered immunocompetent) were not detected 10 days after irradiation.

Our own observations using IL-1 responsiveness as a measure of thymocyte immunocompetence indicates a reduction in these cells from day 6 to 12 postirradiation with 450 cGy. Given that the number of cells recovered from the thymus at 6 days after irradiation represents about 15% of the number of cells in normal thymus and nears normal at 12 days, the frequency of these cells in the thymus must be greatly reduced. Together with the finding on reduced frequency of CTL precursor cells [29,30] and the scarcity of PNA<sup>-</sup>, Lyt1<sup>+</sup>2<sup>-</sup>, weakly Thy-1 stained cells repopulating the thymus after irradiation [28,30] the degree of maturation of radioresistant cells and the types of proliferating cells in a regenerating thymus need to be re-evaluated.

There have been numerous demonstrations that various thymic hormones preparations are effective in treatment of immunodeficiencies [8-14]. The capacity of these hormones to promote maturation, proliferation, and marker acquisition of T-cells in bone marrow or in spleen has been reported [31-33]. However, the majority of the successful experiments demonstrating the effect of thymic hormones have been conducted in vivo despite the fact that most of the in vitro experiments use doses of the hormones many fold higher than the doses used in the living animal [34]. Possibly the action of this hormone is amplified in vivo via a mediating mechanism absent in the in vitro systems. The relatively narrow range of optimal doses necessary to achieve beneficial in vivo effects as well as necessity for daily injections of the hormone represent some of the not yet understood complexities of the system.

Although our results clearly demonstrate an enhancement of IL-1 responsiveness following administration of TF5 to irradiated mice, the mechanism of this enhancement remains unclear. Several possibilities should be considered. (a) Stimulation of the traffic of the bone marrow derived T-precursor cells into the thymus, (b) promotion of maturation of intrathymic cells, and (c) enrichment for IL-1 reactive cells as a result of selective depletion by thymic hormones of immunologically immature cells present in the thymus. The latter possibility does

not seem likely as the recovery of cells per thymus on a given day does not vary much between the different experimental groups. Treatment with TF5 enhanced the level of IL-1 responsiveness in all three strains examined when the age of the mice was 10-12 weeks. The role of genetic factors is suggested by the finding that 5-6 months old C3H/HeJ mice responded to treatment (Table 1) while DBA/1 mice of the same age did not respond (Fig. 4). This difference parallels the previously observed effect of TF5 in these two strains when resistance to *C. albicans* and in vivo release of IFN- $\gamma$  and MIF were compared [13,14]. The same two mouse strains also varied in their responses to IL-1. Three month old C3H/HeJ mice had tenfold higher response than 10 week old DBA/1 mice (data not presented). Although at 5 months the response of normal C3H/HeJ mice to IL-1 had declined, it was still at least two- to threefold higher than the response of thymocytes from 5 month old DBA/1 mice. This apparent difference to a comitogenic effect of IL-1 may be a reflection of differences in the percentages of mature, immunocompetent cells in the thymuses of these strains. For example, the percent of medullary PNA<sup>-</sup> cells differed from 14.6% in CBA mice to 9.5% in C57Bl/6 mice [1]. Perhaps these differences in the numbers of immunocompetent cells in the thymuses of different strains may be the result of differences in the levels of endogenous thymic hormones or of cell responses to thymic hormones. The responsiveness of 5-6 month old C3H/HeJ mice to thymic hormones may be the reason for this strain's high level of IL-1 responses, and therefore the greater number of immunocompetent cells in the thymus. The unresponsiveness of the DBA/1 mice of the same age would result in lower numbers of IL-1 responsive cells in the thymus of this strain as observed in the present study. As reagents to evaluate thymic hormone levels in mice of different strains become available, this hypotheses may be examined.

#### ACKNOWLEDGMENTS

This work was supported by the Armed Forces Radiobiology Research Institute, Defense Nuclear Agency, under Research Work Unit MJ 00148. The views presented in this paper are those of the authors; no endorsement by the Defense Nuclear Agency has been given or should be inferred. Research was conducted according to the principles enunciated in the "Guide for the Care and Use of Laboratory Animals" prepared by the Institute of Laboratory Animal Resources, National Research Council. We thank Marianne Owens for the preparation of this manuscript.



## REFERENCES

1. Scollay R, Shortman K (1983) Thymocyte subpopulations: an experimental review, including flow cytometric cross-correlations between the major murine thymocyte markers. *Thymus* 5:245.
2. Mathieson BJ, Fowlkes BJ (1984) Cell surface antigen expression on thymocytes: Development and phenotypic expression of intrathymic subsets. *Immunol Rev* 82:141.
3. Zinkernagel RM, Calahan GN, Klein J, Dennert G (1978) Cytotoxic T-cells learn specificity for self H-2 during differentiation in the thymus. *Nature* 271:251.
4. Wagner H, Hardt C, Stockinger H, Pflennmayer K, Barlet R, Rollinghoff M (1981) The impact of the thymus on the generation of immunocompetence and diversity of antigen specific, MHC-restricted cytotoxic T-lymphocyte precursors. *Immunol Rev* 58:95.
5. Low TLK, Goldstein AL (1982) Role of the thymosins as immunomodulating agents and maturation factors. In *Maturation Factors and Cancer*, Moore MAS, ed. Raven Press, New York p. 229.
6. Ho AD, Ma DDF, Price G, Hunstein W, Hoffrand AV (1983) Biochemical and immunological differentiation of human thymocytes induced by thymic hormones. *Immunol* 50:471.
7. Andrews P, Shortman K, Scollay R, Potworowski EF, Kruisbeek AM, Goldstein G, Trainin N, Bach JF (1985) Thymus hormones do not induce proliferative ability or cytolytic function in PNA<sup>+</sup> cortical thymocytes. *Cell Immunol* 91:455.
8. Wara DW, Goldstein AL, Doyle N, Ammann AJ (1975) Thymosin activity in patients with cellular immunodeficiency. *New Eng J Med* 292:70.
9. Morrison NE, Collins FM (1976) Restoration of T-cell responsiveness by thymosin: Development of anti-tuberculous resistance in BCG infected animals. *Infect Immun* 13:554.
10. Mawhinney H, Gleadhill VF, McCrea S (1979) In vitro and in vivo responses to thymosin in severe combined immunodeficiency. *Clin Immunol Immunopathol* 14:196.
11. Bonagura VR, Pitt J (1981) Hypoparathyroidism with T-cell deficiency and hypogammaglobulinemia: Response to thymosin therapy. *Clin Immunol Immunopathol* 18:375.
12. Petro TM, Chien G, Watson RR (1982) Alteration of cell mediated immunity to *Listeria monocytogenes* in protein malnourished mice treated with thymosin fraction 5. *Infect Immun* 35:601.
13. Neta R, Salvin SB (1983) Resistance and susceptibility to infection in inbred murine strains. II. Variations in the effect of treatment with thymosin fraction 5 on the release of lymphokines in vivo. *Cell Immunol* 75:173.
14. Salvin SB, Neta R (1983) Resistance and susceptibility to infection in inbred murine strains. I. Variations in the response to thymic hormones in mice infected with *Candida albicans*. *Cell Immunol* 75: 160.
15. Takada A, Takada Y, Huang CC, Ambrus JL (1969) Biphasic pattern of thymus regeneration after whole body irradiation. *J Exp Med* 129:445.
16. Salvin SB, Neta R (1984) The in vivo effect of thymosin on cell-mediated immunity. In *Thymic Hormones and Lymphokines*, Goldstein AL, ed. Plenum, New York, p. 439.
17. Oppenheim JJ, Northoff H, Greenhill A, Mathieson BJ, Smith K, Gillis S (1980) Properties of human monocyte derived lymphocyte activating factor (LAF) and lymphocyte derived mitogenic factor (LMF). In *Biochemical Characterization of lymphokines*, DeWeck AL, Kristensen F, Landy M, eds, Academic Press, New York, p. 399.
18. Oppenheim JJ, Stadler BM, Siraganian RP, Mage M, Mathieson BJ (1982) Lymphokines: Their role in lymphocyte responses. Properties of interleukin-1. *Fed Proc* 41:257.
19. Conlon PJ, Henney CS, Gillis S (1982) Cytokine-dependent thymocyte responses: Characterization of IL-1 and IL-2 target subpopulations and mechanism of action. *J Immunol* 128:797.
20. Puri J, Shinitzky M, Lonai P (1980) Concomitant increase in antigen binding and in T-cell membrane lipid viscosity induced by the lymphocyte activating factor, LAF. *J Immunol* 124:1937.
21. Gery I, Davies P, Derr J, Krett N, Barranger JA (1981) Relation between production and release of lymphocyte activating factor (interleukin-1) by murine macrophages. I. Effects of various agents. *Cell Immunol* 64: 293.
22. O'Brien AO, Scher I, Formal SB (1975) Effect of silica on the innate resistance of inbred mice to *Salmonella typhimurium* infection. *Infect Immun* 25:513.
23. Blyden G, Handschumacher RE (1977) Purification and properties of human lymphocyte activating factor (LAF). *J Immunol* 118:1631.
24. Blomgren H, Andersson B (1970) Characteristics of the immunocompetent cells in the mouse thymus: Cell population changes during cortisone-induced atrophy and subsequent regeneration. *Cell Immunol* 1:545.
25. Konda S, Stockert E, Smith RT (1973) Immunologic properties of mouse thymus cells: Membrane antigen patterns associated with various

- cell subpopulations. *Cell Immunol* 7:275.
26. Kadish JL, Basch RS (1975) Thymic regeneration after lethal irradiation: Evidence for an intrathymic radioresistant T-cell precursor. *J Immunol* 114:452.
  27. Sharp JG, Thomas DB (1975) Thymic regeneration in lethally x-irradiated mice. *Radiat Res* 64:293.
  28. Sharrow SO, Singer A, Hammerling U, Mathieson BJ (1983) Phenotypic characterization of early events of thymus repopulation in radiation bone marrow chimeras. *Transplantation* 35:355.
  29. Korngold R, Bennink JR, Doherty PC (1981) Early dominance of irradiated host cells in the responder profiles of thymocytes from P-F1 radiation chimeras. *J Immunol* 127:124.
  30. Ceredig R, MacDonald HR (1982) Phenotypic and functional properties of murine thymocytes. II. Quantitation of host- and donor-derived cytolytic T-lymphocyte precursors in regenerating radiation bone marrow chimeras. *J Immunol* 128:614.
  31. Bach JF, Dardenne M, Goldstein AL, Guha A, White A (1971) Appearance of T-cell markers in bone marrow rosette-forming cells after incubation with thymosin, a thymic hormone. *Proc Natl Acad Sci USA* 68:2734.
  32. Pazmino NH, Ihle JN, Goldstein AL (1978) Induction in vivo and in vitro of terminal dioxynucleotidyl transferase by thymosin in bone marrow cells from athymic mice. *J Exp Med* 147:708.
  33. Goldschneider I, Ahmed A, Bollum FJ, Goldstein AL (1981) Induction of terminal deoxynucleotidyl transferase and Lyt antigens with thymosin. Identification of multiple subsets of prothymocytes in mouse bone marrow and spleen. *Proc Natl Acad Sci USA* 78:2469.
  34. Zatz MM, Oliver J, Samuels C, Skotnicki AB, Sztein MB, Goldstein AL (1984) Thymosin increases production of T-cell growth factor by normal human peripheral blood lymphocytes. *Proc Natl Acad Sci USA* 81: 2882.

## Acute Toxicity of Petroleum- and Shale-Derived Distillate Fuel, Marine: Light Microscopic, Hematologic, and Serum Chemistry Studies<sup>1</sup>

GEORGE A. PARKER,\* VICTOR BOGO,<sup>†,2</sup> AND ROBERT W. YOUNG<sup>†</sup>

\*P.O. Box 350, Great Falls, Virginia 22066; and <sup>†</sup>Behavioral Sciences Department, Armed Forces Radiobiology Research Institute, Bethesda, Maryland 20814-5145

Acute Toxicity of Petroleum- and Shale-Derived Distillate Fuel, Marine: Light Microscopic, Hematologic, and Serum Chemistry Studies. PARKER, G. A., BOGO, V., AND YOUNG, R. W. (1986). *Fundam. Appl. Toxicol.* 7, 101-105. Rats were gavaged with 60, 48, 38, 30, or 24 ml/kg of either petroleum (P) or shale (S)-derived distillate fuel, marine (DFM). Surviving rats were killed 14 days after dosing. There was a slight difference in toxicity of the two fuels but neither fuel was very toxic. The LD<sub>50</sub>/14 was 43 ml/kg for P-DFM and 50 ml/kg for S-DFM. Lesions in rats that died indicated hepatic and renal toxicity. In another study, rats were gavaged with 24 ml/kg of either P- or S-DFM and killed at 1, 2, or 3 days after dosing. Prominent clinicopathologic findings included loss of body weight, hematologic evidence of dehydration, transient leukopenia, and serum chemistry and histopathologic alterations indicative of mild hepatic and renal toxicity.

© 1986 Society of Toxicology.

As a result of projected shortages in fossil fuels, the U.S. Department of Defense instituted programs to evaluate liquid hydrocarbon fuels derived from alternative fossil sources, namely coal, oil shale, and tar sands (Parker *et al.*, 1981). Current attention centers on shale crude, which has proven to be a reasonable substitute in demonstration trials. Numerous physical and functional characteristics of shale-derived distillate fuel, marine (S-DFM) are being compared to petroleum-derived DFM (P-DFM) in order to determine whether the shale products are suitable for military use.

Knave *et al.* (1976, 1978, 1979) indicated

neurotoxicity associated with long-term exposure to petroleum-derived jet fuel. Work in this laboratory suggested that acute oral or subchronic inhalation exposure to petroleum- or shale-derived JP5 jet fuel is nephrotoxic in rats (Bogo *et al.*, 1983 and 1984; Parker *et al.*, 1981). Systematic toxicity studies on petroleum hydrocarbons were done by Carpenter *et al.* (1978), but no such studies exist for P-DFM or S-DFM. Oral dosing was chosen to obtain data on the lethality of both S-DFM and P-DFM, and to determine sites of pathologic alteration. The present paper describes and compares the early morphologic, hematologic, and serum chemistry changes that occurred in rats following gavage exposure to P- and S-DFM.

### METHODS

*Subjects.* Subjects were male Sprague-Dawley rats (Tac: N(SD)fBR). The first experiment was a 14-day LD<sub>50</sub> study; the other was a 3-day study of serum chemistry, hematology, and histopathology of liver and kidney. Rats were maintained as previously described (Parker *et al.*, 1981).

<sup>1</sup> Research was conducted under Work Unit Number 60215, and according to the principles enunciated in the *Guide for the Care and Use of Laboratory Animals*, prepared by the Institute of Laboratory Resources, National Research Council. This research was supported by the Armed Forces Radiobiology Research Institute, Defense Nuclear Agency (DNA). Views presented in this paper are those of the authors; no endorsement by DNA has been given or should be inferred.

<sup>2</sup> To whom requests for reprints should be sent.



**Fuels.** The P-DFM was refined by Hess St. Croix from a crude mixture consisting primarily of Iranian stock (55%) and Nigerian crude (25%). The S-DFM was derived by the Paraho above-ground retorting process and was refined by Sohio in 1978–1979. The fuels were prepared in accordance with military specifications, with no special additives.

**Fourteen-day varied dose study.** Six groups, each consisting of six male rats ( $368 \pm 3$  g) were gavaged with a plastic syringe and a polyvinyl chloride tube, as described by Parker *et al.* (1981). Rats received the following amounts of either fuel: 60, 48, 38, 30, or 24 ml/kg of body wt. Control rats received 60 ml/kg water. Rats that died during the 2 weeks after fuel administration were necropsied immediately after discovery, gross lesions were recorded, and tissues were fixed in buffered Formalin. Two weeks following fuel exposure, the surviving rats were killed with carbon dioxide, necropsied, and the tissues fixed.

**Three-day uniform-dose study.** Three groups of 18 male rats each ( $315 \pm 3$  g) were gavaged as above with 24 ml/kg of body wt, a nonlethal dose, in the 14-day study. Six rats from each group were killed at 24, 48, and 72 hr after being gavaged. Body weights were taken at gavage and sacrifice. At sacrifice, each rat was anesthetized with methoxyfluorane and approximately 8 ml of blood was collected from the abdominal aorta. One milliliter of blood was placed in glass EDTA anticoagulant tube, and the remainder was allowed to clot.

Histopathology, hematology, and clinical chemistry methodology was as described in the companion JP5 study (Parker *et al.*, 1981).

**Data analysis.** Probit analysis was used to obtain the lethality profiles in the LD50 studies (Finney, 1971). In the 3-day study, the body weight, hematologic, and clinical chemistry data were analyzed by one-way analysis of variance (ANOVA) with a Bonferroni allocation sufficient to each ANOVA to compensate for potential multiple analyses errors (Winer, 1962; Miller, 1981). The Newman-Keuls multiple range tests were used to identify differences between the means of the daily test periods.

## RESULTS

### 14-Day Varied-Dose Studies

**LD50.** The LD50 for P-DFM was 43 ml/kg, with lower and upper 95% confidence limits of 37 and 50 ml/kg, respectively. The LD50 for S-DFM was 50 ml/kg, with lower and upper 95% confidence limits of 40 and 79 ml/kg, respectively.

**Necropsy findings.** There was no consistent pattern of gross lesions in rats that died following DFM administration. Congestion of a

number of organs and accentuation of the hepatic lobular pattern were seen in a few rats. Ventral alopecia was common in rats that survived to termination.

**Microscopic findings.** Congestion of multiple organs was seen in nearly all rats that died following S-DFM gavage, regardless of the survival interval. Congestion was much less common in rats that received P-DFM. Two rats that died following S-DFM gavage had pulmonary edema. Lymphoid depletion in the thymus was seen in six rats that died following S-DFM exposure, in three intercurrent-death rats from the P-DFM group, and in one terminal-kill P-DFM rat. Lymphoid depletion in the spleen accompanied the thymic change in one S-DFM and in one P-DFM rat, both of which died spontaneously. Cytoplasmic vacuolization of periportal hepatocytes was seen in one S-DFM rat that died 67 hr after gavage and in three P-DFM rats that died 66 hr after gavage. The affected rat from the S-DFM exposure group also had karyorrhexis of periportal hepatocytes. Renal hyaline droplet formation was noted in some of the rats that died 60–90 hr after gavage. Suppurative dermatitis was seen in three terminal-kill rats from the S-DFM group, one terminal-kill rat from the P-DFM group, and two rats from the P-DFM group that died spontaneously.

### Three-Day Uniform Dose Studies

**Survival.** All rats from dosed and control groups survived until scheduled termination.

**Body weight.** Terminal body weights of dosed rats were significantly ( $p < 0.05$ ) less than controls on all 3 days. Following P-DFM dosing, there was progressive weight loss throughout the 3-day period. By contrast, weight loss after S-DFM was maximal at Day 2.

**Hematology.** Significant differences among test and control groups were noted in the packed cell volume (PCV), red blood cell (RBC), white blood cell (WBC), hemoglobin values, mean corpuscular volume (MCV), mean corpuscular hemoglobin (MCH), and

absolute neutrophil and lymphocyte counts (Table 1). Eosinophil counts, basophil counts, monocyte counts, relative neutrophil counts,

and mean corpuscular hemoglobin content were approximately equal in dosed versus control rats (data not presented).

*Serum chemistry and electrolytes.* Significant differences were noted in urea nitrogen (BUN), creatinine, alkaline phosphatase, creatine phosphokinase (CPK), lactate dehydrogenase (LDH), glutamic oxaloacetic transaminase (SGOT), glutamic pyruvic transaminase (SGPT), sodium, and potassium (Table 2).

*Necropsy findings.* There was no consistent pattern of gross lesions in the P-DFM or S-DFM groups.

*Microscopic findings.* Mild to moderate cytoplasmic vacuolization of periportal hepatocytes was seen in nearly all dosed rats that were killed on Days 2 and 3, regardless of the type of fuel administered. The lesion was most severe on Day 3 in both groups, and on each day was more severe in the P-DFM group. The sharply bounded cytoplasmic vacuoles stained positively with oil red O on frozen sections. Periportal hepatocytic karyorrhexis and mitotic figures were seen in both groups, beginning at Day 2. Hyaline droplet degeneration was noted in the renal cortex of rats from both groups. These changes were first noted on Day 2, but were most prominent and numerous on Day 3.

## DISCUSSION

The survival data in the 14-day study indicated only a slight difference in toxicity of P- and S-DFM; neither type of fuel was highly toxic. The differences in toxicity may be related to the origin and chemical constituents of the raw crude or the refining process (Parker *et al.*, 1981).

Morphologic and serum chemistry changes in the 3-day study suggested that liver and kidney alterations were produced by both fuels, as was found in a previous study of shale- and petroleum-derived JP5 (Parker *et al.*, 1981). The periportal distribution of the hepatic lesions in the 3-day study was notably

TABLE 1  
HEMATOLOGY

	Day 1	Day 2	Day 3
Hematocrit (PVC) (%)			
Control <sup>a</sup>	44 ± 0.4	42 ± 0.8	41 ± 0.5
Petroleum <sup>b</sup>	47 ± 1.0 <sup>c</sup>	45 ± 0.8 <sup>c</sup>	42 ± 1.3
Shale <sup>b</sup>	43 ± 1.0	43 ± 1.0	39 ± 0.6 <sup>c</sup>
Red blood cells/ $\mu$ l (RBC) ( $\times 10^6$ )			
Control	6.50 ± 0.1	6.13 ± 0.2	6.33 ± 0.1
Petroleum	7.49 ± 0.2 <sup>c</sup>	6.87 ± 0.2 <sup>c</sup>	6.31 ± 0.2
Shale	6.63 ± 0.3	6.52 ± 0.2	6.14 ± 0.1
White blood cells/ $\mu$ l (WBC) ( $\times 10$ )			
Control	623 ± 58	458 ± 50	402 ± 74
Petroleum	220 ± 26 <sup>c</sup>	230 ± 28 <sup>c</sup>	667 ± 144
Shale	146 ± 19 <sup>c</sup>	232 ± 42 <sup>c</sup>	478 ± 85
Hemoglobin (gm/dl)			
Control	14.2 ± 0.2	13.8 ± 0.3	13.6 ± 0.2
Petroleum	15.3 ± 0.3 <sup>c</sup>	14.7 ± 0.2 <sup>c</sup>	13.8 ± 0.4
Shale	13.9 ± 0.3	14.1 ± 0.3	12.9 ± 0.1
Mean corpuscular volume (MCV) (fliters)			
Control	67.5 ± 0.5	68.2 ± 1.2	65.0 ± 0.5
Petroleum	63.1 ± 0.6 <sup>c</sup>	66.1 ± 0.7	65.8 ± 0.5
Shale	65.7 ± 2.1	66.2 ± 0.8	63.8 ± 1.0
Mean corpuscular hemoglobin (MCH) (pg)			
Control	21.8 ± 0.2	22.5 ± 0.3	21.4 ± 0.3
Petroleum	20.5 ± 0.3 <sup>c</sup>	20.5 ± 0.3 <sup>c</sup>	21.8 ± 0.2
Shale	21.2 ± 0.9	21.2 ± 0.9	21.1 ± 0.3
Absolute neutrophil (count/ $\mu$ l)			
Control	499 ± 107	402 ± 74	413 ± 112
Petroleum	224 ± 29 <sup>c</sup>	241 ± 47	1410 ± 718
Shale	165 ± 37 <sup>c</sup>	114 ± 35 <sup>c</sup>	661 ± 162
Absolute lymphocyte count/ $\mu$ l ( $\times 10$ )			
Control	538 ± 62	414 ± 44	324 ± 82
Petroleum	197 ± 24 <sup>c</sup>	205 ± 27 <sup>c</sup>	510 ± 76 <sup>c</sup>
Shale	127 ± 16 <sup>a</sup>	217 ± 39 <sup>c</sup>	406 ± 73

<sup>a</sup> Control values are mean  $\pm$  SE of the mean for six rats/group gavaged on Day 0 with 24 ml water/kg body wt.

<sup>b</sup> Values for petroleum and shale are mean  $\pm$  SE of the mean for six rats/group gavaged on Day 0 with 24 ml DFM/kg body wt.

<sup>c</sup> Significant at  $p \leq 0.05$  as compared to control.

TABLE 2  
SERUM CHEMISTRIES AND ELECTROLYTES

	Day 1	Day 2	Day 3
Blood urea nitrogen (BUN) (mg/dl)			
Control <sup>a</sup>	21 ± 1	21 ± 1	24 ± 1
Petroleum <sup>b</sup>	22 ± 1	32 ± 2 <sup>c</sup>	25 ± 2
Shale <sup>b</sup>	22 ± 2	26 ± 2 <sup>c</sup>	21 ± 2
Creatinine (mg/dl)			
Control	0.9 ± 0.04	0.9 ± 0.02	0.9 ± 0.03
Petroleum	1.3 ± 0.09 <sup>c</sup>	1.5 ± 0.07 <sup>c</sup>	1.4 ± 0.06 <sup>c</sup>
Shale	1.7 ± 0.13 <sup>c</sup>	1.7 ± 0.05 <sup>c</sup>	1.2 ± 0.06 <sup>c</sup>
Alkaline phosphatase (IU/liter)			
Control	114 ± 4	145 ± 9	142 ± 6
Petroleum	143 ± 8 <sup>c</sup>	243 ± 23 <sup>c</sup>	260 ± 28 <sup>c</sup>
Shale	136 ± 13	152 ± 9	197 ± 9 <sup>c</sup>
Creatine phosphokinase (CPK) (IU/liter)			
Control	214 ± 19	166 ± 24	130 ± 21
Petroleum	174 ± 14	179 ± 31	215 ± 23 <sup>c</sup>
Shale	209 ± 32	192 ± 16	256 ± 41 <sup>c</sup>
Lactate dehydrogenase (LDH) (IU/liter)			
Control	1035 ± 103	1085 ± 73	1059 ± 123
Petroleum	1371 ± 114 <sup>c</sup>	1975 ± 170 <sup>c</sup>	1625 ± 159 <sup>c</sup>
Shale	1250 ± 71 <sup>c</sup>	1875 ± 238 <sup>c</sup>	1520 ± 178
Glutamic oxaloacetic transaminase (SGOT) (IU/liter)			
Control	77 ± 4	77 ± 2	74 ± 4
Petroleum	117 ± 10 <sup>c</sup>	230 ± 28 <sup>c</sup>	135 ± 8 <sup>c</sup>
Shale	113 ± 3 <sup>c</sup>	142 ± 21 <sup>c</sup>	111 ± 7 <sup>c</sup>
Glutamic pyruvic transaminase (SGPT) (IU/liter)			
Control	16 ± 1	16 ± 1	13 ± 1
Petroleum	37 ± 4	83 ± 17 <sup>c</sup>	37 ± 3 <sup>c</sup>
Shale	38 ± 1 <sup>c</sup>	47 ± 12 <sup>c</sup>	28 ± 2 <sup>c</sup>
Serum Na <sup>+</sup> (meq/liter)			
Control	150 ± 0.2	152 ± 1.8	154 ± 1.2
Petroleum	154 ± 0.7 <sup>c</sup>	155 ± 0.9	158 ± 0.6 <sup>c</sup>
Shale	156 ± 0.6 <sup>c</sup>	157 ± 0.9 <sup>c</sup>	158 ± 0.6 <sup>c</sup>
Serum K <sup>+</sup> (meq/liter)			
Control	4.7 ± 0.08	5.2 ± 0.17	5.0 ± 0.09
Petroleum	5.7 ± 0.22 <sup>c</sup>	5.8 ± 0.13 <sup>c</sup>	5.4 ± 0.18
Shale	5.1 ± 0.06 <sup>c</sup>	5.6 ± 0.19	5.9 ± 0.17 <sup>c</sup>

<sup>a</sup> Control values are mean ± SE of mean for six rats/group gavaged on Day 0 with 24 ml water/kg body wt.

<sup>b</sup> Values for petroleum and shale are mean ± SE of mean for six rats/group gavaged on Day 0 with 24 ml DFM/kg body wt.

<sup>c</sup> Significant at  $p \leq 0.05$ .

different from the centrilobular changes which are seen with classical hepatotoxins such as carbon tetrachloride (Recknagel, 1967; Robbins, 1974). Periportal hepatocytic degeneration has been associated with particularly potent hepatotoxins (Smith *et al.*, 1983), but in this study other data do not indicate that these compounds were potent hepatotoxins.

Hyaline droplet formation in the renal tubular epithelium is known to result when an increased amount of protein passes the glomerulus (Straus and Oliver, 1955), and may follow impairment of the mechanism by which the tubular epithelial cells degrade pinocytosed protein (Oliver *et al.*, 1954). The possibility of renal vascular damage has been proposed following chronic dermal application of DFM in mice (Easley *et al.*, 1982), and this may include damage to glomerular capillaries.

Weight loss in the 3-day study was attributed to dehydration and inappetance. Hematologic findings indicated that dehydration was a major contributor to the weight loss in rats which received P-DFM, while inappetance alone appeared to be the major contributor in the S-DFM rats. Additional studies in which feed and water consumption were measured (Bogo and Young, 1983) revealed a significant reduction in feed and water consumption for at least 2 days following administration of 24 ml/kg of S-DFM.

Alterations in neutrophil and lymphocyte counts were compatible with early migration of neutrophils to some extravascular site, perhaps inflamed gastrointestinal tract or skin, and depletion of lymphocytes due to stress and adrenocorticosteroid release (Miale, 1977). The alterations in serum electrolyte levels were presumed to reflect altered renal function.

In conclusion, neither fuel appeared to be highly toxic. Oral administration resulted in renal and hepatic damage, as indicated by morphologic alterations and changes in serum chemical indicators of renal and hepatic function. S-DFM was slightly less toxic than P-DFM, as evidenced by lethality, serum chemistry, and histopathologic lesions. Further research is required to identify (a) the mech-



anism of toxicity at the cellular and subcellular level, and (b) the toxic chemical components in these complex compounds.

### ACKNOWLEDGMENTS

We are grateful to Mr. Chester A. Boward, Ms. June Egan, Ms. Carol L. Feser, and Mr. Gerald G. Kessell for their technical assistance.

### REFERENCES

- BOGO, V., AND YOUNG, R. W. (1983). Effects of petroleum- and shale-derived diesel fuel marine (DFM) on the behavior of rats. In *Proceedings of the Fourth Annual Meeting of the American College of Toxicology*. Washington, D.C.
- BOGO, V., YOUNG, R. W., HILL, T. A., CARTLEDGE, R. M., NOLD, J., AND PARKER, G. A. (1984). Neurobehavioral toxicology of petroleum- and shale-derived jet propulsion fuel No. 5 (JP5). In *Advances in Modern Environmental Toxicology, Volume VI: Applied Toxicology of Petroleum Hydrocarbons*, (M. A. Mehlman, ed.). Princeton Scientific, Princeton, N.J.
- BOGO, V., YOUNG, R. W., HILL, T. A., FESER, C. L., NOLD, J., PARKER, G. A., AND CARTLEDGE, R. M. (1983). The toxicity of petroleum and shale JP5. In *Proceedings of the American Petroleum Institute Meeting, The Toxicology of Petroleum Hydrocarbons*. Washington, D.C.
- CARPENTER, C. P., GEARY, G. L., MYERS, R. C., NACHREINER, D. J., SULLIVAN, L. J., AND KING, J. M. (1978). Petroleum hydrocarbon toxicity studies. XVII. Animal response to n-Nonane vapor. *Toxicol. Appl. Pharmacol.* **44**, 53-61.
- EASLEY, J. R., HOLLAND, J. M., GIPSON, L. C., AND WHITTAKER, M. J. (1982). Renal toxicity of middle distillates of shale and petroleum in mice. *Toxicol. Appl. Pharmacol.* **65**, 84-91.
- FINNEY, D. J. (1971). *Probit Analysis*. Cambridge Univ. Press, London.
- KNAVE, B., MINDUS, P., AND STRUWE, G. (1979). Neurasthenic symptoms in workers occupationally exposed to jet fuel. *Acta Psychiatr. Scand.* **60**, 39-49.
- KNAVE, B., OLSON, B. A., ELOFSSON, S., GAMBERALE, F., ISAKSSON, A., MINDUS, P., PERSSON, H. E., STRUWE, G., WENNBERG, A., AND WESTERHOLM, P. (1978). Long-term exposure to fuel. II. A cross-sectional epidemiological investigation on occupationally exposed industrial workers with special reference to the nervous system. *Scand. J. Work Environ. Health* **4**, 19-45.
- KNAVE, B., PERSSON, H. E., GOLDBERG, J. M., AND WESTERHOLM, P. (1976). Long-term exposure to jet fuel. An investigation on occupationally exposed workers with special reference to the nervous system. *Scand. J. Work Environ. Health* **3**, 152-164.
- MIALE, J. B. (1977). *Laboratory Medicine: Hematology*. Mosby, St. Louis.
- MILLER, R. G., JR. (1981). *Simultaneous Statistical Inference*, p. 8. Springer-Verlag, New York.
- OLIVER, J., MACDOWELL, M., AND LEE, Y. C. (1954). Cellular mechanisms of protein metabolism in the nephron: I. The structural aspects of proteinuria; tubular absorption, droplet formation, and the disposal of protein. *J. Exp. Med.* **99**, 589-604.
- PARKER, G. A., BOGO, V., AND YOUNG, R. W. (1981). Acute toxicity of conventional versus shale-derived JP5 jet fuel: Light microscopic, hematologic, and serum chemistry studies. *Toxicol. Appl. Pharmacol.* **57**, 302-317.
- RECKNAGEL, R. O. (1967). Carbon tetrachloride hepatotoxicity. *Pharmacol. Rev.* **19**, 145-208.
- ROBBINS, S. L. (1974). *Pathologic Basis of Disease*, p. 521. Saunders, Philadelphia.
- SMITH, H. A., JONES, T. C., AND HUNT, R. D. (1983). *Veterinary Pathology*, p. 1416. Lea and Febiger, Philadelphia.
- STRAUS, W., AND OLIVER, J. (1955). Cellular mechanisms of protein metabolism in the nephron: VI. The immunological demonstration of egg white in droplets and other cellular fractions of the rat kidney after intraperitoneal injection. *J. Exp. Med.* **102**, 1-9.
- WINER, B. J. (1962). *Statistical Principles in Experimental Design*. McGraw-Hill, New York.

# Role of the Area Postrema in Radiation-Induced Taste Aversion Learning and Emesis in Cats<sup>1</sup>

BERNARD M. RABIN,\*†‡ WALTER A. HUNT,\* ALAN L. CHEDESTER‡  
AND JACK LEE\*

*\*Behavioral Sciences Department, Armed Forces Radiobiology Research Institute  
Bethesda, MD 20814-5145*

*†Department of Psychology, University of Maryland Baltimore County, Catonsville, MD 21228  
and ‡Walter Reed Army Institute of Research, Washington DC 20307*

Received 6 March 1986

RABIN, B. M., W. A. HUNT, A. L. CHEDESTER AND J. LEE. *Role of the area postrema in radiation-induced taste aversion learning and emesis in cats.* *PHYSIOL BEHAV* 37(5) 815-818, 1986.—The role of the area postrema in radiation-induced emesis and taste aversion learning and the relationship between these behaviors were studied in cats. The potential involvement of neural factors which might be independent of the area postrema was minimized by using low levels of ionizing radiation (100 rads at a dose rate of 40 rads/min) to elicit a taste aversion, and by using body-only exposures (4500 and 6000 rads at 450 rads/min) to produce emesis. Lesions of the area postrema disrupted both taste aversion learning and emesis following irradiation. These results, which indicate that the area postrema is involved in the mediation of both radiation-induced emesis and taste aversion learning in cats under these experimental conditions, are interpreted as being consistent with the hypotheses that similar mechanisms mediate both responses to exposure to ionizing radiation, and that the taste aversion learning paradigm can therefore serve as a model system for studying radiation-induced emesis.

Emesis      Taste aversion      Radiation      Cat      Area postrema

A conditioned taste aversion (CTA) is produced when a novel tasting solution is paired with exposure to ionizing radiation, such that the organism will avoid ingestion of that solution at a subsequent presentation. In common with many chemical toxins, irradiation not only will produce a CTA, but will also cause vomiting in organisms that are capable of making that response. Because the functional effects of a CTA are similar to those of emesis, to limit the intake and/or absorption of toxic substances, it has been proposed that both CTA and emesis are part of a "gut defense system" that functions to maintain internal homeostasis within the organism [6,7]. As such, it has been suggested that the CTA paradigm can serve as a model system for the study of emesis [18].

For the most part, the study of the neural mechanisms of both emesis and CTA learning has focused on the role of the area postrema (AP), the brainstem chemoreceptive trigger zone, in mediating these behaviors [2, 4, 12-14]. If, as suggested above, CTA and emesis are related behaviors in the maintenance of internal homeostasis and if CTA can

serve as a model system for the study of emesis, then similar neural mechanisms should be involved in the regulation of both behaviors [16]. Because cats show both responses following exposure to ionizing radiation [9], they would seem to provide the best animal model for studying the relationship between CTA and emesis. However, while AP lesions in the rat disrupt the acquisition of a CTA following exposure to ionizing radiation [12-14], these lesions have been reported to be ineffective in disrupting radiation-induced emesis in the cat [1,11]. In this regard, cats differ from both dogs and monkeys in which AP lesions prevent radiation-induced emesis [3, 8, 22].

It may be, however, that the AP mediation of the emetic response to irradiation, like the CTA response [15], depends upon the dose used. Compared to dogs, in which the ED<sub>100</sub> is 800 rads [5], and monkeys, in which the ED<sub>100</sub> is 600 rads [10], the approximately 5500 rads needed to elicit consistent emesis in the cat [1,11] is so high that other neural mechanisms unrelated to the AP may be involved. It may be that AP lesions are not effective in disrupting radiation-induced

<sup>1</sup>We would like to gratefully acknowledge the assistance of Dr. Herbert L. Borison, who generously shared his knowledge of the procedures for making area postrema lesions in the cat with us. We also wish to acknowledge the support of the Veterinary Medicine Department of AFRRRI for its invaluable assistance with the surgical and histological procedures. This research was conducted according to the principles described in the "Guide for the Care and Use of Laboratory Animals" prepared by the Institute of Laboratory Animal Research, National Research Council.

<sup>2</sup>Requests for reprints should be addressed to Bernard M. Rabin, Department of Psychology, University of Maryland Baltimore County, Catonsville, MD 21228.

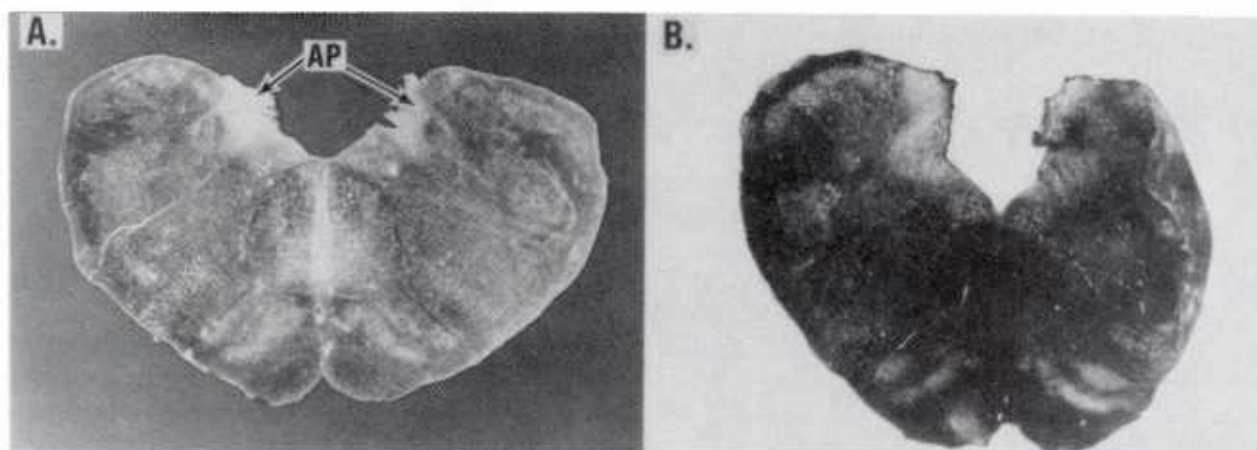


FIG. 1. Photomicrographs of representative sections of the brainstem of an intact cat showing the area postrema (A, "AP"), and a cat with lesions of the area postrema (B).

emesis in cats, in contrast to the effects of the lesions on vomiting in dogs and monkeys and on CTA learning in rats, because the effective dose in cats is so high that other, non-AP-mediated, mechanisms are brought into play.

An alternative hypothesis to account for these differences in the effectiveness of AP lesions involves the possibility that because the CTA is a conditioned response to a conditioned stimulus while emesis is an unconditioned response to an unconditioned stimulus, different neural mechanisms may mediate the two responses to irradiation. Similarly the failure of AP lesions to disrupt emesis in cats, in contrast to the effectiveness of the lesions in disrupting CTA learning in rats and emesis in dogs and monkeys, may be due to species differences (e.g., [18]), in the role of the AP in mediating these behaviors and to the fact that CTA learning is typically studied in rats which are incapable of vomiting.

The present experiments were designed to evaluate the role of the AP in radiation-induced emesis in the cat and its relationship with CTA learning under conditions that might be expected to minimize the involvement of neural mechanisms that are unrelated to the AP. These conditions involved the use of low dose (100 rad) irradiation for CTA learning and the use of head shielding for emesis. If the neural mechanisms of CTA and emesis involve similar AP-mediated mechanisms and if the dose and site of irradiation are critical factors in accounting for the failure to observe an effect of AP lesions on radiation-induced emesis in the cat, then AP lesions should be equally effective in disrupting both CTA learning and emesis under these experimental conditions.

#### METHOD

##### Subjects

The subjects were 40 cats weighing 4.5–5.5 kg at the start of the experiment. Twenty intact cats served as subjects for the CTA experiment. An additional 3 intact cats and the 6 sham-operated cats served as subjects for the emesis testing. All 11 cats with lesions of the AP participated first in the CTA experiment and then, 2–4 weeks later, in the emesis experiment. The cats were housed in individual cages in a room with a 12:12 light:dark cycle. Food and water were

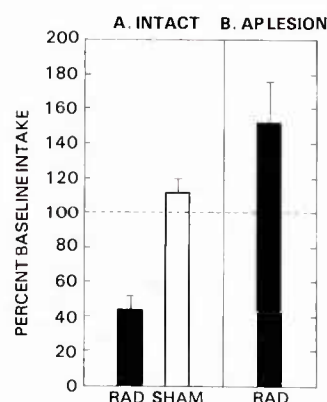


FIG. 2. Taste aversion learning in intact cats (A) and cats with lesions of the area postrema (B) following exposure to ionizing radiation (100 rads at a dose rate of 40 rads/min). Test day intake is presented as the percentage of conditioning day intake. Error bars indicate the standard error of the mean.

continually available except as required by the experimental protocol.

##### Surgery and Histology

Lesions were placed in the AP of 11 cats while 6 cats served as sham operated controls. All surgery was performed under sterile conditions using the procedures detailed by Borison and his coworkers [1, 20, 21]. Briefly, the cats were anesthetized with halothane and the AP was exposed. The tissue was destroyed using a cautery probe under direct visual control. For the sham-operated controls, the AP was exposed but not cauterized. Following surgery, all cats were given 3–4 months to recover from the effects of the surgery before beginning behavioral testing.

At the conclusion of the emesis testing, all operated cats were given an IV injection of T-61. They were then perfused intracardially with isotonic saline followed by 10% formalin saline. The brains were fixed in 10% formalin saline and 50  $\mu$ m sections were cut through the brainstem at the level of



TABLE 1  
EFFECTS OF RADIATION AND AP LESIONS ON CS INTAKE

Condition	Conditioning Day Intake (ml)	Test Day Intake (ml)
Intact		
Radiation	101.80 $\pm$ 16.38*	50.25 $\pm$ 13.60
Sham Exposure	102.50 $\pm$ 17.76	106.70 $\pm$ 15.57
AP Lesion		
Radiation	76.00 $\pm$ 12.63	97.56 $\pm$ 12.88

\*Mean  $\pm$  Standard Error of the Mean.

the AP and stained with thionin. Representative samples of the brainstem of an intact and a lesion animal are shown in Fig. 1.

#### Procedure

Taste aversions were established in cats using a modification of the procedure described by Kimeldorf *et al.* [9]. Briefly, all cats were deprived of food and water starting 20 hr prior to the conditioning day. On the conditioning day they were presented with a measured amount of the conditioned stimulus (CS), either milk flavored with 5% vanilla extract (v/v) or eggnog, for 1 hr, and their intake measured. In order to make certain that the cats had sampled a sufficient quantity of the CS to observe a CTA, any cat which did not show an intake of at least 15 ml of the CS was excluded from the experiment. Immediately following the drinking period, the experimental cats were exposed to ionizing radiation using a  $^{60}\text{Co}$  source. The sham-irradiated control cats were carried to the source, but not exposed. Four hr later, food and water were returned for 24 hr. Food and water were then removed for 20 hr before the test day. On the test day, the cats were again presented with the CS for 1 hr and intake recorded.

For radiation-induced emesis, all cats were deprived of food and water for 24 hr. One hr prior to the scheduled exposure time, food and water were returned. The cats were then exposed to a  $^{60}\text{Co}$  source and returned to their home cages. All cats were monitored continually for emesis for 3–4 hr post-irradiation and intermittently for an additional 1–2 hr. Those cats which did not vomit within this time period were typically allowed to survive over night and their cages were inspected for signs of emesis the following morning. All cats were sacrificed within 24 hr following irradiation.

#### Radiation

For radiation exposure, the cats were placed in a clear plastic restraining cage, and carried to a  $^{60}\text{Co}$  source. For the CTA experiment, the cats were given a whole-body unilateral exposure of 100 rads at a dose rate of 40 rads/min. For the emesis experiment, the cats were given unilateral, body-only exposures of either 4500 or 6000 rads at a dose rate of 450 rads/min. Shielding for the head was provided by combining lead bricks to a thickness of approximately 11 cm in an "L"-shaped pattern, such that the shielding ran from the shoulder of the cat on the side facing the source around the front of the animal's head.

Dosimetry was performed using a 3.3 ml Victoreen chamber and using thermoluminescent detectors (LIF TLD

TABLE 2  
AP LESIONS AND RADIATION-INDUCED EMESIS IN CATS

Condition	n	Dose (rad)	Frequency of Emesis	Mean Latency (min)	Range (min)
Intact	3	4500	3	106	60–178
Sham Operated	3	6000	3	86	52–120
	3	4500	3	124	72–163
AP Lesion	4	6000	0	—	—
	7	4500	0	—	—

100s) on a cat phantom. The dosimetry indicated that the shoulders of the cat received an exposure of 4.6% of the total dose, while at the base of the skull the exposure dropped off to 2.5% and at the nose of the cat it was 1.4% of the total dose. This means that for the 6000 rad irradiation, the brainstem was exposed to a dose of approximately 150 rads while the exposure level at the nose of the cat was only 80 rads. Therefore, the brains of the subjects were only exposed to radiation doses well below the reported thresholds for eliciting radiation-induced emesis.

#### RESULTS

The effect of AP lesions on the acquisition of a radiation-induced CTA in cats is summarized in Fig. 2, which presents test day CS intake as the percentage of conditioning day CS intake. Exposing intact cats to 100 rads whole-body radiation produced a significant decrease in CS intake relative to their pre-exposure intake,  $t(9)=5.42$ ,  $p<0.001$ . In contrast, both the sham-irradiated intact control cats,  $t(9)=1.26$ ,  $p<0.10$ , and the irradiated cats with AP lesions,  $t(8)=1.74$ ,  $p<0.10$ , showed nonsignificant increases in CS intake on the test day (Table 1). Analysis of the individual intakes of the irradiated cats indicated that 9 of the 10 intact cats showed a test day reduction in CS intake, while only 1 of the 9 cats with AP lesions showed a similar reduction in intake.

The data on the effects of AP lesions on emesis produced by body-only irradiation are presented in Table 2. Of the 9 control cats, all vomited within 3 hr following exposure to either 4500 or 6000 rad doses of ionizing radiation. The major difference between the two doses was the slightly shorter latency in which emesis was observed following exposure to the higher dose. There were no major differences between the responses of the cats that had undergone the control surgical procedures and those that had not. In contrast to the controls, no signs of emesis were observed in any of the 11 cats with AP lesions.

Examination of the histological material of the operated cats showed that the extent of the brainstem lesions was somewhat variable, ranging from lesions that were restricted to the AP to lesions that encompassed varying amounts of surrounding tissue, including portions of the nucleus of the solitary tract and the dorsal motor nucleus of the vagus. However, because the AP was the only brainstem structure that was consistently included within the region of tissue destruction across all 11 operated cats, it seems reasonable to infer that the disruption of the radiation-induced emesis by these lesions must have involved the destruction of the AP; although the participation of adjacent structures in this behavior cannot be completely ruled out.

## DISCUSSION

The present results on radiation-induced taste aversion learning in the cat are in agreement with previous research [9] showing that exposing cats to non-lethal levels of ionizing radiation is sufficient to lead to the acquisition of a CTA. In addition, these results clearly show that this behavioral response to ionizing radiation is mediated by the AP in the cat, as in the rat [12–14].

With regard to radiation-induced vomiting the present data similarly show that lesions involving the AP and adjacent structures will disrupt the emetic response to ionizing radiation under experimental conditions that have been designed to minimize the involvement of brain mechanisms that may be independent of the AP. In the present experiment, these conditions were met by shielding the head of the cat during irradiation. As such these results would be consistent with the hypothesis that the high dose of radiation needed to produce emesis in the cat, in contrast to the dose needed in the dog or monkey [5,10], may activate mechanisms that do not involve the AP in the regulation of the behavior. This observation would be consistent with the results of studies of CTA learning in the rat which have shown that AP lesions are less effective in disrupting the acquisition of a CTA when the radiation is restricted to the head of the organism [15]. Similarly, other research using rats has shown that AP lesions are less effective in disrupting CTA learning when the dose of a toxin (WR-2721) is increased to levels much greater than required to produce a CTA [17].

These factors, the dose and site of irradiation, probably account for the differences between the present data and the data reported by Borison [1,11] who found that AP lesions

had no effect on radiation-induced emesis. In his experiments, high-dose, whole-body irradiation was used to produce emesis. These conditions might be expected to facilitate the involvement of mechanisms not restricted to the AP in the regulation of emesis. In contrast, the partial-body exposures used in the present experiments might be expected to minimize the involvement of such factors.

While some of the lesions in the present experiment did extend beyond the borders of the AP, it is not likely that this additional tissue destruction was a key factor in the observed disruption of radiation-induced emesis for several reasons. First, a comparison of the lesions which were restricted to the AP with those that included additional tissue indicated that there were no differences in the effectiveness of the different lesions in producing disruption of the radiation-induced emesis. Second, Harding *et al.* [8] have shown that the disruption of radiation-emesis in the dog does not depend upon the inclusion of brainstem tissue adjacent to the AP, but is also observed when the lesions are completely restricted to that structure. Therefore, it seems most likely that the disruption of radiation-induced emesis in cats observed in the present experiment resulted from the combination of the AP lesions with the partial-body exposures.

The present results, which clearly show that lesions of the AP in cats disrupt both emesis and CTA learning following exposure to ionizing radiation, are consistent, therefore, with the hypotheses proposed above that both radiation-induced emesis and radiation-induced CTA learning are mediated by the same neural structure, the AP, and that the CTA paradigm can be used as a model system for the study of radiation-induced emesis.

## REFERENCES

1. Borison, H. L. Site of emetic action of X-radiation in the cat. *J Comp Neurol* 107: 439–453, 1957.
2. Borison, H. L. Area postrema: Chemoreceptive trigger zone for emesis—is that all? *Life Sci* 14: 1807–1817, 1974.
3. Brizzee, K. R. Effect of localized brain stem lesions and supradiaphragmatic vagotomy on X-irradiation emesis in the monkey. *Am J Physiol* 187: 567–570, 1970.
4. Carpenter, D. O., D. B. Briggs and N. Strominger. Behavioral and electrophysiological studies of peptide-induced emesis in dogs. *Fed Proc* 43: 2952–2954, 1984.
5. Chinn, H. I. and S. C. Wang. Locus of emetic action following irradiation. *Proc Soc Exp Biol Med* 85: 472–474, 1954.
6. Coil, J. D., R. C. Rogers, J. Garcia and D. Novin. Conditioned taste aversions: Vagal and circulatory mediation of the toxic unconditioned stimulus. *Behav Biol* 24: 509–519, 1978.
7. Garcia, J., P. S. Lasiter, F. Bermudez-Rattoni and D. A. Deems. A general theory of taste aversion learning. *Ann NY Acad Sci* 443: 8–21, 1985.
8. Harding, R. K., H. Hugenholz, M. Keany and J. Kucharczyk. Discrete lesions of the area postrema abolish radiation-induced emesis in the dog. *Neurosci Lett* 53: 95–100, 1985.
9. Kimeldorf, D. J., J. Garcia and D. O. Rubadeau. Radiation-induced conditioned avoidance behavior in rats, mice and cats. *Radiat Res* 12: 710–718, 1960.
10. Mattson, J. L. and M. G. Yochmowitz. Radiation-induced emesis in monkeys. *Radiat Res* 83: 191–198, 1980.
11. McCarthy, L. E., H. L. Borison and E. B. Douple. Radiation-induced emesis in cats prevented by 24-hr prior exposure but not ablation of the area postrema. Abstract of paper presented at the 33rd Meeting of the Radiation Research Society, Los Angeles, CA, 1985.
12. Ossenkopp, K.-P. Taste aversions conditioned with gamma radiation: Attenuation by area postrema lesions in rats. *Behav Brain Res* 7: 295–305, 1983.
13. Ossenkopp, K.-P. and L. Giugno. Taste aversions conditioned with multiple exposures to gamma radiation: Abolition by area postrema lesions in rats. *Brain Res* 346: 1847, 1985.
14. Rabin, B. M., W. A. Hunt and J. Lee. Attenuation of radiation- and drug-induced conditioned taste aversions following area postrema lesions in the rat. *Radiat Res* 93: 388–394, 1983.
15. Rabin, B. M., W. A. Hunt and J. Lee. Effects of dose and of partial body ionizing radiation on taste aversion learning in rats with lesions of the area postrema. *Physiol Behav* 32: 119–122, 1984.
16. Rabin, B. M., W. A. Hunt and J. Lee. Recall of a previously acquired conditioned taste aversion in rats following lesions of the area postrema. *Physiol Behav* 32: 503–506, 1984.
17. Rabin, B. M., W. A. Hunt and J. Lee. Effect of area postrema lesions on taste aversions produced by treatment with WR-2721 in the rat. *Neurobehav Toxicol Teratol* 8: 83–87, 1986.
18. Rabin, B. M., W. A. Hunt, A. C. Bakarich, A. L. Chedester and J. Lee. Angiotensin II-induced taste aversion learning in cats and rats and the role of the area postrema. *Physiol Behav* 36: 1173–1178, 1986.
19. Smith, J. C., J. T. Blumsack, F. S. Bilek, A. C. Spector, G. R. Hollander and D. L. Baker. Radiation-induced taste aversion as a factor in cancer therapy. *Cancer Treat Rep* 68: 1219–1227, 1984.
20. Tron, C. D., J. A. Riancho and H. L. Borison. Lack of protection against ouabain cardiotoxicity after chronic ablation of the area postrema in cats. *Exp Neurol* 85: 574–583, 1984.
21. Wang, S. C. and H. L. Borison. The vomiting center: A critical experimental analysis. *Arch Neurol Psychiatr* 63: 928–941, 1950.
22. Wang, S. C., A. A. Renzi and H. I. Chinn. Mechanisms of emesis following X-irradiation. *Am J Physiol* 193: 335–339, 1958.

## Radioprotective Properties of Detoxified Lipid A from *Salmonella minnesota* R595

STEPHEN L. SNYDER, THOMAS L. WALDEN,<sup>1</sup> MYRA L. PATCHEN,  
THOMAS J. MACVITTIE, AND PINHAS FUCHS<sup>2</sup>

*Biochemistry and Experimental Hematology Departments, Armed Forces Radiobiology  
Research Institute, Defense Nuclear Agency, Bethesda, Maryland 20814-5145*

SNYDER, S. L., WALDEN, T. L., PATCHEN, M. L., MACVITTIE, T. J., AND FUCHS, P. Radioprotective Properties of Detoxified Lipid A from *Salmonella minnesota* R595. *Radiat. Res.* **107**, 107-114 (1986).

In the past, the toxicity of bacterial lipopolysaccharide (LPS) or its principal bioactive component, lipid A, has detracted from their potential use as radioprotectants. Recently, a relatively nontoxic monophosphoryl Lipid A (LAM) that retains many of the immunobiologic properties of LPS has been isolated from a polysaccharide deficient Re mutant strain of *Salmonella minnesota* (R595). The ability of the native endotoxic glycolipid (GL) from *S. minnesota* (R595) as well as diphosphoryl lipid A (LAD) and nontoxic monophosphoryl lipid A (LAM) derived from GL to protect LPS responsive (CD2F1 or C3H/HeN) and nonresponsive (C3H/HeJ) mice from <sup>60</sup>Co γ irradiation has been studied. Administration of GL, LAD, or LAM to CD2F1 or C3H/HeN mice (400 μg/kg) 24 h prior to exposure provided significant radioprotection. No protection was afforded to C3H/HeJ mice. Experiments were also conducted to determine the relative abilities of GL, LAD, and LAM to stimulate hematopoiesis as reflected by the endogenous spleen colony (E-CFU) assay. Protection was not correlated with the ability of these substances to increase E-CFUs or to induce colony-stimulating activity (CSA). © 1986 Academic Press, Inc.

### INTRODUCTION

Endotoxic lipopolysaccharide (LPS) has long been known to protect mice against lethal doses of ionizing radiation (1, 2). In addition, LPS elicits numerous immunobiologic responses capable of enhancing host resistance to infectious agents (3) or malignant tumors (4, 5). Several investigators have chemically or physically altered the structure of native LPS in an attempt to reduce its toxicity while maintaining its beneficial properties (6-8). Protection against ionizing radiation has been achieved using LPS derivatives that have been detoxified by alkylation (9), emulsification (10), radiation exposure (7), treatment with chromium ions (8), and hydrolysis (11). Previous studies using various LPS fragments obtained by sequential hydrolysis suggest that the radioprotective properties of LPS are located principally within the polysaccharide region of the molecule (11, 12). Furthermore, when glycolipid or lipid A fractions were

<sup>1</sup> National Research Council Research Associate.

<sup>2</sup> National Research Council Senior Research Associate. Current address: Israel Institute for Biological Research, P.O. Box 19, Ness-Ziona, Israel.



used in radioprotection experiments, little or no increase in survival was observed (11, 12).

In this communication we report some recent observations showing that endotoxin obtained from a polysaccharide deficient Re mutant strain of *Salmonella minnesota* (R595), sometimes referred to as endotoxic glycolipid (GL), markedly increased the survival of CD2F1 and C3H/HeN mice exposed to lethal doses of  $^{60}\text{Co}$   $\gamma$  irradiation. More significantly, it was found that detoxified monophosphoryl lipid A (LAM) obtained from *S. minnesota* (R595), described by Ribí and associates as a potent immunostimulatory agent (13, 14), also protected mice from the lethal effects of ionizing radiation. In contrast to the GL parent, the increased survival afforded mice by pre-treatment with detoxified lipid A was not correlated with its capacity to enhance the proliferation of endogenous spleen colonies (E-CFU) following sublethal irradiation or to induce plasma colony-stimulating activity (CSA).

#### METHODS AND MATERIALS

**Mice.** The male CD2F1 mice were obtained from Harland Sprague Dawley, Indianapolis, IN. The female C3H/HeJ and C3H/HeN mice were purchased from the Jackson Laboratory, Bar Harbor, ME. Mice were acclimated to laboratory conditions for 2 weeks before use. During this time they were quarantined until a random sample was found to be free of histologic lesions of common murine diseases and water bottle cultures (trypticase soy broth) of all animals were found to be free of *Pseudomonas* spp. Mice 10–14 weeks old were used throughout. All animals were maintained on a 6 AM–6 PM light–dark cycle and were allowed a standard laboratory diet (pellets) and acidified water *ad libitum*.

**Radioprotectants.** The endotoxic glycolipid (GL) from *S. minnesota* (R595) as well as diphosphoryl lipid A (LAD) and the detoxified monophosphoryl lipid A (LAM) from this same organism were obtained from RIBI Immunochem, Hamilton, MO. These substances were routinely dissolved at a concentration of 100  $\mu\text{g}/\text{ml}$  in distilled water containing 0.5% triethylamine.

**Irradiation.** Mice were placed in Plexiglas boxes and irradiated bilaterally with  $^{60}\text{Co}$   $\gamma$  photons [1.17 and 1.33 MeV] at a midline tissue exposure rate of 1.0 Gy/min. The AFRRI Co-60 Facility consists of two planar sources which were raised together to irradiate the mice bilaterally. To measure the midline tissue dose rate, a tissue-equivalent ionization chamber, with calibration traceable to the National Bureau of Standards, was placed midline in a plastic mouse phantom. The variation across the array of mice was measured to be less than 1%, and the uncertainty in the dose measurements is about 5%. In protection experiments mice received 0.1–0.2 ml of GL, LAD, or LAM intraperitoneally. Following exposure survival was monitored for 30 days. Both before and after exposure mice were kept in boxes equipped with microfilter tops to protect them from airborne infections.

**In vitro assay of colony-stimulating activity (CSA).** Ten micrograms of GL, LAD, or LAM were injected ip into male CD2F1 mice. Three hours later, the animals were anesthetized and bled retroorbitally into heparinized tubes. Each plasma sample was obtained from the pooled blood of three mice. The pooled plasma samples of normal and experimental mice were assayed for their ability to stimulate the growth of bone-marrow-derived granulocyte-macrophage colonies by the double-layer soft agar technique (15). CMRL 1066 culture medium for this procedure was prepared as previously described (16). Dose-response curves indicated that a 1:6 dilution of test plasma added as 10% (v/v) of total culture volume to the lower layer of agar provided maximum colony-stimulating activity. Colony-stimulating activity was expressed as the number of colonies formed per  $1 \times 10^5$  murine bone marrow cells. Cultures were incubated at 37°C in a humidified 5%  $\text{CO}_2$  atmosphere. Colonies of more than 50 cells were counted after 10 days of incubation. Four separate plasma samples were used to determine each value. Each culture was performed in duplicate.

**Endogenous spleen colony assay (E-CFU).** Endogenous spleen colony-forming units (E-CFU) were evaluated by the method of Till and McCulloch (17). CD2F1 mice were injected with 2.0  $\mu\text{g}$  of GL, LAM, or LAD intraperitoneally 24 h before exposure to 6.5, 7.0, and 7.5 Gy of total body irradiation from the  $^{60}\text{Co}$  source. Ten days after exposure the spleens of irradiated mice were removed and fixed in Bouin's fixative, and the number of macroscopic spleen colonies was counted. Two separate experiments were performed involving

five animals per group. Data are expressed as the mean of the number of colonies found on the spleens of 10 animals,  $\pm$  the standard error of the mean (SEM).

## RESULTS

### *Radiation Protection Experiments*

The results presented in Table I which were analyzed using a chi-squared distribution test show that intraperitoneal administration of 10–20  $\mu$ g of endotoxic glycolipid (GL), diphosphoryl lipid A (LAD), or detoxified monophosphoryl lipid A (LAM) conferred significant protection to LPS-responsive CD2F1 and C3H/HeN mice when given 24 h before exposure to a lethal dose of radiation. No significant differences were observed between the two doses employed or among GL, LAD, or LAM ( $P > 0.05$ ) in CD2F1 mice. On the other hand, no protection was afforded by these glycolipids to LPS-nonresponsive C3H/HeJ mice. Although the detoxified LAM increased survival of CD2F1 mice exposed to 10 Gy to about the same extent as the more toxic GL, LAM was found to be more radioprotective than the latter substance in survival experiments using the C3H/HeN mice ( $P < 0.005$ ). Maximum protection using GL or LAM in CD2F1 mice was achieved when these substances were given 24 to 48 h prior to exposure (Fig. 1). Duplicate experiments were performed at each time using a total of 20 mice per group. A two-way analysis of variance (GL or LAM vs time) was conducted on the data presented in Fig. 1. There was no statistical difference between

TABLE I  
Radioprotection of Mice Using Endotoxic Glycolipid (GL), Diphosphoryl Lipid A (LAD) and Detoxified Monophosphoryl Lipid A (LAM) from *Salmonella minnesota* R595<sup>a</sup>

Mouse strain	Compound	Dose ( $\mu$ g)	No. animals surviving	Percent survival
CD2F1 <sup>b</sup>	LAM	10	43/50	86
	LAM	20	15/20	75
	LAD	10	45/50	90
	LAD	20	27/30	90
	GL	10	18/20	90
	GL	20	8/10	80
	Controls	0	0/30	0
C3H/HeN <sup>c</sup>	LAM	20	10/10	100
	LAD	20	3/10	30
	GL	10	4/10	40
	Controls	0	1/10	10
C3H/HeJ <sup>c</sup>	LAM	20	0/10	0
	LAD	20	0/10	0
	GL	10	0/10	0
	Controls	0	0/10	0

<sup>a</sup> Mice injected ip 24 h prior to exposure to <sup>60</sup>Co  $\gamma$  radiation.

<sup>b</sup> CD2F1 mice received 10 Gy.

<sup>c</sup> C3H/HeN and C3H/HeJ mice received 9.5 Gy.

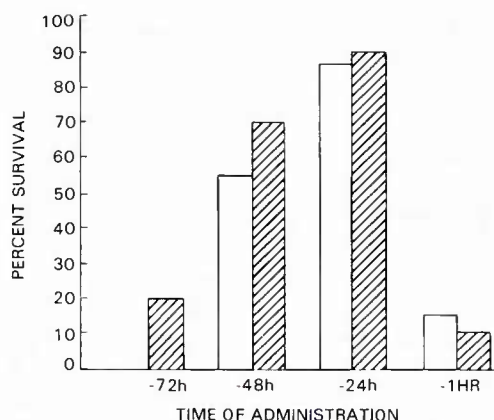


FIG. 1. Effect of time of administration of GL or LAM (10  $\mu\text{g}/\text{mouse}$ ) on the survival of CD2F1 mice exposed to 10 Gy  $^{60}\text{Co}$   $\gamma$ . Closed bars = GL treated; open bars = LAM treated.

GL or LAM although there was a significant difference over time ( $P < 0.01$ ). Using a Neuman-Keul comparison test, there was no significant difference between radioprotection at 24 to 48 h, but there was a significant decrease for these two times in comparison to treatment 72 h prior to irradiation.

Figure 2 compares the survival of untreated with GLY and LAM treated CD2F1 mice as a function of radiation dose. A minimum of 20 mice were used at each dose of radiation. From these experiments the  $\text{LD}_{50/30}$  dose for the untreated control mice was found to be 9.39 Gy [95% of confidence limits = 9.29–9.49]. In the case of mice receiving the parent GL, the  $\text{LD}_{50/30}$  was shifted to 11.28 [10.93, 11.64], or a dose reduction factor (DRF) of 1.20. For LAM the  $\text{LD}_{50/30}$  was estimated to be 11.0 Gy [10.75, 11.25] or a DRF = 1.17 using a probit analysis.

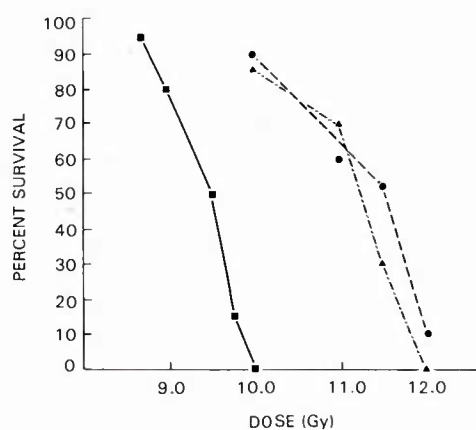


FIG. 2. Effect of  $^{60}\text{Co}$   $\gamma$ -radiation dose on the survival of CD2F1 mice pretreated with GL or LAM. ■, Controls; ▲, LAM-treated mice; ●, GL-treated mice.



*Endogenous Spleen Colony Formation (E-CFU)*

Table II illustrates the capacity of the three radioprotective glycolipids from *S. minnesota* to stimulate the formation of endogenous spleen colonies (E-CFU) in irradiated CD2F1 mice. Both GL and LAD markedly increased E-CFU content at all three radiation doses studied, while no stimulation of E-CFUs was observed in mice challenged with LAM.

*Factors with Colony-Stimulating Activity (CSA)*

The effect of GL, LAD, and LAM on the induction of plasma factors (CSA) which stimulate the growth of granulocyte-macrophage colonies *in vitro* was also studied (Table III). Table III was analyzed using a Mann-Whitney test with a Bonferroni allocation of Type I error ( $P = 0.05$ ). There was no difference in the effects of GL and DP at 3 and 6 h post infection. Both compounds significantly increased the plasma level of CSA at these times. The plasma of mice challenged with LAM contained significantly less CSA than those receiving either GLY or LAD.

## DISCUSSION

The radioprotective effect of bacterial endotoxins has been known for over 30 years (1, 2). Subsequent studies demonstrated that radioprotection could also be achieved using "detoxified" endotoxin preparations (7-11). Collectively these studies suggested that the locus for radioprotection is situated in a region of the endotoxin molecule separate from that responsible for its toxicity. Evidence presented by Nowotny *et al.* (11) and by Urbaschek (18) has tended to confirm this notion. Using derivatives obtained by mild hydrolysis of *Salmonella minnesota* 1114 endotoxin it was shown that the lipid A component conferred no radioprotection to mice (11). On the other hand the nontoxic polysaccharide fraction (PS) obtained from the same hydrolysate retained a radioprotective activity approximately equal to that of the parent endotoxin. In further experiments it was shown that the toxic activities of endotoxin could be selectively neutralized using homologous antiserum directed at the lipid moiety, but that the resulting "immune complex" was fully radioprotective (12). These observations also gave support to the notion that the PS region of molecule is the principal active

TABLE II  
Effect of GL, LAD, and LAM on E-CFU in Sublethally Irradiated CD2F1 Mice<sup>a</sup>

Radiation dose (Gy)	E-CFUs (d10)			
	Controls	GL	LAD	LAM
6.5	1.2 ± 1.2	14.0 ± 2.6*	8.8 ± 2.2*	0.2 ± 0.2
7.0	0.6 ± 0.4	12.0 ± 3.4*	7.6 ± 2.4*	0.2 ± 0.2
7.5	0.2 ± 0.2	11.2 ± 1.8*	5.0 ± 1.8*	0.0 ± 0.0

<sup>a</sup> Mice received 2 µg of GL, LAD, or LAM 24 h prior to exposure to <sup>60</sup>Co γ radiation. Each value is the mean of ten determinations ± SEM.

\*  $P \leq 0.01$  with respect to control using Student's *t* test.

TABLE III  
Effect of GL, LAD, and LAM on Plasma Colony Stimulating Factor (CSA) Levels in CD2F1 Mice<sup>a</sup>

Time (h)	No. of colonies			
	Controls	GL	LAD	LAM
3	0	70 ± 6	57 ± 6	9 ± 4
6	4 ± 2	62 ± 9	44 ± 10	15 ± 5
24	0	10 ± 3	0	0
48	0	0	0	0

<sup>a</sup> Mice received 10 µg GL, LAM, or LAD ip at  $t = 0$ . Each value represents the mean of four determinations. Errors are ± SEM.

site responsible for radioprotection. Furthermore, endotoxic glycolipid isolated from the polysaccharide-deficient rough mutant of *S. minnesota* (R595) was reported to have a significantly diminished capacity to confer radioprotection (11, 12).

In contrast to the literature cited above we have found that relatively low doses (400 µg/kg) of endotoxic glycolipid (GL) from *S. minnesota* conferred significant protection to endotoxin-responsive strains of mice (CD2F1 and C3H/HeN). The magnitude of the dose reduction factor (DRF  $\cong$  1.2) is approximately the same as that achieved previously using endotoxin from smooth *Salmonella typhosa* (2). The results of our studies employing endotoxic glycolipid and diphosphoryl lipid A from *S. minnesota* (R595) suggest that the radioprotective properties of lipopolysaccharide may not be restricted solely to the PS region of the molecule. More significantly it was found that the detoxified monophosphoryl lipid A from *S. minnesota* (R595) was approximately equal to the parent endotoxin in its capacity to confer protection to lethally irradiated mice. This confirms and extends the observations of Ribi and associates who showed that beneficial properties of lipid A can be uncoupled from its toxic properties by removing a single phosphate group from the reducing end of the glucosamine disaccharide unit (13, 14).

Although the precise mechanism by which endotoxins promote survival in irradiated animals is not entirely understood, it has been generally accepted that increased survival is associated with their ability to stimulate hematopoietic recovery (19, 20). Presumably, this process is initiated by the action of endotoxin on reticuloendothelial macrophages (21), triggering the release of humoral factors such as CSA (15, 22) that enhance stem cell proliferation.

In this study both the parent glycolipid and the diphosphoryl lipid A markedly enhanced the formation of E-CFUs in irradiated mice. These substances also induced elevated plasma levels of CSA within 3 h after administration. The detoxified monophosphoryl lipid A (LAM), on the other hand, did not promote the formation of E-CFU in the spleen and was much less effective than either GL or LAD in elevating plasma levels of CSA. Nevertheless, LAM was found to be just as effective as GL or LAD in protecting against lethal doses of <sup>60</sup>Co radiation. Previous investigators have also found that the ability of endotoxin to increase hematopoiesis in the spleen does not necessarily correlate with increased survival following irradiation (23–25). It is possible that E-CFUs in the spleen are not representative of changes in whole-body

numbers of hematopoietic stem cells (26). On the other hand, it is also conceivable that the radioprotective effect of the bacterial glycolipids as well as polysaccharides (PS) used in previous studies may be unrelated to their ability to stimulate hematopoiesis and/or induce CSA. Along these same lines evidence has been reported suggesting that the CSA-inducing component obtained from endotoxin hydrolysates is not the same as the PS component eliciting radioprotection (11).

Addison and Berry (27) have recently presented evidence suggesting that protection of mice against lethal irradiation with serum mediators elicited by injection of endotoxin is not solely dependent on the presence of CSA alone. Our observations showing that LAM is radioprotective but does not stimulate E-CFUs and is only a weak inducer of CSA suggest that bacterial glycolipids may exert their radioprotective effects by mechanisms other than hematopoietic stimulation. We are currently exploring the possibility that bacterial lipopolysaccharides and glycolipids can elicit the production of endogenous radioprotective factors *in vivo*.

Although the DRF of 1.2 determined in this study for LAM is much lower than those generally observed for aminothiols such as S-2-(3-aminopropylamino) ethylphosphorothioic acid (WR 2721), the application of LAM in combination with radiotherapy offers intriguing possibilities for treating tumors. There has been a great deal of recent interest in using chemical agents to modify the sensitivity of neoplastic vis-a-vis normal cells to obtain a selective advantage in radiation killing of tumors (28, 29). It has already been reported that LAM administered in combination with mycobacterial cell wall skeleton (CWS) causes tumor regression (14). It is therefore conceivable that LAM could be used to promote radiation-induced killing of neoplasms while simultaneously conferring protection to normal tissues.

#### ACKNOWLEDGMENTS

The authors express their gratitude to Mr. William E. Jackson for performing the statistical analysis of the data presented in this paper. This research was supported by the Armed Forces Radiobiology Research Institute, Defense Nuclear Agency, under Research Work Unit 00142. The views presented in this paper are those of the authors. No endorsement by the Defense Nuclear Agency has been given or should be inferred. Research was conducted according to the principles enunciated in the "Guide for the Care and Use of Laboratory Animals," prepared by the Institute of Laboratory Animal Resources, National Research Council.

RECEIVED: September 30, 1985; REVISED: April 9, 1986

#### REFERENCES

1. R. B. MEFFERD, JR., D. T. HERKEL, and J. B. LOEFER, Effect of Piromen on survival in irradiated mice. *Proc. Soc. Exp. Biol. Med.* **83**, 54-56 (1953).
2. W. W. SMITH, I. M. ALDERMAN, and R. E. GILLESPIE, Increased survival of irradiated animals treated with bacterial endotoxins. *Am. J. Physiol.* **191**, 124-130 (1957).
3. M. PARANT, Effect of LPS on nonspecific resistance to bacterial infections. In *Beneficial Effects of Endotoxins* (A. Nowotny, Ed.), pp. 179-196. Plenum, New York, 1983.
4. L. A. BOBER, M. J. KRUNEPOL, and V. P. HOLLANDER, Inhibitor effect of endotoxin on the growth of plasma cell tumor. *Cancer Res.* **36**, 927-929 (1976).
5. E. A. CARSWELL, L. J. OLD, L. KASSEL, S. GREEN, N. FIORE, and B. WILLIAMSON, An endotoxin-induced serum factor that causes necrosis of tumors. *Proc. Natl. Acad. Sci. USA* **72**, 3666-3670 (1975).



6. L. CHEDID, Biologic activities of detoxified bacterial lipopolysaccharides. *Bull. de L'Institute Pasteur* **74**, 103-105 (1976).
7. L. BERTOK, Radio-detoxified endotoxin as a potent stimulator of nonspecific resistance. *Prospect. Biol. Med.* **24**, 61-66 (1980).
8. S. SNYDER, R. I. WALKER, T. J. MACVITTIE, and J. M. SHEIL, Biologic properties of bacterial lipopolysaccharides treated with chromium chloride. *Can. J. Microbiol.* **24**, 495-501 (1978).
9. L. CHEDID, F. AUDIBERT, C. BONA, C. DAMAIS, F. PARANT, and M. PARANT, Biologic activities of endotoxins detoxified by alkylation. *Infect. Immun.* **12**, 714-721 (1975).
10. S. J. PRINGAL, Protection of neonates against whole-body irradiation by the administration of a single emulsified injection of lipopolysaccharide during pregnancy. *Nature (London)* **191**, 159-169 (1969).
11. A. NOWOTNY, U. H. BEHLING, and H. L. CHANG, Relation of structure to function in bacterial endotoxins. VIII. Biologic activities in a polysaccharide-rich fraction. *J. Immunol.* **115**, 199-203 (1975).
12. U. H. BEHLING, The radioprotective effect of bacterial endotoxin. In *Beneficial Effects of Endotoxin* (A. Nowotny, Ed.), pp. 127-148. Plenum, New York, 1983.
13. E. RIBI, Beneficial modification of the endotoxin molecule. *J. Biol. Resp. Modif.* **3**, 1-9 (1984).
14. E. RIBI, K. AMANO, J. L. CONTRELL, S. SCHWARTZMAN, R. PARKER, and K. TAKAYAMA, Preparation and antitumor activity of nontoxic lipid A. *Cancer Immunol. Immunother.* **12**, 91-96 (1982).
15. P. QUESENBERRY, A. MORLEY, F. STOHLMAN, JR., K. RICHARD, D. HOWARD, and M. SMITH, Effect of endotoxin on granulopoiesis and colony stimulating factor. *N. Engl. J. Med.* **286**, 227-232 (1972).
16. T. J. MACVITTIE and K. F. MCCARTHY, Inhibition of granulopoiesis in diffusion chambers by a granulocyte chalone. *Exp. Hematol.* **2**, 182-194 (1974).
17. J. TILL and E. MCCULLOCH, Early repair processes in marrow cells irradiated and proliferating *in vivo*. *Radiat. Res.* **18**, 96-105 (1963).
18. R. URBASCHEK, Effects of bacterial products on granulopoiesis. *Adv. Exp. Med. Biol. B* **121**, 51-64 (1980).
19. W. W. SMITH, G. BRECHER, R. A. RUDD, and S. FRED, Effects of bacterial endotoxin on the occurrence of spleen colonies in irradiated mice. *Radiat. Res.* **27**, 369-374 (1966).
20. W. H. TALIAFERRO, L. G. TALIAFERRO, and B. N. JAROSLOW, *Radiation and Immune Mechanisms*, p. 152. Academic Press, New York, 1964.
21. R. N. APTE, C. F. HERTOFS, and D. H. PLUZNIK, Regulation of lipopolysaccharide induced granulopoiesis and macrophage formation by spleen cells. II. Macrophage-lymphocyte interaction in the process of generation of colony-stimulating factor. *J. Immunol.* **124**, 1223-1229 (1980).
22. R. URBASCHEK, S. E. MERGENHAGEN, and B. URBASCHEK, Failure of endotoxin to protect C3H/HeJ mice against lethal irradiation. *Infect. Immun.* **18**, 860-862 (1977).
23. K. KUMAGAI, H. IZUMI, M. TSURUSAWA, and K. J. MORI, Radioprotection of C3H/HeJ mice by RES-blockade. *Experientia* **38**, 861 (1982).
24. G. E. HANKS and E. J. AINSWORTH, Repopulation of colony-forming units in mice. *Nature (London)* **215**, 20-22 (1967).
25. E. J. AINSWORTH and R. M. LARSEN, Colony forming units and survival of irradiated mice treated with AET or endotoxin. *Radiat. Res.* **40**, 149-176 (1969).
26. S. AIZAWA, I. AMAKI, J. FUJITA, M. TSURUSAWA, and K. J. MORI, LPS induces migration of bone marrow cells in LPH non-responsive C3H/HeJ mice. *J. Radiat. Res.* **25**, 191-198 (1984).
27. P. D. ADDISON and L. J. BERRY, Passive protection against X-irradiation with serum from zymosan-primed and endotoxin-injected mice. *J. Reticuloendothelial Soc.* **30**, 301-310 (1983).
28. J. M. YUHAS, M. YURCONI, M. KLIGERMAN, and D. F. PETERSON, Combined use of radioprotective and radiosensitizing drugs in experimental radiotherapy. *Radiat. Res.* **70**, 433-443 (1977).
29. K. TANAKA and K. AOKI, Protective effect and clinical trials of WR-2721 (YM-08310). *Nippon Acta Radiol.* **41** (Suppl), 79 (1981).

# Brain Areas Involved in Production of Morphine-Induced Locomotor Hyperactivity of the C57Bl/6J Mouse

KAREN E. STEVENS,\* G. ANDREW MICKLEY†<sup>1</sup> AND LOIS J. McDERMOTT\*

\**Department of Psychology, University of Colorado, Austin Bluffs Parkway, Colorado Springs, CO 80907*  
and †*Behavioral Sciences Department, Armed Forces Radiobiology Research Institute*  
*Naval Medical Command National Capital Region, Bethesda, MD 20814-5145*

Received 12 November 1984

STEVENS, K. E., G. A. MICKLEY AND L. J. McDERMOTT. *Brain areas involved in production of morphine-induced locomotor hyperactivity of the C57Bl/6J mouse.* PHARMACOL BIOCHEM BEHAV 24(6) 1739-1747, 1986.—Previous studies reveal a dose-dependent increase in locomotor activity of the C57Bl/6J mouse after administration of morphine or amphetamine. Concurrent partial lesions of both the dorsomedial caudate and lateral septal nuclei resulted in a significant decrease in morphine-induced, but not amphetamine-induced, hyperactivity. Concurrent partial lesions of the nucleus accumbens and stria terminalis produced only a nonsignificant decrease in the morphine-induced hyperactivity. Lesions of the individual brain structures did not significantly affect the morphine-induced locomotor hyperactivity. Microinjections of the opiate antagonist naloxone into discrete portions of the caudate and septal nuclei produced suppression of the morphine-induced hyperactivity response without affecting the hyperactivity caused by amphetamine injections. Only a slight suppression of morphine-induced locomotion was produced when naloxone was injected into the nucleus accumbens and stria terminalis. These data suggest that portions of the caudate and septum may be involved in the mediation of morphine-induced hyperactivity in the C57Bl/6J mouse.

Morphine	Caudate nucleus	Septal nucleus	Amphetamine	Locomotion	Mice
----------	-----------------	----------------	-------------	------------	------

MORPHINE, in high doses, produces immobility in most species [4]. However, when administered systemically to certain strains of mice, it evokes instead a dose-dependent locomotor hyperactivity [12,26]. This hyperactivity is characterized by a stereotypic "running fit" [16], usually around the perimeter of the cage, and is accompanied by an elevated or "straub" tail [12,16].

Several studies have attempted to identify brain areas that might mediate opioid-induced locomotor hyperactivity. Some of these experiments have implicated the nucleus accumbens as a primary locus of both morphine and endorphin actions. For example, locomotor hyperactivity follows the injection of morphine or enkephalin into the nucleus accumbens of the rat [5,17]. Naloxone reverses both of these effects [24]. Similarly, lesions involving the nucleus accumbens partially block the morphine-induced locomotor hyperactivity of the C57Bl/6J mouse [26]. The behavioral findings that have implicated the nucleus accumbens as a partial mediator of morphine-induced locomotion are further supported by immunohistochemical studies. Experiments have isolated endorphins as well as large numbers of enkephalin receptors, and beta-endorphin receptors in this brain area [2, 7, 8, 20, 24, 25, 28-30].

However, the failure of the lesions of nucleus accumbens to completely eliminate morphine-induced hyperactivity [26]

suggests that other brain areas may also be partially involved in the production of this behavior. Candidate nuclei include several brain structures that are connected to the nucleus accumbens and also contain both beta-endorphin and enkephalin and their receptors [3, 7, 20, 22, 24, 25, 28-30]. For example, some opioid-containing cells in the nucleus accumbens project to the stria terminalis, including its bed nucleus [14, 15, 31]. The accumbens is also anatomically connected, both directly and indirectly (through the cells of the A9 group), to the caudate nucleus [14,31], which is known to contain endorphins and enkephalins [1]. Massive nucleus accumbens and septal connections have also been reported as part of the brain's endogenous opiate system [18].

Since the nucleus accumbens projects to the caudate, septum and stria terminalis (areas which contain opioid peptides and their receptors), one or more of the brain structures in these systems may also be involved in the mediation of morphine-induced locomotor hyperactivity. The present investigation sought to specify other brain areas involved in the production of this behavior in the C57Bl/6J mouse.

## EXPERIMENT 1

Ablation of brain structures that mediate morphine-induced hyperactivity should reduce or eliminate this behav-

<sup>1</sup>Requests for reprints should be addressed to G. Andrew Mickley.

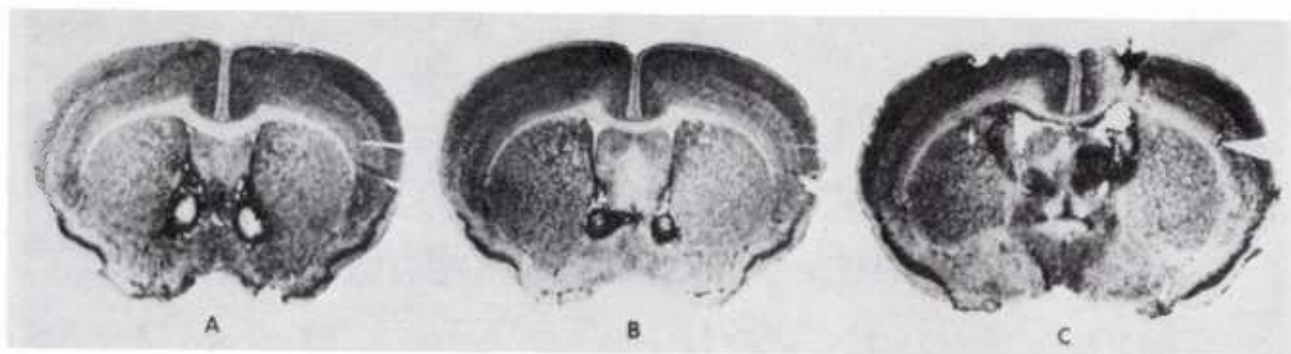


FIG. 1. Representative micrographs of lesioned brains. A and B are two different sections from the same brain, and show the lesion in both the nucleus accumbens and stria terminalis target areas. C shows combined lesions of the dorsomedial caudate and lateral septal nuclei.

ioral response. In this experiment, bilateral lesions were made in the nucleus accumbens, the stria terminalis, or a combination of these areas. In other animals, bilateral lesions were made in the dorsomedial portion of the caudate nucleus, the lateral septal nucleus, or a combination of these two areas.

#### Method

The subjects were C57Bl/6J male mice (Jackson Laboratories, Bar Harbor, ME), weighing between 16 and 22 grams. The mice were individually housed and were maintained on a 12-hour light/dark cycle (lights on at 6:00 a.m.). Purina rodent chow and water were continuously available.

Bilateral lesions were placed either in (a) nucleus accumbens (ACCUM), (b) stria terminalis (STRIA), (c) nucleus accumbens and stria terminalis (ACCUM + STRIA), (d) dorsomedial portion of the caudate nucleus (CAUD), (e) lateral septal nucleus (SEPT), or (f) dorsomedial caudate and lateral septal nuclei (CAUD + SEPT). Stereotaxic surgery was accomplished using atropine sulfate (0.4 mg/kg, IP) as a pre-anesthetic treatment and also sodium pentobarbital (75 mg/kg, IP) anesthetic. Methoxyflurane was used as an auxiliary anesthetic. Bilateral lesions were placed using the following coordinates: ACCUM—anterio-posterior (AP) +1.0 mm from bregma, lateral (LAT)  $\pm 0.9$  mm from midline, and depth (DEP) -4.2 mm from skull; STRIA—AP bregma, LAT  $\pm 0.6$  mm, and DEP -4.0 mm; ACCUM + STRIA—AP +0.6 mm, LAT  $\pm 0.6$  mm and DEP -4.5; CAUD—AP bregma, LAT  $\pm 1.5$  mm DEP -2.5 and 3.3 mm; SEPT—AP bregma, LAT  $\pm 0.5$  mm DEP -2.5 and -3.3 mm; and CAUD + SEPT—AP bregma, LAT  $\pm 1.0$  mm DEP -2.5 and -3.3 mm. All coordinates were determined by using a mouse stereotaxic atlas [23]. The lesions were made at two different depths in animals with CAUD, SEPT, and combined CAUD + SEPT lesions in order to achieve an elliptical lesion rather than a spherical lesion. Lesions were produced by passing a 1.5 mA current through a 0.27-mm enamel-coated nickel-chromium wire for 7 seconds. This produced a lesion approximately 0.6 mm in diameter. Animals were allowed to recover for a minimum of 1 week before postsurgical testing began.

Activity was measured on Columbus Instruments' Animal Activity Monitors Automex D and Automex 2 SDII (Columbus Instruments, Columbus, OH). Prior to surgery, baseline activity was measured in the following manner: on the first day of baselines, each animal received an injection

TABLE 1  
MEAN CHANGES\* IN LOCOMOTOR ACTIVITY "DIFFERENCE SCORES"† AFTER BRAIN LESION(S): SECOND 30-MINUTES OF RECORDING

Brain Lesion Site	Morphine	Amphetamine	Saline
Nucleus Accumbens	926	-142	370
Stria Terminalis	-214	-783	35
Nucleus Accumbens and Stria Terminalis	-48	160	-138
Caudate Nucleus (dorsomedial)	798	951‡	-44
Lateral Septal Nucleus	576	813‡	-147
Caudate (dorsomedial) and Lateral Septal Nuclei	-1062‡	360	-237

\*Post-surgical locomotion minus pre-surgical locomotion.

†Difference score=activity recorded after an injection of saline, morphine or amphetamine minus activity after an initial saline injection (baseline).

‡ $p < 0.05$ , Newman-Keuls. For purposes of this table we present only the results of the Newman-Keuls analysis of pre- vs. post-surgical locomotor activity (here represented by the change statistic). The actual Newman-Keuls comparison included pre- and post-surgical activity after all 3 drug treatments within each lesion group only (therefore, a total of 6 groups were involved in each post-hoc analysis).

(IP) of saline followed by a 5-minute waiting period and two 30-minute periods of recorded locomotor activity. Immediately following the baseline activity readings, mice received a second IP injection of 30 mg/kg morphine sulfate, or 4 mg/kg amphetamine sulfate (which produced nonopiate mediated hyperactivity), or saline. Again, there was a 5-minute waiting period followed by two more 30-minute locomotor activity recordings. On the two following days, each animal received one of the other remaining drug solutions as the second injection. The order of drug presentation was randomized for each animal. Activity data from these three combinations of saline and drug injections (saline/amphetamine, saline/morphine, saline/saline) constituted the baseline measurements.

Postsurgical testing was performed in the same manner as presurgical baselines. Each animal received the three drug solutions (IP) following the saline injection (IP), one each



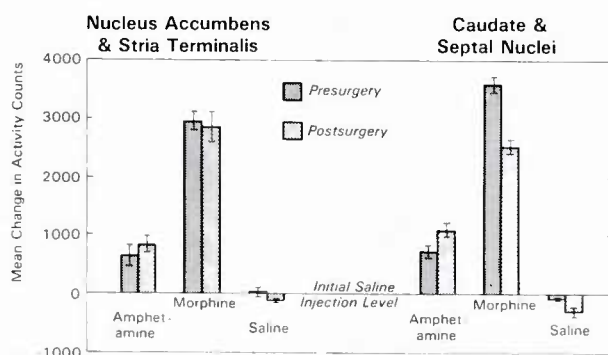


FIG. 2. Average change in locomotor activity counts after experimental drug injections (counts after the drug injection minus counts after initial saline injection) for each drug used (amphetamine 4.0 mg/kg, morphine 30 mg/kg or saline). Data presented are for the second 30 minutes of activity recorded. Bars show average activity changes both before and after surgery for the two combination brain lesion areas: (1) nucleus accumbens and stria terminalis (ACCUM + STRIA), and (2) dorsomedial caudate and septal nuclei (CAUD + SEPT). Variability indicators are the standard error of the means.

day, over the course of 3 days of testing. A randomized pattern of order of drug presentation was used for each animal.

After completion of testing, animals were sacrificed by perfusion, and brain tissue from each was sliced. The tissue was stained with thionin and lesion placements were verified. Only animals with well-defined bilateral lesions were retained in the experiment which resulted in the following distribution of lesion placements: ACCUM, (N=10); STRIA, (N=15); ACCUM + STRIA, (N=13); CAUD, (N=12); SEPT, (N=16); and CAUD + SEPT, (N=22). The lesions were, for the most part, discrete, but in some cases slight damage to adjacent structures had occurred. However, damage to other structures was random and slight, relative to the bulk of the lesioned area (see Fig. 1).

Data were analyzed using difference scores (activity after second injection of saline, morphine, or amphetamine minus activity after the initial saline injection). This was done to control for any hyperactivity caused by the injection procedures. Difference scores were computed for both time periods (first and second 30 minutes of activity recorded after injections) for presurgical baselines and postsurgical testing. The data were analyzed separately for the first and second 30 minutes of activity by 2, 3-way analyses of variance: (F)—lesion site by drug (second injection) by pre- or postsurgery. Newman-Keuls *a posteriori* tests were performed to locate specific differences between means [11]. In some instances, *t*-tests were performed if they were more applicable to the data. An alpha level of 0.05 was adopted throughout.

## Results

Statistically significant differences occurred with respect to the interaction of lesion site and drug injection at both time frames:  $F(12,170)=2.59$ ,  $p<0.003$ , for the first 30 minutes of activity, and  $F(12,170)=2.905$ ,  $p<0.003$ , for the second 30 minutes of activity (see Table I).

During the first 30 minutes of behavioral testing,

amphetamine-induced increases in activity were observed postsurgically in CAUD, SEPT, and CAUD + SEPT animals ( $p<0.05$ , Newman-Keuls). These were the only statistically significant changes in locomotion observed in this early time period.

During the second 30 minutes of activity, morphine-injected animals with CAUD + SEPT lesions showed a significant decrease ( $p<0.05$ , Newman-Keuls) in locomotor activity, compared to morphine-stimulated activity before lesioning. In these same animals, amphetamine induced a small nonsignificant increase in activity postsurgically compared to presurgical amphetamine-induced hyperactivity, the drug's effect was potentiated after CAUD, SEPT, lesions ( $p<0.05$ ).

ACCUM + STRIA lesioned mice displayed a slight nonsignificant postsurgical reduction in morphine hyperactivity, which was not reflected in amphetamine-induced hyperactivity. Individual lesions of the STRIA, and ACCUM produced nonstatistically significant changes in both morphine- and amphetamine-induced locomotor hyperactivity.

To verify that systemic injections of morphine and amphetamine caused an increase in locomotor activity in the C57Bl/6J mouse, *t*-tests were performed on the baseline (presurgical) difference score activity counts for morphine and amphetamine compared to saline control injections. As expected, the results show a significant increase in locomotor activity for both drugs ( $p<0.001$  for both).

## Discussion

This study reveals two different brain regions that may be involved in the mediation of morphine-induced hyperactivity: the dorsomedial caudate and lateral septal nuclei. Combined lesions of the dorsomedial caudate and lateral septal nuclei (CAUD + SEPT) caused a reduction in morphine-induced hyperactivity. This reduction cannot be described as a generalized lethargy since no similar postsurgical decrease was seen in the saline or amphetamine responses; indeed, in these animals a trend was seen towards an increase in amphetamine hyperactivity, although statistical significance was not achieved. The lesioned brain areas that produced decrements, corresponded very closely to areas known to contain opiate receptors (primarily enkephalin) [1,28]. It may be that the CAUD + SEPT lesions destroyed the endorphinergic neurons that partially mediate the morphine-induced locomotor response. These areas are probably not solely responsible for the mediation of morphine-induced hyperactivity, since ablation did not totally eliminate the morphine response, but only reduced it.

Combined partial CAUD + SEPT lesions produced a statistically significant reduction in morphine-induced activity while similarly-sized lesions of the individual areas did not. It may be the case that lesions of either the CAUD or SEPT alone leave enough opiate receptors intact (in other brain areas) to maintain the hyperactivity observed after morphine administration. Alternatively, the two brain areas may work in a synergistic way to produce this drug-induced locomotor hyperactivity response.

ACCUM + STRIA lesions produced a small decrease in morphine-induced hyperactivity and failed to block amphetamine-induced locomotion. This latter result is similar to that described in rats after anterior nucleus accumbens lesions [32]. In addition, large kainic acid lesions, which destroyed portions of the striatum and nucleus accumbens, also apparently spared amphetamine-induced locomotion

while attenuating morphine-stimulated activity [21]. Thus, it may be the case that the present lesions spared dopaminergic neurons while damaging at least a portion of the endorphinergic neurons in the region. The results of the present study are somewhat inconsistent with other data [10,26] that have demonstrated a significant reduction in amphetamine-stimulated locomotion after lesions of the posterior nucleus accumbens. However, direct comparisons between the 2 studies are not justified since the lesions of the present study were more posterior (consistently involving the stria terminalis) than those previously reported [26].

## EXPERIMENT 2

Experiment 1 established two brain areas which seemed to be involved in mediation of morphine-induced hyperactivity: the dorsomedial caudate and the lateral septal nuclei. In addition, the nucleus accumbens and stria terminalis area may be involved [21,26]. As further verification of the role of these areas in the mediation of morphine-induced activity, naloxone, an opiate antagonist, was microinjected into the caudate and septal nuclei or the nucleus accumbens and stria terminalis of mice that had also received an intraperitoneal injection of morphine.

### Method

The subjects were again C57Bl/6J male mice (Jackson Laboratories, Bar Harbor, ME) and were housed in the same manner as Experiment 1.

The mice were surgically implanted, bilaterally, with 23-gauge stainless-steel guide cannulas aimed at both the nucleus accumbens and stria terminalis (ACCUM + STRIA), or at both of the dorsomedial caudate and lateral septal nuclei (CAUD + SEPT). Because of the proximity of the lateral ventricles to both implant areas, a third group of mice was added in which guide cannulas were directed into only the lateral ventricles (VENT). This was done to control for the effect of possible backwash of intracerebrally injected solutions up the guide cannulas into the lateral ventricles and traveling to other brain structures. Stereotaxic coordinates for the placement of cannulas were: ACCUM + STRIA—anterior-posterior (AP) +0.6 mm from bregma, lateral (LAT)  $\pm 0.6$  mm from midline; and depth (DEP) -4.0 mm from skull; VENT—AP +0.6 mm, LAT  $\pm 0.6$  mm and DEP -3.0 mm and CAUD + SEPT—AP +0.6 mm, LAT  $\pm 2.8$  mm and DEP -2.5 mm. Coordinates were determined using a mouse stereotaxic atlas [23]. In order to effect intracerebral injections to both the caudate and the septal nuclei, an angular placement of guide cannulas was used as well as two different lengths of injection cannula. The guide cannulas were placed at an angle of 30 degrees to the vertical midline plane. Surgery was accomplished using atropine sulfate (0.4 mg/kg, IP) presurgically and sodium pentobarbital (75 mg/kg, IP) anesthetic. Methoxyflurane was also used as an auxiliary anesthetic. Mice were allowed a minimum of 1 week recovery from surgery before testing.

Activity was measured using Columbus Instruments' Animal Activity Monitors Automex D and Automex 2 SDII. Intracerebral injections were made using a 30-gauge injection cannula attached to a Hamilton microliter syringe inserted into a Stoelting syringe assembly with a Starrett Micrometer head. Injection cannulas for mice with ACCUM + STRIA and VENT implants extended 0.5 mm beyond the end of the

guide cannulas. Intracerebral injection volumes for these two groups were 1  $\mu$ l per cannula (hemisphere). Intracerebral injections in the CAUD + SEPT group were made at two depths (0.5 mm and 1.5 mm beyond the end of the guide cannula) to introduce the drug into both the caudate and septal nuclei. Injections in this group were 0.5  $\mu$ l per injection per depth, or a total of 1  $\mu$ l per hemisphere. Injection cannulas were left in the guide cannulas for 30 seconds following injections of the solution to allow complete delivery of the dose.

On the first day of testing, each animal received an intraperitoneal injection of 30 mg/kg morphine sulfate, 4 mg/kg amphetamine sulfate or saline, followed immediately by 30, 1-minute activity readings. Then an intracerebral injection of 1  $\mu$ g naloxone in 1  $\mu$ l saline or saline alone was administered [12], and 45 1-minute activity readings were taken immediately following completion of the injection. On each of the following 5 days, each animal received one of the following combinations of intraperitoneal plus intracerebral injections: saline plus saline, saline plus naloxone, morphine plus saline, morphine plus naloxone, amphetamine plus saline, or amphetamine plus naloxone. Each animal received all six combinations of intraperitoneal and intracerebral injections during the course of the testing period. The order of presentation was randomized for each animal.

At the completion of testing, 1  $\mu$ l of Evans Blue dye was injected into each cannula. Mice were sacrificed by decapitation, and the brain quickly dissected out and frozen in freon 12. The frozen tissue was sectioned, and drawings and photographs of the spread of dye were taken to verify the cannula placement and the relative diffusion of fluid into the brain (see Figs 3-5). Only animals with "dye-marked" tissue corresponding closely to target areas were retained in the experiment. After elimination of animals with inaccurate "dye-marked" areas, the following animals were retained in the experiment: ACCUM + STRIA, (N=10); CAUD + SEPT (N=7); and VENT (N=12). Examination of ACCUM + STRIA placements showed an area of dye approximately 0.5 mm in diameter centering in the ACCUM + STRIA area, with some extension into the anterior commissure. VENT implant animals had dye only in the ventricles, primarily the lateral, but with some diffusion into the third ventricle. CAUD + SEPT implant animals had areas of dye extending angularly from the medial caudate into the lateral septal area but, surprisingly, no dye in the lateral ventricles. The entire length of the dye area in the CAUD + SEPT group was approximately 1.5 mm with a diameter of about 0.4 mm. The most posterior portions of the "dye-marked" tissue occasionally extended into the edges of the STRIA.

Data analysis was performed on individual activity scores for each fifth minute (from 5 to 45 minutes after injection). Data were analyzed by 2-way analysis of variance (F), drug (intracerebral) by time (after intracerebral injection) for each implant area, for each intraperitoneal drug injection. Newman-Keuls a posteriori tests [11] were used to locate specific differences between means. In order to compare the effects of IP saline plus IC naloxone against IP saline plus IC saline (to ascertain any depressant effects of naloxone alone), *t*-tests were performed on data accumulated in the following way. For each animal, under each drug condition, scores for the 5th, 10th, 15th . . . 45th minute of activity were summed to yield two total scores (saline versus naloxone effects) for each animal. These scores were then analyzed by a *t*-test for matched pairs. Again, an alpha level of 0.05 was adopted throughout.



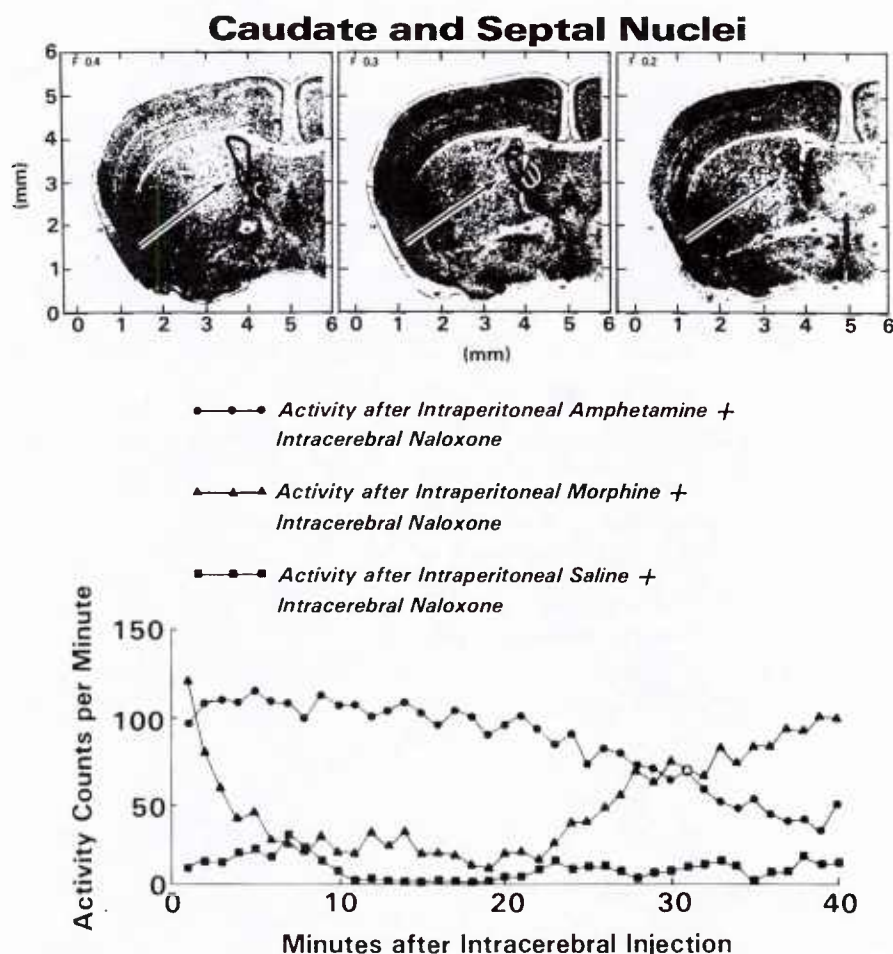


FIG. 3. Locomotor activity counts for each minute after bilateral injections of naloxone (1  $\mu$ g/hemisphere) into the dorsomedial caudate and lateral septal nuclei. Lines on the brain sections (photographs from Slotnick and Leonard [23]) indicate probable diffusion areas as imaged by postexperimental dye injections. Intracerebral naloxone injections challenged the locomotion observed after IP amphetamine (4 mg/kg), morphine (30 mg/kg), or saline injections. Mean activity counts for IC injections of saline after IP amphetamine, morphine or saline injections were 90, 127, and 29, respectively.

## Results

Naloxone, injected in the CAUD + SEPT area, produced a significant suppression of peripherally induced morphine hyperactivity,  $F(8,102)=5.149$ ,  $p<0.01$ , but not amphetamine-induced hyperactivity (see Fig. 3). This decrease in activity following morphine plus naloxone injections was apparent at the 5th minute following intracerebral injection, and it continued through the 25th minute ( $p<0.001$  for the 5th, 10th, and 15th minutes,  $p<0.002$  for the 20th minute, and  $p<0.001$  for the 25th minute; Newman-Keuls). At the 30th minute, and minutes thereafter, morphine plus naloxone activity was not significantly different from activity after morphine plus saline. Naloxone injections in the ACCUM + STRIA or VENT failed to significantly alter morphine-induced locomotion (see Figs. 4,5).

Intracerebral naloxone did not significantly alter the peripherally induced amphetamine hyperactivity of any group (as compared to IC saline),  $F(3,442)=0.756$ ,  $p=0.84$ .

Intracerebral naloxone, in and of itself, did not alter spontaneous (IP saline injection-induced) activity, and intracerebral saline also did not. As expected, intraperitoneal injections of morphine or amphetamine significantly increased locomotor activity over that of saline controls,  $F(2,52)=48.445$ ,  $p<0.001$ .

## Discussion

Intracerebral injections of naloxone significantly suppressed morphine-stimulated locomotor activity in animals with the CAUD + SEPT implants but not in the subjects with ACCUM + STRIA or VENT implants animals. However, a small (not statistically significant) decrease was observed in the ACCUM + STRIA lesioned group. These quantitative representations of activity were corroborated by behavioral observations. After intracerebral naloxone challenges to morphine-induced locomotion, VENT implant mice contin-



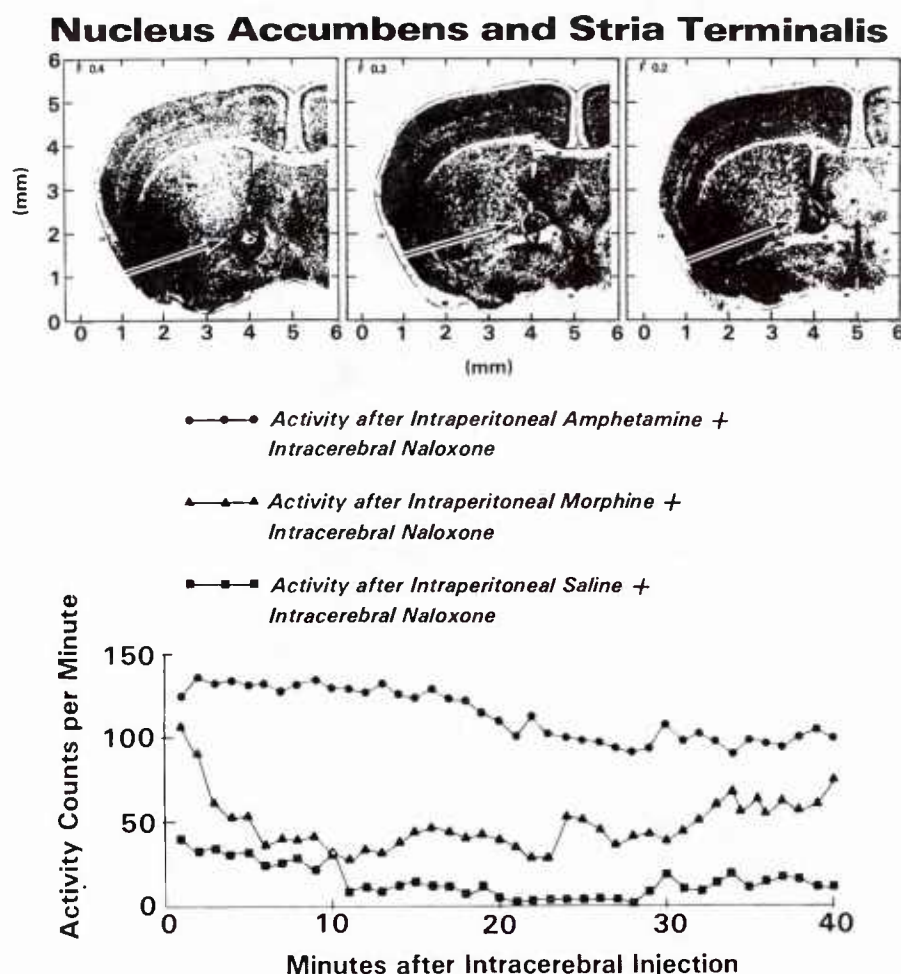


FIG. 4. Locomotor activity counts for each minute after bilateral injections of naloxone ( $1 \mu\text{g}/\text{hemisphere}$ ) into the nucleus accumbens and stria terminalis. Lines on the brain sections (photographs from Slotnick and Leonard [23]) indicate probable diffusion areas as imaged by postexperimental dye injections. Intracerebral naloxone injections challenged the locomotion observed after IP amphetamine ( $4 \text{ mg/kg}$ ), morphine ( $30 \text{ mg/kg}$ ), or saline injections. Mean activity counts for IC injections of saline after IP amphetamine, morphine or saline injections were 110, 145, and 35, respectively.

ued to exhibit the "running fit" and straub tail associated with morphine hyperactivity; they just ran a little more slowly. ACCUM + STRIA animals showed a decrease in morphine stereotypic behavior, with short periods of rearing and grooming interspersed throughout the "running fit." During the period of greatest suppression of activity, the CAUD + SEPT implanted mice exhibited almost no stereotypic behavior at all. They groomed, reared, and sometimes explored but they did not exhibit the elevated straub tail response. Some mice rested with eyes closed in the nest area of the home cage. Later (approximately 25 to 30 minutes), the stereotypic running returned, so that by the end of the 45-minute period they were behaviorally indistinguishable from the mice injected with intraperitoneal morphine plus intracerebral saline.

The suppressant effect of naloxone was limited to the

morphine response and did not affect the amphetamine-induced hyperactivity in any group. The small decrease in amphetamine activity seen late in the CAUD + SEPT implant animals was also observed after intraperitoneal amphetamine plus intracerebral saline injections, and may represent a wearing off of the amphetamine hyperactivity. These animals seemed to slow down from the amphetamine hyperactivity and spend more time in the nest area, but did not go to sleep.

The possibility that naloxone alone is a depressant was eliminated by the lack of difference in activity between intraperitoneal saline and intraperitoneal saline plus intracerebral naloxone activity counts. Intracranial pressure caused by microinjections into the brain was also eliminated as a possible explanation for the reduction in morphine hyperactivity, since no difference was seen between the lo-

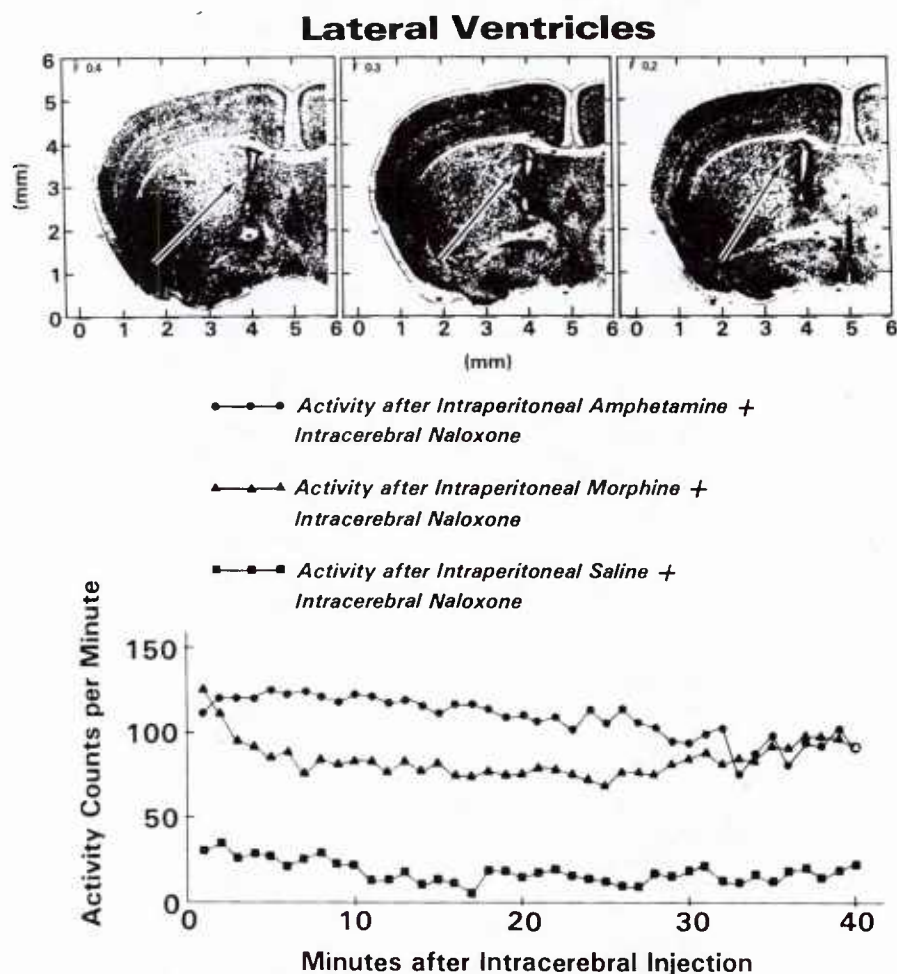


FIG. 5. Locomotor activity counts for each minute after bilateral injections of naloxone ( $1 \mu\text{g}/\text{hemisphere}$ ) into the lateral ventricles. Lines on the brain sections (photographs from Slotnick and Leonard [23]) indicate probable diffusion areas as imaged by postexperimental dye injections. Intracerebral naloxone injections challenged the locomotion observed after IP amphetamine ( $4 \text{ mg}/\text{kg}$ ) morphine ( $30 \text{ mg}/\text{kg}$ ), or saline injections. Mean activity counts for intracerebral injections of saline after IP amphetamine, morphine or saline injections were 119, 130, and 15, respectively.

comotor activity of mice injected with intraperitoneal saline alone and those that received intraperitoneal saline plus intracerebral saline.

#### GENERAL DISCUSSION

Destruction of caudate and septal neurons as well as injection of naloxone to the same sites produced significant decreases in morphine-induced locomotor hyperactivity, although neither procedure completely eliminated this response. It remains unclear whether ablation of a greater number of endorphinergic neurons in this area, or injection of more naloxone, would reduce morphine-induced locomotion to premorphine levels. It is known that morphine-induced hyperactivity in C57 mice may depend on dopaminergic mechanisms. For example, morphine injections

stimulate dopamine receptors in C57Bl/6J mice [27] and increase dopamine release in the striatum [19]. The results from experiment I indicate that dopamine and norepinephrine receptors were functional since amphetamine activity was not diminished significantly by any of the lesions. Perhaps this may account for the inability of any lesion to fully eliminate the morphine-induced hyperactivity.

The present experiments did not demonstrate significant reductions in morphine- or amphetamine-induced hyperactivity after either lesions of the ACCUM + STRIA or naloxone injections in these brain areas. However, the literature suggests a role for these structures in opiate-stimulated locomotion [26]. The current studies may not be directly comparable with those of Teitelbaum *et al.* since the present lesions were more caudal.

It is possible that all four areas (the nucleus accumbens,

the stria terminalis, the dorsomedial caudate, and the lateral septal nuclei, which are interconnected [1, 14, 15, 18] and all contain endorphins) are necessary for full mediation of the morphine-induced hyperactivity effect. This suggestion is in consonance with the findings of a recent experiment in which kainic acid lesions involving portions of the striatum and nucleus accumbens apparently produced a near-complete reduction in morphine-induced locomotion while sparing amphetamine-stimulated activity [21]. Another study has proposed, for example, that activity is divided into two parts—fine and gross motor activity—and that these two types of activity are mediated by different opiate receptor subpopulations [6]. The current data are consistent with this theory. The areas of caudate and septal nuclei studied contain primarily enkephalinergic neurons, which could indicate high concentrations of delta receptors [28,29]. The nucleus accumbens and stria terminalis areas contain more endorphinergic neurons than enkephalinergic neurons [2, 8, 28, 29]. This may indicate large numbers of mu receptors. Perhaps both regions are involved in the mediation of the hyperactivity induced by morphine, with the neurons of one region controlling predominantly fine activity and the neurons in the other controlling predominantly gross activity. This speculation concerning the possibly different role of

opiate receptor subtypes is consistent with a recent report revealing that selective mu receptor antagonism produces only a partial reduction of morphine-induced hyperactivity in the C57BL/6J mouse [9].

#### ACKNOWLEDGEMENTS

The authors wish to thank Robert L. Stewart and Joseph Dannelley for their fine technical assistance during the course of these experiments. The naloxone hydrochloride was kindly supplied by Endo Laboratories. We thank Mrs. Marion Golightly for her help in typing this manuscript and Ms. Junith VanDeusen for her useful editing suggestions. Research was conducted according to the principles enunciated in the "Guide for the Care and Use of Laboratory Animals" prepared by the Institute of Laboratory Animal Resources, National Research Council. This research was conducted in part at the Department of Behavioral Sciences and Leadership, USAF Academy, Colorado Springs, CO, and was supported by Defense Nuclear Agency (DNA) under research project grant U99QMXMK.0041 awarded to G. Andrew Mickley. These experiments were performed as partial fulfillment of requirements for the M.A. degree awarded to Karen E. Stevens by the University of Colorado, Colorado Springs, CO.

#### REFERENCES

1. Akil, H., S. J. Watson, E. Young, M. E. Lewis, H. Khachaturian and J. M. Walker. Endogenous opioids: Biology and function. *Annu Rev Neurosci* 7: 223-255, 1984.
2. Barchas, J. P., H. Akil, G. R. Elliott, R. B. Holman and S. J. Watson. Behavioral neurochemistry: Neuroregulators and behavioral states. Location of enkephalin and endorphin receptors. *Science* 200: 964-973, 1978.
3. Bloom, F., E. Battenberg, J. Rossier, N. Ling and R. Guillemin. Neurons containing beta-endorphin in rat brain exist separate from those containing enkephalin: Immunocytochemical study. *Proc Natl Acad Sci USA* 75: 1591-1595, 1978.
4. Browne, R. G., D. C. Derrington and C. S. Segal. Comparison of opiate and opioid-peptide-induced immobility. *Life Sci* 24: 933-942, 1979.
5. Costall, B., D. H. Fortune and R. J. Naylor. The induction of catalepsy and hyperactivity by morphine administered directly into the nucleus accumbens of rats. *Eur J Pharmacol* 49: 49-64, 1978.
6. DeRosetti, S. E. and S. F. Holtzman. Effects of naloxone and diprenorphine on spontaneous activity in rats and mice. *Pharmacol Biochem Behav* 17: 347-351, 1982.
7. Elde, R., T. Hokfelt, O. Johansson and L. Terenius. Immunohistochemical studies using antibodies to leu-enkephalin: Initial observations in the nervous systems of the rat. *Neuroscience* 1: 349-351, 1976.
8. Finley, J. C. W., P. Lindstrom and P. Petrusz. Immunocytochemical localization of B-endorphin-containing neurons in the rat brain. *Neuroendocrinology* 33: 28-42, 1981.
9. Frischknecht, H.-R., B. Siegfried, G. Riggio and P. W. Waser. Inhibition of morphine-induced analgesia and locomotor activity in strains of mice: A comparison of long-acting opiate antagonists. *Pharmacol Biochem Behav* 19: 939-944, 1983.
10. Kelly, P. H., P. W. Seviour and S. D. Iversen. Amphetamine and apomorphine responses in the rat following 6-OHDA lesions of the nucleus accumbens septi and corpus striatum. *Brain Res* 94: 507-522, 1975.
11. Kirk, R. E. *Experimental Design: Procedures for the Behavioral Sciences*. Belmont, CA: Brooks/Cole, 1968, p. 91.
12. Lee, J. R. and M. R. Fennessy. Effects of morphine on brain histamine, antinociception and activity in mice. *Clin Exp Pharmacol Physiol* 3: 179-189, 1976.
13. Myers, R. D. *Methods in Psychobiology*, vol III. New York: Academic Press, 1977, pp. 281-313.
14. Nauta, W. J. H. and V. B. Domesick. Interconnections of limbic system and corpus striatum. *Psychol Med* 11: 1103-1114, 1978.
15. Nauta, W. J. H., G. P. Smith, R. L. M. Faull and V. B. Domesick. Efferent connections and nigral afferents of the nucleus accumbens septi in the rat. *Neuroscience* 3: 385-402, 1978.
16. Oliverio, A. Genotype-dependent electroencephalographic, behavioral and analgesic correlates of morphine: An analysis in normal mice and mice with septal lesions. *Brain Res* 83: 135-141, 1975.
17. Pert, A. and C. Sivit. Neurochemical focus for morphine and enkephalin-induced hypermotility. *Nature* 256: 645-647, 1977.
18. Powell, E. W. and R. B. Leman. Connections of the nucleus accumbens. *Brain Res* 105: 389-403, 1976.
19. Racagni, G., F. Bruno, E. Iuliano and R. Paoletti. Differential sensitivity to morphine-induced analgesia and motor activity in two inbred strains of mice: Behavioral and biochemical correlations. *J Pharmacol Exp Ther* 209: 111-116, 1979.
20. Sar, M., W. E. Stumpf, R. J. Miller, K. Chang and P. Cautrecasas. Immunohistochemical localization of enkephalin in rat brain and spinal cord. *J Comp Neurol* 182: 17-37, 1978.
21. Siegfried, B., U. Filibeck, S. Gozzo and C. Castellano. Lack of morphine-induced hyperactivity in C57BL/6J mice following striatal kainic acid lesions. *Behav Brain Res* 4: 389-399, 1982.
22. Simon, E. J. and J. M. Hiller. *In vitro* studies on opiate receptors and their ligands. *Fed Proc* 37: 141-146, 1978.
23. Slotnick, B. M. and C. M. Leonard. *A Stereotaxic Atlas of the Albino Mouse Forebrain* (HEW Publication No. 75-100). Rockville, MD: Department of Health Education and Welfare, 1975.
24. Snyder, S. H. and S. R. Childers. Opiate receptors and opioid peptides. *Annu Rev Neurosci* 2: 35-64, 1979.



25. Szara, S. Opiate receptors and endogenous opiates: Panorama of opiate research. *Prog Neuropsychopharmacol Biol Psychiatry* 6: 3-15, 1982.
26. Teitelbaum, H., P. Giammateo and G. A. Mickley. Differential effects of localized lesions of the n. accumbens on morphine- and amphetamine-induced locomotor hyperactivity in the C57BL/6J mouse. *J Comp Physiol Psychol* 93: 745-751, 1979.
27. Trabucchi, M., P. F. Spano, G. Racagni and A. Oliverio. Genotype-dependent sensitivity to morphine: Dopamine involvement in morphine-induced running in the mouse. *Brain Res* 114: 536-540, 1976.
28. Wamsley, J. K., W. S. Young, III and M. J. Kuhar. Immunohistochemical localization of enkephalin in rat forebrain. *Brain Res* 190: 153-174, 1980.
29. Wamsley, J. K., W. S. Young, II and M. J. Kuhar. Anatomical localization of enkephalin immuno-reactive sites in rat forebrain. In: *Neural Peptides and Neuronal Communication*, edited by E. Costa and W. Trabucchi. New York: Raven Press, 1980.
30. Watson, S. J., H. Akil, S. Sullivan and J. P. Barchas. Immunohistochemical localization of methionine enkephalin: Preliminary observations. *Life Sci* 21: 733-738, 1977.
31. Williams, D. J., A. R. Crossman and P. Slater. The efferent projections of the nucleus accumbens in the rat. *Brain Res* 130: 217-227, 1977.
32. Wirtshafter, D., K. E. Asin and E. W. Kent. Nucleus accumbens lesions reduce amphetamine hyperthermia but not hyperactivity. *Eur J Pharmacol* 51: 449-452, 1978.

# **AFRRI** **TECHNICAL REPORT**

## **Preliminary evaluation of U.S. Army RADIAC detector DT-236/PD and RADIAC computer-indicator CP-696/UD**

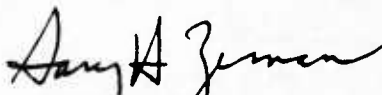
**G. H. Zeman  
M. Dooley  
T. M. Mohaupt**

**DEFENSE NUCLEAR AGENCY  
ARMED FORCES RADIOBIOLOGY RESEARCH INSTITUTE  
BETHESDA, MARYLAND 20814-5145**

---

**APPROVED FOR PUBLIC RELEASE; DISTRIBUTION UNLIMITED**

REVIEWED AND APPROVED

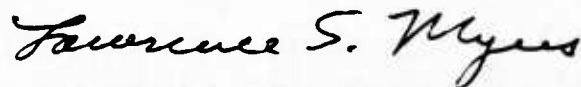


GARY H. ZEMAN

CDR, MSC, USN

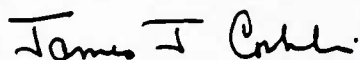
Chairman

Radiation Sciences Department



LAWRENCE S. MYERS, Ph.D.

Scientific Director



JAMES J. CONKLIN

Col, USAF, MC

Director



Preliminary evaluations of the DT-236/PD U.S. Army battlefield personnel dosimeter were performed at the Armed Forces Radiobiology Research Institute (AFRRI) from the summer of 1984 to the spring of 1985. This personnel dosimetry system is being procured by the U.S. Army for use by combat forces in theaters of operation where tactical nuclear weapons could be used.

In operation, the wristwatch-style dosimeter is worn by a soldier to record both instantaneous and residual gamma and neutron radiations that are released from the detonation of a nuclear weapon, plus gamma radiation from fallout. The dosimeter contains a block of radiophotoluminescent glass as the gamma detector and a silicon diode as the neutron detector. Properties of these detectors have been described in various review articles (1). The reader unit simultaneously evaluates both of the radiation detectors and presents a total dose reading on a panel meter.

Earlier tests of this dosimetry system at the U.S. Army Pulsed Radiation Facility at Aberdeen Proving Ground, Maryland, were reported by Basso (2). Other calculational evaluations of this dosimetry system have also been done (3). The present report describes AFRRI results of the irradiation of DT-236/PD dosimeters with (a) reactor-produced neutron and gamma radiations to simulate a nuclear detonation and (b) cobalt-60 gamma radiation to simulate nuclear fallout.

## MATERIALS AND METHODS

About 500 RADIAC detectors DT-236/PD and 1 prototype RADIAC computer indicator CP-696/UD were obtained from the U.S. Army Communications-Electronics Command, Fort Monmouth, New Jersey. The CP-696/UD reader unit was of the original analog readout type (4) as shown in Figure 1. Nameplate information on the reader was type 3146Y, serial 19, with no modifications. The DT-236/PD dosimeters used in the tests had serial numbers between 005400 and 006594.

To operate the CP-696/UD dosimeter reader, a 24-volt DC laboratory power supply was connected to the power input. Readout from the CP-696/UD was taken from the analog panel meter and from a digital voltmeter connected internally in parallel with the analog panel meter. The use of a digital voltmeter allowed more rapid and precise readings to be made, and allowed estimation of those readings that were off-scale on the analog meter. Before using this technique, it was verified that the digital voltmeter connected to the analog meter did not change the reading of the meter. Also, a calibration curve for the voltmeter was constructed by comparing concurrent analog and digital meter readings. This curve was found to have two linear segments described by the following equation:

$$\text{Dose (rads)} = \begin{cases} 2 + 1441 \times V & (V < 0.172 \text{ volts}) \\ -518 + 4443 \times V & (V > 0.172 \text{ volts}) \end{cases}$$

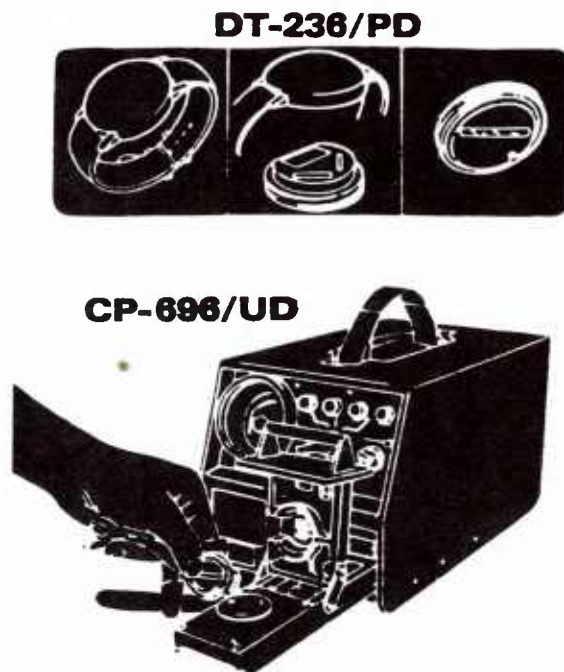


Figure 1. DT-236/PD dosimeter and CP-696/UD reader

Calibration and operating procedures for the reader unit were taken directly from the technical manual (4). These procedures give a single total (neutron plus gamma) dose reading in rads for each dosimeter. To attain separate evaluations of the neutron and gamma doses, a second read cycle was required. This second cycle was done with the reader unit set to the "gamma test" position. In this position, a gamma-only readout of the dosimeter was attained. The neutron component of the total reading was then obtained by subtraction.

Radiation sources for these tests were the AFRRI Cobalt-60 Whole-Body Irradiation Facility (5) and the TRIGA Mark-F Nuclear Reactor (6). Reference dosimetry measurements were performed as described in reference 7, using a tissue-equivalent ionization chamber with flowing tissue-equivalent gas and a magnesium chamber with argon.

The cobalt-60 irradiations were carried out in a unilateral mode at 0.40 Gy/min. The dosimeters were free in air; that is, no phantom or backscattering material was used for the cobalt-60 irradiation. For reactor irradiation, the dosimeters were mounted on the surface of a cylindrical lucite phantom 30 cm in diameter and 60 cm tall. Eight dosimeters were arranged in a 10-cm-diameter array on a curved phantom surface facing the reactor. The entrance surface of the phantom was located 85 cm from the reactor tank wall, and a 15-cm-thick lead shield was positioned midway between the phantom and the tank wall. The dose rate on the phantom surface was 0.55 Gy/min with a neutron-to-gamma ratio of 5.0; i.e., 17% of the dose on the phantom surface was due to gamma rays. The neutron and gamma-ray free-in-air energy spectra and spatial variation are shown in Figures 2 and 3a,b.

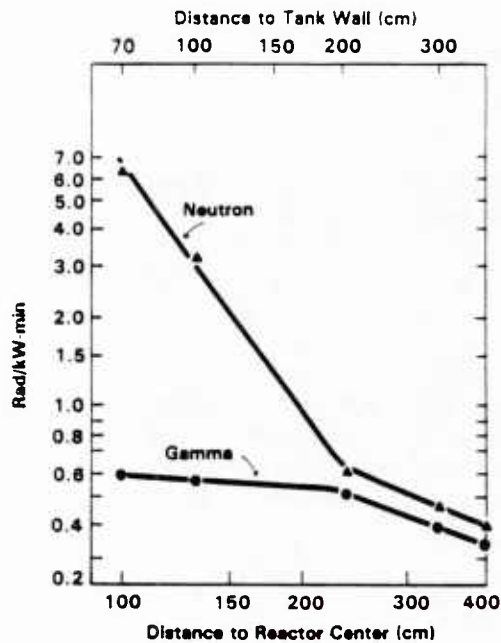
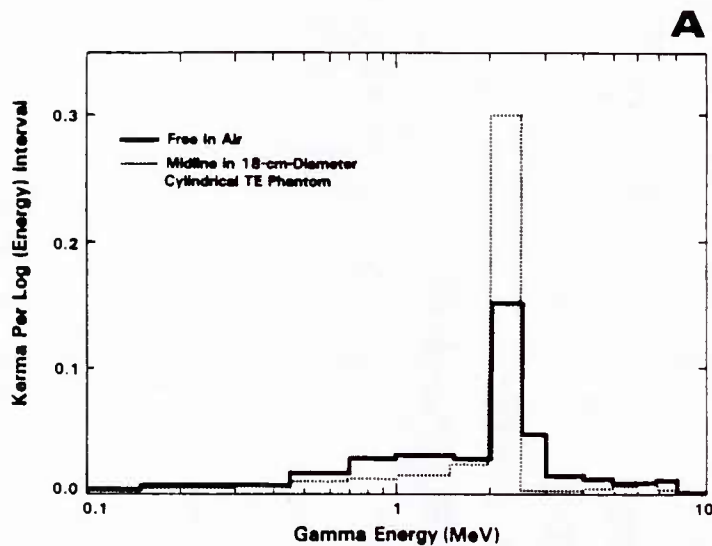
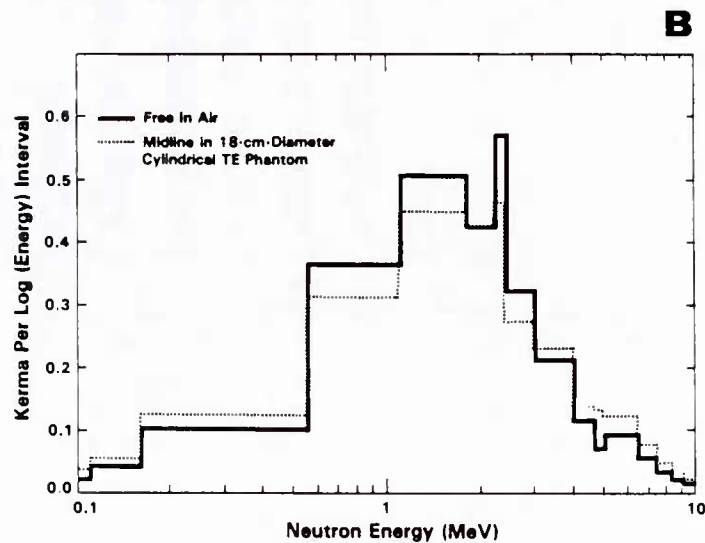


Figure 2. Free-in-air kerma rates in AFRR TRIGA reactor exposure room 1, with a 15-cm-thick lead shield in place. Irradiation of dosimeters was done with front face of phantom 85 cm from tank wall, or 115 cm from reactor center. Neutron-to-gamma ratio was 8 for free in air and 5 at phantom surface.



Figures 3a,b. Neutron and gamma-ray energy spectra free in air and at midline of 18-cm-diameter phantom in exposure room 1, with the 15-cm-thick lead shield in place. Spectra were derived from reference 8.





## RESULTS

### DOSIMETER READER

During initial tests, the calibration readings of the dosimeter reader were checked after every few dosimeters. These readings proved to be very constant, and the calibrations did not have to be adjusted if the unit had been powered ON for 24 hours. During the first 24 hours after turning the unit on, frequent calibration adjustments were necessary.

The reproducibility of sequential readings of the same dosimeter was within  $\pm 5\%$  except for occasional aberrant readings markedly lower than expected. Because of this, the dose received by a dosimeter was usually taken to be the median of three sequential readings. The cause of the occasional low readings was not positively identified. Firmly holding the read-switch in position during the read cycle did lessen the number of aberrant readings.

### DOSIMETER PREIRRADIATION READINGS

All nonirradiated dosimeters tested gave a nonzero dose reading. Individual dosimeter readings ranged from 20 to 60 rads total dose. Figures 4a,b,c summarize the readings of 70 nonirradiated dosimeters that were later used in further tests. These baseline or predose readings of the dosimeters could have been reduced by appropriate adjustments of the reader unit zero-levels. However, for the initial tests described in this report, no further zero-level adjustments were made.

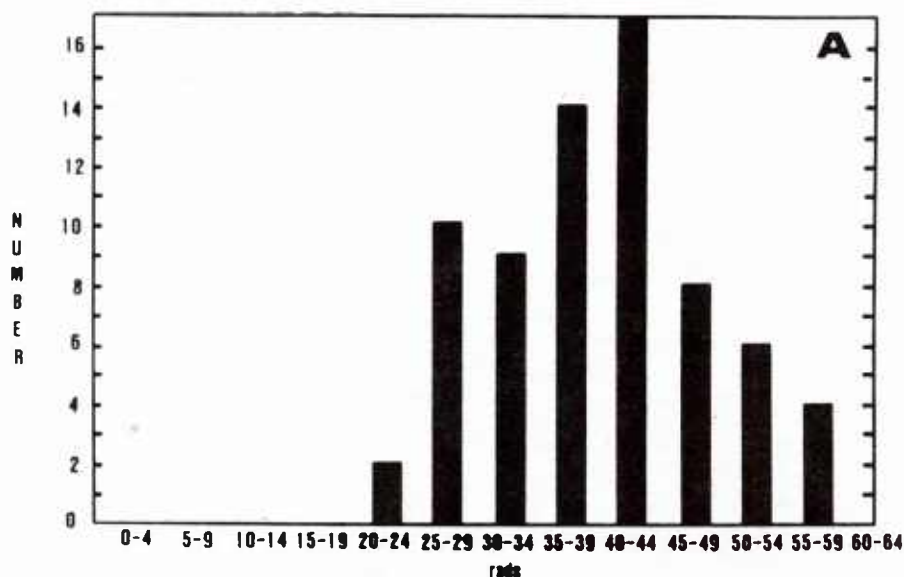


Figure 4a. Readings of 70 nonirradiated dosimeters. Total dose: average 37.8 rads, SD 8.9 rads.

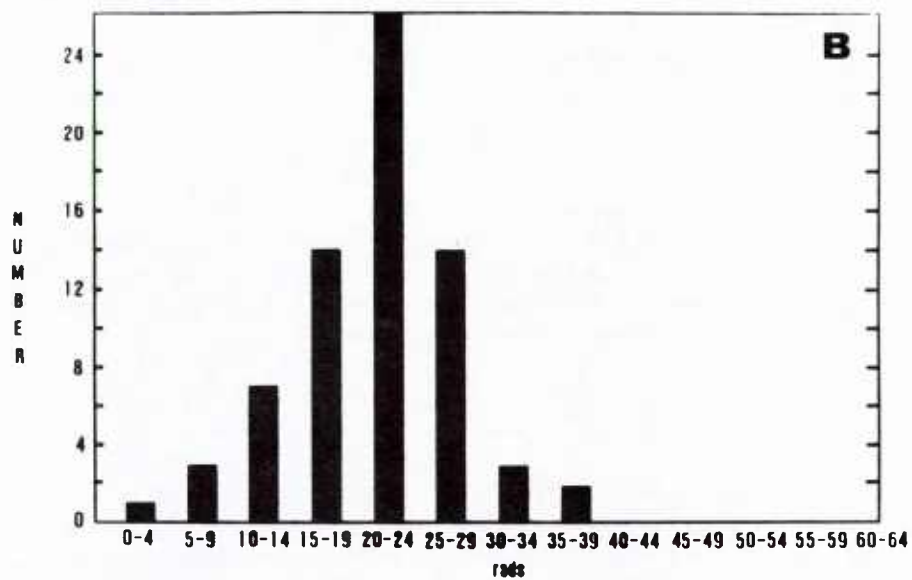


Figure 4b. Readings of 70 nonirradiated dosimeters. Gamma dose: average 19.4 rads, SD 6.8 rads.

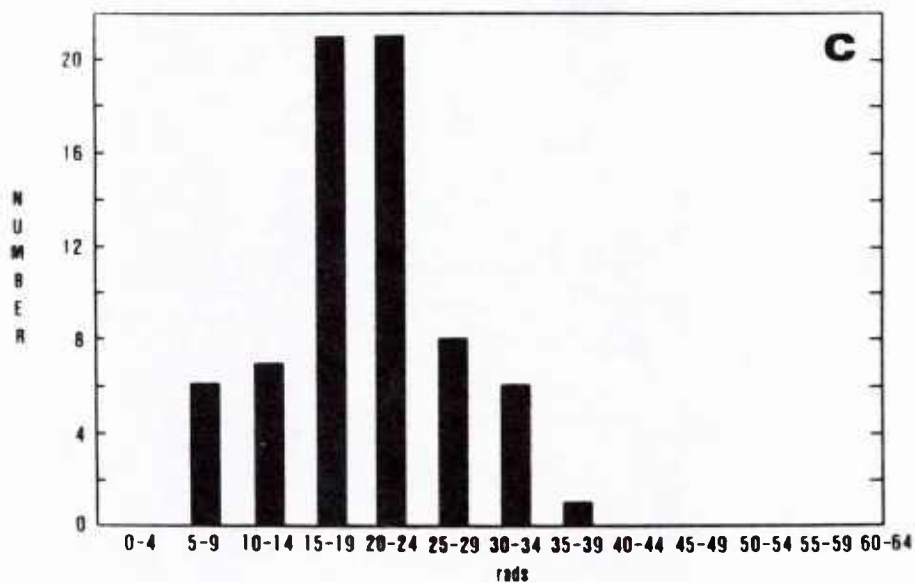


Figure 4c. Readings of 70 nonirradiated dosimeters. Neutron dose: average 18.5 rads, SD 7.1 rads.

Lower limits of detection (LLD) of the DT-236/PD dosimetry system can be inferred from observed variability of predose readings. Following the convention of U.S. Nuclear Regulatory Commission Regulatory Guide 8.14, "Personnel Neutron Dosimeters," the LLD is defined as follows:

$$LLD = 4.66 \sqrt{N} \cdot S$$

where N is the number of dosimetry exchange periods in a calendar quarter (N = 1 in the present case) and S is the standard deviation (SD) of the normal background. Using the data in Figures 4a,b,c, the LLD of the DT-236/PD system is 33 rads neutron, 32 rads gamma, and 41 rads total dose.

### COBALT-60 IRRADIATION

Dosimeters were irradiated with cobalt-60 gamma rays to doses of 500 rads, 100 rads, and 25 rads. The dosimeters were evaluated just after irradiation and at various times through the next 5 days. Figures 5a,b,c show the dosimeter gross readings uncorrected for baseline readings. The cobalt-60 data display the expected increase in phosphate glass gamma reading over the first day post-irradiation followed by a plateau or slow fading of readings. The variability of response between individual dosimeters, as determined from the five 500-rad dosimeters, was  $\pm 20\%$  (2 SD) at most times, with larger variability of  $\pm 30\%$ - $40\%$  observed within the first 2 hours after irradiation. The average gross response of the 500-rad dosimeters was higher than the delivered doses by +12% to +44% over the course of the measurement period. Correction for baseline readings would reduce this overresponse only slightly.

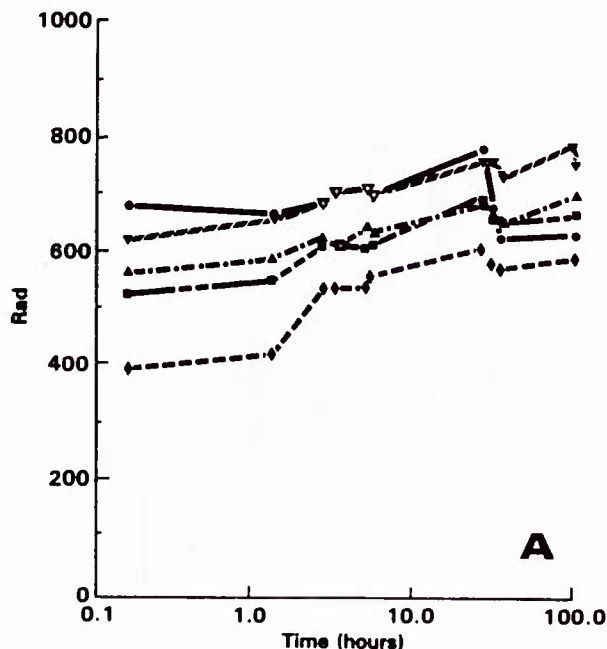


Figure 5a. Readings of dosimeters irradiated with cobalt-60 at 500 rads. Data in Figures 5a,b,c are gross gamma readings, uncorrected for baseline preirradiation readings. Symbols represent separate dosimeters.



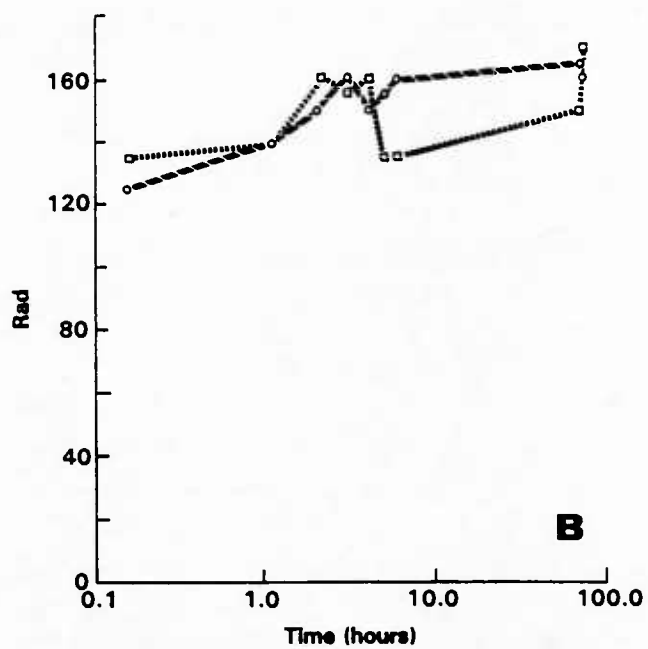


Figure 5b. Readings of dosimeters irradiated with cobalt-60 at 100 rads

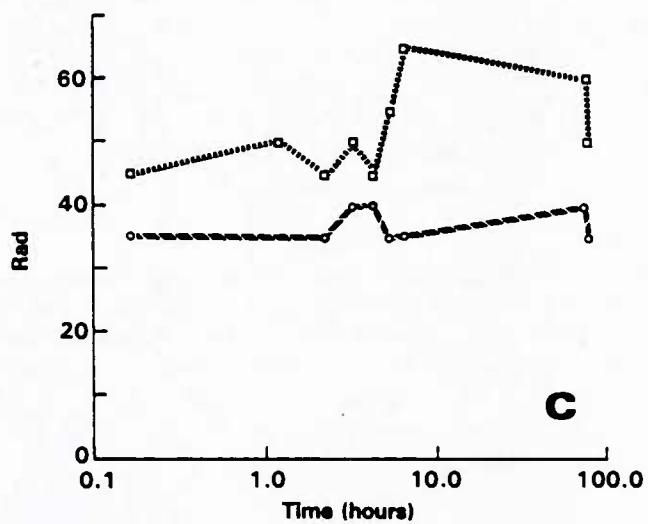


Figure 5c. Readings of dosimeters irradiated with cobalt-60 at 25 rads

## REACTOR IRRADIATION

Three reactor runs were performed with the delivered doses on the surface of the phantom listed in Table 1.

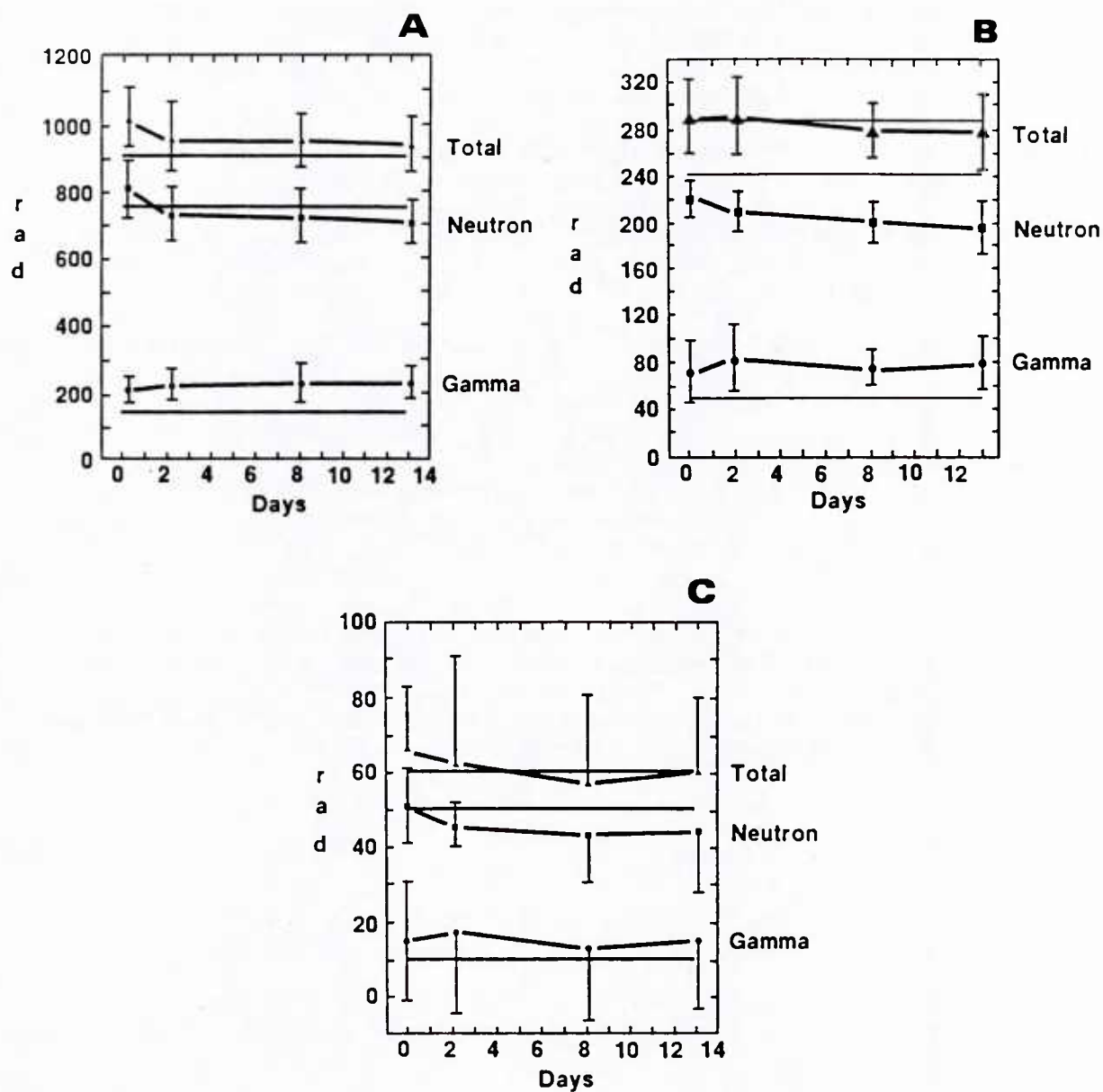
Table 1. Delivered Doses at Surface of Phantom

Run Number	Dose (Rad)		
	Gamma	Neutron	Total
1	10	51	61
2	48	242	290
3	152	757	909

Eight dosimeters were irradiated in each run. The average response of the dosimeters is shown in Figures 6a,b,c. In these graphs, the average gamma, neutron, and total readings of nonirradiated dosimeters (Figure 2) have been subtracted. Thus the graphs represent net dosimeter readings. Error bars in these graphs indicate the 95% confidence interval (2 SD) determined from the eight dosimeters in each group.

The data displayed in Figures 6a,b,c show an overresponse to gamma radiation as observed for cobalt-60 irradiations and, generally, an underresponse to neutron radiation. These opposing biases resulted in total dose readings of the dosimeters that were reasonably accurate. The data also show the loss of neutron reading or fading with time after irradiation. The neutron fading over 13 days was 10%-15% for each of the three dose groups. It is of interest that the initial loss of neutron signal is at least partially compensated for by the increase in gamma signal, so that the total dose readings remain relatively constant for several days after irradiation.

Finally, Figures 6a,b,c show that the precision of the neutron dose readings was noticeably better than that of the gamma dose readings. For the two high-dose groups, the 95% confidence interval for the neutron readings was typically  $\pm 10\%$ , and that for the gamma readings was typically  $\pm 20\%$ . Precision of the total-dose readings was comparable to the neutron precision ( $\pm 10\%$ , 2 SD) for this high-neutron field. This contrasts with the  $\pm 20\%$  total-dose precision obtained for the 500-rad gamma-only irradiations.



Figures 6a,b,c. Readings of dosimeters irradiated with TRIGA reactor at (a) 909 rads, (b) 290 rads, and (c) 61 rads



## DISCUSSION

Performance of the DT-236/PD and CP-696/UD dosimetry system has been studied in preliminary tests at AFRRI in cobalt-60 and in TRIGA-reactor radiation fields. The test results are relevant to the reproducibility of the dosimeter reader, the variability of readings among identically irradiated dosimeters, the fading or growth of dosimeter readings with time after irradiation, and the accuracy of dosimeter response in the AFRRI radiation fields.

The performance specifications (2, 3) for this system list  $\pm 40\%$  accuracy at doses of 50-1000 rads and  $\pm 20$ -rad accuracy at 0-50 rads. The present tests showed the system to be capable of meeting these specifications and, with care, a level of accuracy of  $\pm 10\%$  to  $20\%$  was achieved at high doses. At low doses, the accuracy of the system was limited by the  $\pm 20$ -rad (2 SD) variability in readings of nonirradiated dosimeters.

Factors found to improve the precision of dosimeter readings were (a) warm-up time of several hours for the reader unit, (b) sustained firm pressure on the mechanical switch that initiates the read cycle, (c) triplicate readings of each dosimeter, (d) digital readout of the dose values, (e) proper accounting of dosimeter predose readings, and (f) waiting 2 hours after irradiation before reading the dosimeter. Although these practices were easily implemented in a laboratory setting, they may be totally impractical in field use of the system. Thus, in the field it seems likely that the specification of  $\pm 40\%$  accuracy represents realistic performance of the system.

The test results described in this report represent the performance of a prototype dosimeter system. The final production version of the system, to be designated AN/PDR-75, will require similar tests to be performed. Further tests will also be needed to define the directional and energy response of the dosimeters as well as the performance of the system under extremes in ambient temperature.

## REFERENCES

1. Becker, K. Solid State Dosimetry. CRC Press, Cleveland, 1973, pp. 141-173 and 225-231.
2. Basso, M. J. Response of the UK DT-236 Personnel Dosimeter to a Fast Pulsed Nuclear Reactor Radiation Environment. DELCS-K, MFR, Fort Monmouth, New Jersey, 1982.
3. Scott, W. H., et al. Dosimeter and bone marrow doses in tactical nuclear environments. SAI-133-80-269-LJ. Science Applications Inc., La Jolla, California, 1980.
4. U.S. Army Technical Manual for CP-696/UD Computer Indicator Radiac and DT-236/PD Detector Radiac. DEP TM 11-6665-236-12, Fort Monmouth, New Jersey, 1978.
5. Carter, R. E., and Verrelli, D. M. AFRRI cobalt whole-body irradiator. Technical Note TN73-3, Armed Forces Radiobiology Research Institute, Bethesda, Maryland, 1973.

6. Sholtis, J. A., and Moore, M. L. Reactor facility at Armed Forces Radiobiology Research Institute. Technical Report TR81-2, Armed Forces Radiobiology Research Institute, Bethesda, Maryland, 1981.
7. Goodman, L. J. A practical guide to ionization chamber dosimetry at the AFRRI reactor. Contract Report CR85-1, Armed Forces Radiobiology Research Institute, Bethesda, Maryland, 1985.
8. Verbinski, V. V., et al. Calculation of the neutron and gamma-ray environment in and around the AFRRI TRIGA reactor. DNA 5793F-2, Defense Nuclear Agency, Washington, DC, 1981.

# AFRRI\_\_\_\_\_CONTRACT REPORT



AFRRI CR86-1

## **Calorimetric dose measurements and calorimetric system developed for the Armed Forces Radiobiology Research Institute**

DEFENSE NUCLEAR AGENCY

**ARMED FORCES RADIOBIOLOGY RESEARCH INSTITUTE**

BETHESDA, MARYLAND 20814-5145

---

APPROVED FOR PUBLIC RELEASE; DISTRIBUTION UNLIMITED



Prepared by

Joseph C. McDonald, Senior Research Scientist

Battelle Memorial Institute, Pacific Northwest Laboratory

Richland, Washington 99352

Under Contract No. AI-CR0-0013

## CONTENTS

INTRODUCTION	1
MATERIALS AND METHODS	1
RADIATION SOURCES	4
EXPERIMENTAL PROCEDURES	6
COBALT-60	6
REACTOR	6
LINAC	6
DATA ANALYSIS	7
RESULTS	10
DISCUSSION AND CONCLUSIONS	12
UNCERTAINTIES	12
CONCLUSIONS	12
ACKNOWLEDGMENTS	13
APPENDIX A. DATA LIST	15
APPENDIX B. OPERATIONAL PROCEDURES FOR CALORIMETER	19
REFERENCES	23

## INTRODUCTION

An absorbed-dose calorimeter measures kerma caused by the absorption of gamma rays and fast neutrons. It basically operates through the following principle: The absorption of radiation in material results in an increase of the temperature of the material; this temperature increase is directly proportional to absorbed dose and is not dependent on dose rate or the ionization density of the radiation (1). Since the magnitude of such temperature increases is small (on the order of  $10^{-3}$  K/rad), a sensitive thermistor is used to detect the change.

A calorimeter can be calibrated directly in terms of energy per unit mass by depositing a known amount of energy into the calorimeter's central absorbing element (or core) with an electric heater. When a TE plastic calorimeter is used, a small amount of the energy deposited by radiation does not appear as heat. About 4% of the energy is consumed by radiochemical reactions in the plastic (2), so a correction must be made for this thermal defect.

## MATERIALS AND METHODS

The calorimeter used for these measurements (see Figure 1) was designed specifically to measure kerma in A-150 plastic. To achieve this goal, it was necessary to have a minimum amount of material surrounding the core. The core is a sphere of A-150 plastic, 1.27 cm in diameter. The point of measurement is at the center of the core, which is behind 0.63 cm of A-150 plastic. This amount of material is

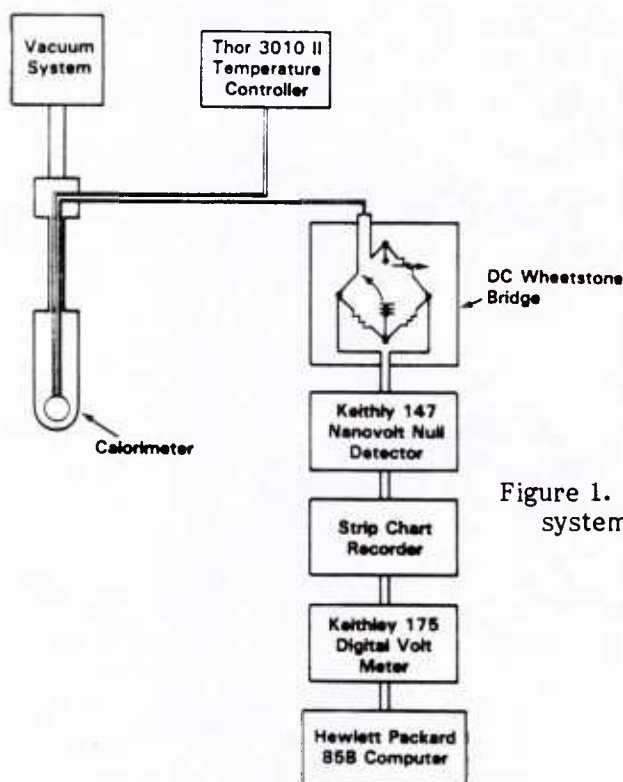


Figure 1. Block diagram of calorimeter system, indicating major components

enough to ensure secondary charged particle equilibrium for cobalt-60 gamma rays, but it is more than is needed to establish secondary charged particle equilibrium for neutrons from the reactor. Therefore, a correction was made for the absorption of neutrons in the material between the point of entry and the center of the core.

An aluminum vacuum shell, approximately 0.02 cm thick, surrounds the calorimeter's central elements. The vacuum provides insulation, which helps reduce heat loss from the core.

Figure 2 shows a block diagram of the equipment used in the calorimetric system. The change in resistance of the core thermistor was measured by the Wheatstone bridge and the null detector. This signal was displayed on a strip chart recorder and interfaced to a computer by means of a voltmeter. An example of the output signal is shown in Figure 3. The vacuum system and temperature controller were used to control the temperature of the calorimeter.

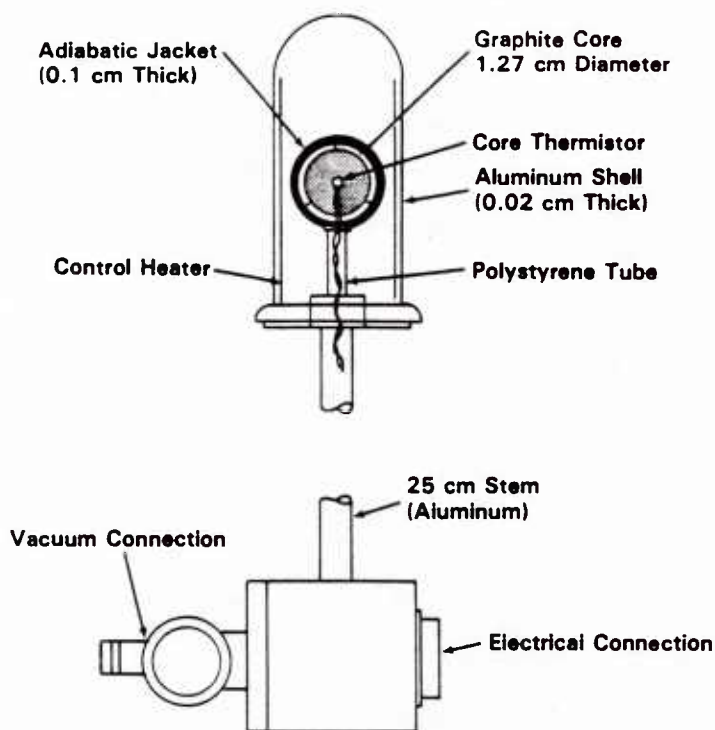


Figure 2. Cutaway drawing of internal construction of calorimeter (not to scale)



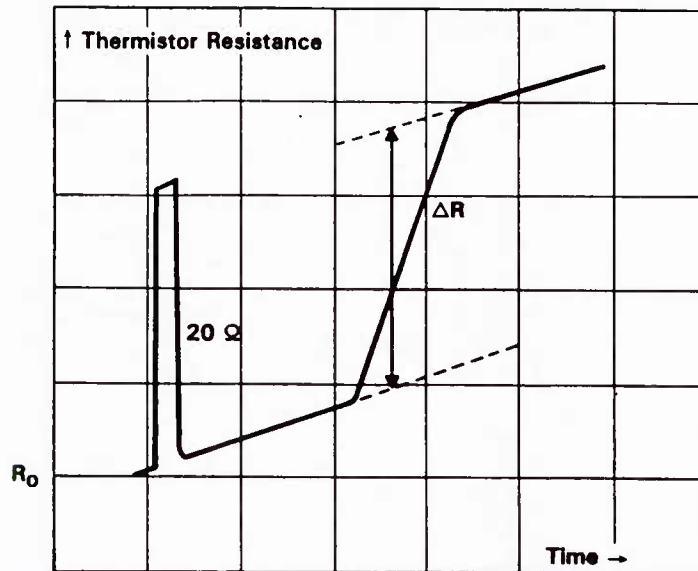


Figure 3. Recorder trace indicating response of Wheatstone bridge to change of 20 ohms and then to change in resistance of core thermistor due to heat deposited in core by radiation

Electrical calibration of the calorimeter was performed with a current source connected to the calibration heater element, which is imbedded in the core. Electrical heating of the core results in a response that corresponds to a known amount of energy per unit mass. This response is measured as the relative change in core thermistor resistance,  $\Delta R$ , divided by the initial resistance value before the input of energy,  $R_0$ . The calibration factor,  $C$ , then becomes:

$$C = \frac{E}{m} \cdot \frac{R_0}{\Delta R}$$

where  $E$  is the energy deposited,  $m$  is the core mass, and  $R_0/\Delta R$  is the fractional thermistor resistance change. The electrical energy deposited is calculated, knowing the core heater resistance and the current flowing through it (1).

During radiation measurement, a value is determined for  $\Delta R/R_0$ , which is then multiplied by the calibration factor to yield dose. An additional correction of 4% is made for the thermal defect; therefore:

$$DA-150 = C \cdot \frac{\Delta R}{R_0} \cdot T$$

where  $C$  is the calibration factor and  $T$  is the thermal defect correction of 1.04.

Kerma in the neutron field is determined by making an additional correction to account for the absorption of neutrons in the A-150 plastic upstream of the center of the core. The absorption in the 0.02-cm-aluminum vacuum shell was considered

negligible. These corrections differed for each irradiation condition, because the relative amounts of neutrons and gamma rays present were different. The three conditions are listed in Table 1 along with the absorption corrections used to calculate kerma (3).

Table 1. Irradiation Conditions and Absorption Corrections

Condition	Absorption Correction
6" lead	1.104
Bare	1.078
12" water	1.006

## RADIATION SOURCES

### Cobalt-60

The Cobalt-60 facility consists of 104 separate cobalt-60 elements stored under approximately 5 meters of water. The total activity was 100,000 curies as of September 1981. Depending on the arrangement of the elements, unilateral or bilateral exposures may be obtained. By varying the number of elements and the distance from the source, the dose rate may be varied from approximately 1 to 5700 rad/min.

When a source is selected, it is automatically raised from its safe storage position by an elevator. There are two such elevators, one on either side of the irradiation support. These elevators can be moved away from the source to distances of several meters. The source drives are controlled with electronic timers so that the duration of the exposure can be preset.

### Reactor

The reactor at AFRRI is a General Atomics (TRIGA) Mark-F pool-type reactor, which is capable of both steady-state and pulsed modes. The reactor produces a modified uranium-235 fission spectrum with neutron-to-gamma ratios ranging from 0.05 to 30. The maximum power limitations are 1.0 MW (thermal) and 2500 MW (thermal) in the steady-state and pulsed modes, respectively.

Dosimetry at AFRRI's TRIGA reactor is currently performed with paired ionization chambers (tissue-equivalent plastic and magnesium). During steady-state reactor runs, where the dose rate is on the order of 40 rad/min, this technique has proven sufficient. However, in the pulsed mode, up to 10,000 rad may be given in a very short time (msec), causing the chambers to saturate. The pulsed mode, although used frequently, has not been adequately studied in terms of the neutron-to-gamma ratio and the spectra in the exposure rooms.

The reactor exposure room is approximately a cube (with 3.5-meter sides). The wall nearest the reactor has a cylindrical protrusion that allows the reactor core to be placed somewhat farther into the room. The normal irradiation reference position is 1 meter from the center of the core.

### LINAC

The AFRRI linear accelerator (LINAC) is a traveling wave electron accelerator powered by a pulsed source of high-power microwave radio frequency. The LINAC may be operated in two distinct modes: one produces electron beams (13-20 MeV) and the other produces either higher energy (20-45 MeV) electron beams or bremsstrahlung fields.

Most experimental work currently done using the AFRRI LINAC requires the use of the first mode, that is, a beam of electrons with initial energy ranging from 13 to 20 MeV. The pulse is from 0.01 to 5.0 microseconds. A water scatterer is often used to decrease the energy of the electron beam and to increase the field size. Occasionally, shielding or a scattering device is placed between the target and the LINAC port to further reduce the energy and broaden the spectrum. The dose rate and the field size then depend on the initial energy of the electrons, use of water scatter, distance from the LINAC, and use of shielding or other scattering devices. Some common experimental configurations are listed in Table 2 (pulse width equal to 4 microseconds).

Table 2. Common Experimental Configurations

Initial Energy (MeV)	Water Scatter	Approx. Energy Striking Target (MeV)	Pulse Rate (pulse/sec)	Target Distance (meters)	Approx. Field Size (cm diam.)	Dose Rate (rad/pulse)
18.6	Yes	13.7	60	1.0	14	160
18.6	Yes	13.7	15	3.5	42	15
18.6	Yes	13.7	15	4.0	49	12
13.5	Yes	9.3	30	1.0	16	250
13.5	No	12.7	15	3.2	21	490
13.5	Yes	8.3	15	5.0	78	7
13.5	No	12.0	30	5.0	47	50

## EXPERIMENTAL PROCEDURES

### COBALT-60

The calorimeter and an AFRRI ionization chamber (Exradin T-2) were placed at the same distance (approximately 30 cm) from the cobalt-60 source elevators. The calorimeter and the chamber were supported on a wooden table placed between the two source elevators. The vacuum pump for the calorimeter was supported on an adjacent table. Cables were strung up to the shielded entry door, and then taped to the wall so that the door could close without crushing the cables. The calorimeter's electronics rack was operated in an area adjacent to the cobalt-60 source control room.

Monitoring was achieved by the use of electronic timers to control the duration of the exposures, and a spherical ionization chamber placed approximately 1 meter from the source elevators.

Appropriate corrections were made to the ionization chamber readings to account for local air temperature and pressure. The calorimetric measurements were taken in sets of approximately ten replicate runs to improve the standard error of the mean for each set.

### REACTOR

Two ionization chambers were set up, along with the calorimeter, at a distance of 1 meter from the reactor core. The ionization chambers were Exradin T-2 model (0.5 cc); one was constructed of A-150 plastic and the other was of magnesium. A 50-cc AFRRI chamber served as a monitor.

The calorimeter's vacuum system was also in the exposure room. The entire vacuum system was shielded with boron-loaded paraffin blocks so that it could not become activated.

A series of steady-state and pulsed exposures was taken at several power levels to determine the saturation corrections for pulsed irradiations.

### LINAC

The measurement configuration at the LINAC was different from that used at the reactor because of the higher energies encountered. Both the calorimeter and the AFRRI ionization chamber (Exradin T-2) were placed within a polystyrene block, which is normally a part of a SCRAD phantom (25 x 25 x 25 cm). Both the chamber and the calorimeter measured the dose at an effective depth of 2.67 g/cm<sup>2</sup>, which is approximately the point of maximum dose within the phantom. With both electron and bremsstrahlung beams, the position of the dose maximum extends over several centimeters.



The calorimeter and chamber were placed on a table at distances ranging from approximately 2 to 6 meters from the beam pipe exit window. The calorimeter's vacuum system was placed on an adjacent table. The calorimetric signal passed through approximately 150 feet of shielded signal cable. The calorimeter's electronics were set up in the LINAC experimental area, near the electrometer for the ionization chamber.

## DATA ANALYSIS

### Calorimetric Calibration

The calorimeter is calibrated electrically by passing a known current through the core heater for a known time and observing the response in terms of the normalized resistance change (i.e.,  $\Delta R/R_0$ ). The electrically equivalent "dose" (J/kg) is computed from the following formula:

$$D = \frac{\left( \frac{V}{1.3 \times 1000} \right)^2 R_H t}{m_c}$$

where V is the calibration circuit voltage,  $R_H$  is the core heater resistance, t is the duration of the heating in seconds, and  $m_c$  is the mass of the core in kg. The factor of 1.3 accounts for the voltage division in the calibration circuit, and the factor of 1000 yields the correct units of joules.

Table 3 shows the calibration circuit voltages, equivalent doses, duration times, and observed  $\Delta R/R_0$  values.

Table 3. Electrical Calibration Parameters

Voltage (V)	Dose (Gy)	Time (s)	$\Delta R/R_0$
.534	17.26	60	$4.49 \times 10^{-4}$
.823	41.42	60	$1.08 \times 10^{-3}$
1.600	148.07	60	$3.86 \times 10^{-3}$

These values yield an average electrical calibration factor of:

$$C_E = 3.84 \times 10^4 \text{ Gy}/\Delta R/R_0$$

To cross-check this calibration, the core thermistor was calibrated in terms of temperature response. The data were fitted with an exponential least squares fit (Figure 4), yielding a value for the percent change per unit temperature of -4.467% per °C with a correlation coefficient of 0.99.

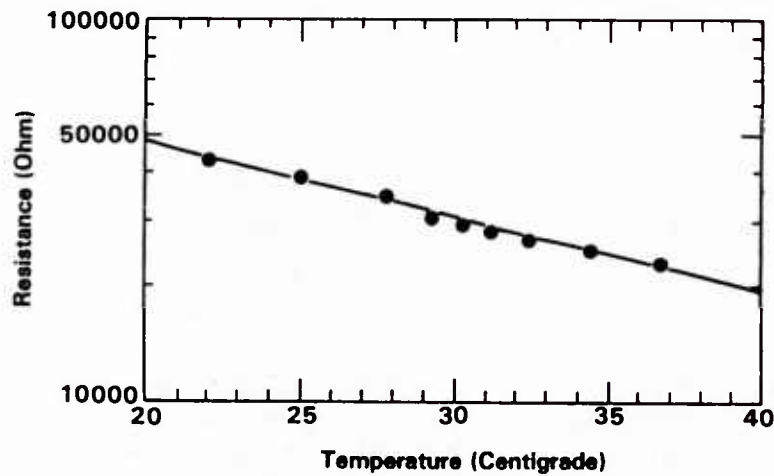


Figure 4. Plot of core thermistor resistance as function of core (A-150 plastic) temperature

The formula for specific heat can be used to evaluate the calorimeter's response another way:

$$S = \frac{E}{m \Delta t}$$

where  $S$  is the specific heat,  $E$  is the quantity of energy put into the substance,  $m$  is its mass, and  $t$  is the resultant temperature increase. Rewritten, this equation yields:

$$\frac{E}{m} = \Delta t S$$

where we can observe that the energy per unit mass will again be the dose.

The calorimeter was irradiated by a series of identical exposures of 12.03 Gy (tissue) of cobalt-60 gamma rays. The average value of the responses was:

$$R = 3.02 \times 10^{-4} \Delta R/R_0$$

Using the thermistor coefficient allows the determination of a temperature increase, and multiplying that by the specific heat of A-150 plastic (1.72 J/°C) measured by Domen (4) yields the dose:

$$\frac{3.02 \times 10^{-4}}{4.467} \cdot 1.72 \cdot 10^5 = 11.63 \text{ Gy}$$

Thus the value of the calibration factor based on the thermal calibration is:

$$\frac{11.63}{3.02 \times 10^{-4}} = 3.85 \times 10^4 \text{ Gy} / \frac{\Delta R}{R_0}$$

This is almost indistinguishable from the electrical calibration:

$$C_E = 3.84 \times 10^4 \text{ Gy} / \frac{\Delta R}{R_0}$$

#### Calorimetric Dose Calculations

When the electrical calibration is used to calculate the dose from the response shown above, it yields:

$$D_{A-150} = R \cdot C_E \cdot T_D$$

where  $T_D$  is the thermal defect correction of 1.04 and the other symbols have their previous definitions.

$$3.02 \times 10^{-4} (1.84 \times 10^6) 1.04 = 12.06 \text{ Gy A-150}$$

This value should be compared to the value of dose computed to have been delivered to the center of the calorimetric core. This dose was computed as follows:

The measured exposure was  $X = 1270$  roentgen  
 $D = f X A_{eq}$   
 $D = 0.957 \ 1270 \ 0.99 \ 0.01 \text{ Gy/rad}$   
 $D = 12.03 \text{ Gy}$

where  $F$  is the ratio of mass-energy absorption coefficients for tissue and air, and  $A_{eq}$  is the attenuation correction factor.

The delivered value is within 0.3% of the measured value. To summarize, the calibrations based on electrical and thermal methods agree, and the electrical calibration yields values of dose that are identical to values computed from National Bureau of Standards-calibrated chambers.

## RESULTS

Tables 4-6 show the results of measurements that were taken during two sessions, July 1984 and March 1985. All of the individual calorimetric runs used to calculate the average values in the tables are shown in Appendix A. The first session concentrated on the reactor, and the second session dealt with the LINAC. Each time, a set of measurements was taken at the cobalt-60 source as a reference.

The cobalt-60 results show good linearity and reproducibility. The reproducibility between the two cobalt-60 measurements demonstrates the long-term stability of the calorimetric response.

Table 4. Cobalt-60 Results, July 1984

Set	Date	Nominal Dose Rate	Measured Dose Rate (A-150 rad/min)
1	7/10	7000	6950
2	7/11	1000	1050
3*	7/12	5000	2500
4	7/12	3000	3030

\* Could be result of one source element not being in place



Table 5. Calorimetric Results at Reactor, July 1984

Date	Condition		Dose (rad)
7/16	Bare	100 kW	3,270
7/17	Bare pulses	6.5 MW	5,050
		13.8 MW	9,450
		19.9 MW	13,300
	12" H <sub>2</sub> O	100 kW	460
7/18	6" Pb	100 kW	570
		200 kW	1,250
7/19	6" Pb pulses	8.8 MW	1,290
		15.4 MW	2,300
		21.3 MW	3,190

Table 6. LINAC Results, March 1985

Date	Radiation	Dose (Gy A-150 Plastic)
3/5	Cobalt-60	35.6
3/5	Cobalt-60	22.5
3/7	LINAC X rays 2.25 m	22.1
3/7	LINAC electrons 2.25 m	54.5
3/7	LINAC electrons 4 m, 4 $\mu$ s	127.0
3/7	LINAC electrons 4 m, 3 $\mu$ s	91.6
3/8	LINAC electrons 4 m, 2 $\mu$ s	62.8
3/8	LINAC electrons 4 m, 1 $\mu$ s	33.0
3/8	LINAC electrons 6 m, 4 $\mu$ s	54.1
3/8	LINAC electrons 4 m, 18.4 MeV	24.6

## DISCUSSION AND CONCLUSIONS

### UNCERTAINTIES

The precision of the measurements primarily depends on the signal-to-noise ratio for the particular irradiation condition. To improve the determination of a particular value of kerma or kerma rate, several replicate runs were taken. The standard error of the mean for most of these measurements was between  $\pm 0.5\%$  and  $1.5\%$ . Other sources of random uncertainty include data analysis imprecision, monitor reproducibility, and calibration uncertainties.

The accuracy, or systematic uncertainty, is dependent on the calibration of the calorimeter and on the correction factors applied in the calculation of kerma. Estimates of the accuracy from similar measurements were approximately  $\pm 2.5\%$  (5). This includes an uncertainty of approximately  $\pm 1.5\%$  in the value used for the thermal defect corrections (6).

The overall uncertainty in the determination of kerma and kerma rate by means of calorimetric measurement was determined by adding the estimated random and systematic uncertainties in quadrature. The individual sources of uncertainty are shown in Table 7. The overall value thus obtained is  $\pm 2.9\%$ .

Table 7. Sources of Uncertainty

Electrical calibration	0.25%
Measurement repeatability	0.5%
Geometry	0.5%
Thermal defect	1.5%
Kerma correction	2.5%

### CONCLUSIONS

The calorimetric system provides an accurate method for determining the absorbed dose from the radiation beams at AFRRI. The calorimeter's response is independent of dose rate and ionization density, which makes it valuable for comparing the performances of dosimetry systems.

It was decided that a TE calorimetric system should be constructed specifically for AFRRI. This project was completed, and the system is described in Appendix B. Instructions for operating the system are also included.

## ACKNOWLEDGMENTS

The author wishes to thank G. H. Zeman, M. Dooley, L. J. Goodman, D. Eagleson, E. J. Golightly, and T. H. Mohaupt for their help during these difficult measurements.





## APPENDIX A. DATA LIST

The following pages contain tables of data from each calorimetric run taken at AFRRRI during two measurement sessions.

### Cobalt-60

$5.89 \times 10^{-4}$   
 $5.73 \times 10^{-4}$   
 $5.80 \times 10^{-4}$   
 $5.56 \times 10^{-4}$   
 $5.65 \times 10^{-4}$   
 $5.57 \times 10^{-4}$   
 $5.87 \times 10^{-4}$   
 $5.60 \times 10^{-4}$   
 $5.61 \times 10^{-4}$   
 $5.61 \times 10^{-4}$

### Electrons 252 cm

$1.38 \times 10^{-3}$   
 $1.38 \times 10^{-3}$   
 $1.37 \times 10^{-3}$   
 $1.39 \times 10^{-3}$   
 $1.38 \times 10^{-3}$   
 $1.38 \times 10^{-3}$   
 $1.38 \times 10^{-3}$   
 $1.37 \times 10^{-3}$   
 $1.39 \times 10^{-3}$   
 $1.40 \times 10^{-3}$   
 $1.41 \times 10^{-3}$

### X-Rays LINAC

$5.65 \times 10^{-4}$   
 $5.65 \times 10^{-4}$   
 $5.66 \times 10^{-4}$   
 $5.58 \times 10^{-4}$   
 $5.50 \times 10^{-4}$   
 $5.59 \times 10^{-4}$   
 $5.51 \times 10^{-4}$   
 $5.52 \times 10^{-4}$   
 $5.56 \times 10^{-4}$

### Electrons 4 m (4 $\mu$ s)

$3.97 \times 10^{-3}$   
 $3.20 \times 10^{-3}$   
 $3.18 \times 10^{-3}$   
 $3.21 \times 10^{-3}$   
 $3.21 \times 10^{-3}$   
 $3.20 \times 10^{-3}$   
 $3.21 \times 10^{-3}$   
 $3.21 \times 10^{-3}$   
 $3.22 \times 10^{-3}$   
 $3.25 \times 10^{-3}$   
 $3.23 \times 10^{-3}$

### Electrons 4 m (3 $\mu$ s)

$2.33 \times 10^{-3}$   
 $2.31 \times 10^{-3}$   
 $2.29 \times 10^{-3}$   
 $2.34 \times 10^{-3}$   
 $2.32 \times 10^{-3}$   
 $2.35 \times 10^{-3}$   
 $2.33 \times 10^{-3}$   
 $2.33 \times 10^{-3}$   
 $2.31 \times 10^{-3}$

### Electrons 4 m (1 $\mu$ s)

$8.28 \times 10^{-4}$   
 $8.39 \times 10^{-4}$   
 $8.40 \times 10^{-4}$   
 $8.31 \times 10^{-4}$   
 $8.32 \times 10^{-4}$   
 $8.33 \times 10^{-4}$   
 $8.43 \times 10^{-4}$   
 $8.34 \times 10^{-4}$   
 $8.40 \times 10^{-4}$

Electrons 4 m (2  $\mu$ s)

1.58 x 10<sup>-3</sup>  
1.59 x 10<sup>-3</sup>  
1.59 x 10<sup>-3</sup>  
1.57 x 10<sup>-3</sup>  
1.57 x 10<sup>-3</sup>  
1.58 x 10<sup>-3</sup>  
1.58 x 10<sup>-3</sup>  
1.61 x 10<sup>-3</sup>  
1.63 x 10<sup>-3</sup>

Electrons 6 m (4  $\mu$ s)

1.36 x 10<sup>-3</sup>  
1.36 x 10<sup>-3</sup>  
1.36 x 10<sup>-3</sup>  
1.37 x 10<sup>-3</sup>  
1.36 x 10<sup>-3</sup>  
1.38 x 10<sup>-3</sup>  
1.39 x 10<sup>-3</sup>  
1.39 x 10<sup>-3</sup>  
1.39 x 10<sup>-3</sup>  
1.38 x 10<sup>-3</sup>

7/12/84 Cobalt-60 3000 rad

2.53 x 10<sup>-3</sup>  
2.40 x 10<sup>-3</sup>  
2.39 x 10<sup>-3</sup>

7/12/84 Cobalt-60 5000 rad

3.33 x 10<sup>-3</sup>  
3.08 x 10<sup>-3</sup>  
3.14 x 10<sup>-3</sup>  
3.08 x 10<sup>-3</sup>

7/11/84 Cobalt-60 1000 rad

1.31 x 10<sup>-3</sup>  
1.34 x 10<sup>-3</sup>  
1.33 x 10<sup>-3</sup>  
1.37 x 10<sup>-3</sup>  
1.33 x 10<sup>-3</sup>

7/10/84 Cobalt-60 7000 rad

8.76 x 10<sup>-3</sup>  
8.81 x 10<sup>-3</sup>  
8.79 x 10<sup>-3</sup>  
8.85 x 10<sup>-3</sup>  
8.88 x 10<sup>-3</sup>

7/16/84 Bare Reactor 100 kW

2.40 x 10<sup>-3</sup>  
2.26 x 10<sup>-3</sup>  
2.58 x 10<sup>-3</sup>  
2.51 x 10<sup>-3</sup>  
2.69 x 10<sup>-3</sup>

7/16/84 Reactor Pulses 6 nVt

9.62 x 10<sup>-4</sup>  
9.44 x 10<sup>-4</sup>  
1.10 x 10<sup>-3</sup>

7/17/84 Reactor 12" H<sub>2</sub>O 100 kW

3.02 x 10<sup>-4</sup>  
3.14 x 10<sup>-4</sup>  
3.38 x 10<sup>-4</sup>  
3.22 x 10<sup>-4</sup>

7/18/84 Reactor 6" Pb 100 kW

7.10 x 10<sup>-4</sup>  
1.01 x 10<sup>-3</sup>  
7.09 x 10<sup>-4</sup>  
5.78 x 10<sup>-4</sup>  
5.08 x 10<sup>-4</sup>

7/18/84 Reactor Pulses 6" Pb 12 nVt

7.81 x 10<sup>-4</sup>  
7.72 x 10<sup>-4</sup>  
7.47 x 10<sup>-4</sup>  
6.60 x 10<sup>-4</sup>

7/19/84 Reactor 6" Pb 100 kW

5.75 x 10<sup>-4</sup>  
5.75 x 10<sup>-4</sup>  
5.77 x 10<sup>-4</sup>  
6.00 x 10<sup>-4</sup>  
5.80 x 10<sup>-4</sup>

7/19/84 Reactor 6" Pb 200 kW

5.91 x 10<sup>-4</sup>  
6.18 x 10<sup>-4</sup>  
4.07 x 10<sup>-4</sup>

## APPENDIX B. OPERATIONAL PROCEDURES FOR CALORIMETER

These procedures are written as a checklist. The user is assumed to be somewhat familiar with the equipment. If you are not familiar with the equipment, study the equipment manuals and then follow the instructions below.

### EQUIPMENT CHECK

The equipment includes:

- Calorimeter
- Vacuum pump with connectors
- HP-85 computer (HP-1B interface and 64K memory needed)
- Keithley voltmeter
- Calibration circuit
- Cables

If any of these items are missing, locate them or contact your supervisor.

### PLACEMENT OF EQUIPMENT

1. The HP-85 computer, the Keithley voltmeter, and the calibration circuit are normally in an equipment cart, along with the cables and the calorimeter in its wooden case (see Figure 4).
2. The vacuum pump does not need to be kept with the other equipment.
3. The electronic equipment should be placed in the control area adjacent to the radiation source to be used.

### EVALUATING THE CALORIMETER

1. The A-150 plastic core must be kept at low pressure. If you suspect that the calorimeter's vacuum valve has been opened to air, evacuate the calorimeter.
2. If the calorimeter has been opened to air for longer than 2 days, you must evacuate the calorimeter and irradiate it to approximately 150 kilorad using cobalt-60 or electrons before attempting measurements.
3. If you have not operated the vacuum system before, consult the equipment manuals before doing so. All valves of the vacuum system should be closed. The calorimeter's vacuum valve should be closed. The mechanical pump should then be switched on. (The diffusion pump will not be switched on until later.)
4. Connect the calorimeter to the brass valve on the pump by means of the stainless steel bellows. Check to be sure that the O-rings are clean and well seated. Secure the calorimeter with a ring stand clamp. Open the brass valve slowly (the bellows will compress and may pull the calorimeter toward the pump).



5. Open the calorimeter's valve slowly. After a few minutes, switch on the diffusion pump. Allow the calorimeter to pump this way for about 1 hour. Observe the vacuum gauge, which should indicate a pressure of just a few torrs.

## CONNECTING CABLES

1. After the calorimeter has been evacuated and the electronics have been placed in the appropriate location, connect the calorimeter to the cable end that has a dark-green female connector. This connector mates with the calorimeter's connector. It is keyed and has a quarter-turn bayonet-type mechanism.

The other end of the cable has a blue male multipin connector that plugs into the rear of the calibration circuit. A short cable with banana jacks at the end is connected from the rear of the calibration circuit to the input of the Keithley digital multimeter.

2. The Keithley will normally be left connected to the HP-85 computer. However, it is prudent to verify that the interconnecting cable and HP-IB interface module are plugged into the Keithley and the HP-85, respectively.

3. The Keithley multimeter should be in the resistance mode, and the display should read approximately 10,000 ohms. If an open circuit or short circuit is indicated, recheck the connections.

4. Turn on the calibration circuit and run it for a few seconds. Select both the core and the jacket on the mode switch, and verify that some voltage appears on the panel meter in both positions. This checks the continuity of the calibration heaters. If the panel meter indicates no voltage, again check the connections.

## SETUP FOR MEASUREMENTS

1. After it has been determined that the calorimeter is operating properly, disconnect the cable and set the calorimeter at the irradiation position. A white line on the exterior of the calorimeter indicates the height of the core, and the top of the calorimeter has a centering spot.

2. Make sure that the vacuum valve is not inadvertently opened while you are setting up the system.

3. Bring the cable into the irradiation room and connect it to the calorimeter. After the final fine position adjustments and checks, tape the cable down or otherwise secure it into position.

## TEMPERATURE EQUILIBRATION

After the calorimeter has been set in place for measurements, it must be allowed to come to equilibrium with its surroundings. Although the temperatures of most rooms are within a few degrees of each other, such differences are very large compared to the temperatures that the calorimeter will actually be measuring when it is irradiated. (These are on the order of  $10^{-3}^{\circ}\text{C}$ .) Allow a few hours for the calorimeter to equilibrate.

The reactor presents the most serious equilibration problem. The calorimeter should be placed in the reactor's exposure room some time during the afternoon preceding a measurement session. It should be connected to the electronic system and left on overnight. No further entries into the exposure room should be made until early the next morning (approximately 6:30 a.m.), when the reactor room lights should be turned on and left on. These lights create a rise of several degrees in room temperature, so the calorimeter will have to equilibrate again for approximately 2 hours. If the lights are turned on at 6:30, the system should be ready by 9:00 a.m.

The drift rate of the calorimeter can be checked periodically by acquiring the plotting data with the READIN program or by observing the reading of the Keithley digital multimeter.

## COMPUTER ROOM

The operation of the HP-85 computer requires the program tape cassette and a blank tape (or tapes). The program tape should be "write inhibited," and the blank data tapes should be capable of being written.

The program will autostart. The program tape should be inserted into the HP-85, and the power switch should then be turned on. At this point, a menu will appear on the screen with a list of the following subprograms:

LOADR  
READIN  
LSTSQ  
DNLOAD  
EPLOT

The control keys K1 through K9 are used to select the subprograms. The programs are self-prompting and require either a yes or no (Y/N) or an input of numerical data.

### Procedure

1. Enter date (D,M,Y) and time (H,M,S).
2. Select READIN. This program will ask for file names and run parameters.

3. When data entry is finished, write the data onto a blank tape with DNLOAD. This program will also prompt the user.
4. When the data are to be analyzed, run the EPLOT program to select the intervals of analysis. This program automatically scales the plot to display maximum sensitivity.
5. Program LSTSQ analyzes the data and calculates a net slope value and a displacement. Either of these quantities can be calibrated to produce dose or dose-rate values.

## REFERENCES

1. Laughlin, J. S., and Genna, S. Calorimetry. In: Radiation Dosimetry, Vol. 2. Attix, F. H., Roesch, W. C., and Tochilin, E., eds. Academic Press, New York, 1966, pp. 389-439.
2. Fleming, D. M., and Glass, W. A. Endothermic radiochemical reactions in tissue equivalent plastic. Radiation Research 37: 316, 1969.
3. Goodman, L. J. A practical guide to ionization chamber dosimetry at the AFRRI reactor. Contract Report CR 85-1, Armed Forces Radiobiology Research Institute, Bethesda, Maryland, 1985.
4. Domen, S. R. Thermal diffusivity, specific heat, and thermal conductivity of A-150 plastic. Physics in Medicine and Biology 25: 93-102, 1980.
5. McDonald, J. C., Ma, I., Liang, J., and Laughlin, J. S. Absorbed dose determination in high-LET and conventional radiotherapy beams. Biomedical Dosimetry: Physical Aspects, Instrumentation, Calibration. Publ. No. 567. International Atomic Energy Agency, Vienna, 1981, pp. 259-270.
6. McDonald, J. C., and Goodman, L. J. Measurements of the thermal defect for A-150. Physics in Medicine and Biology 27: 229-233, 1982.